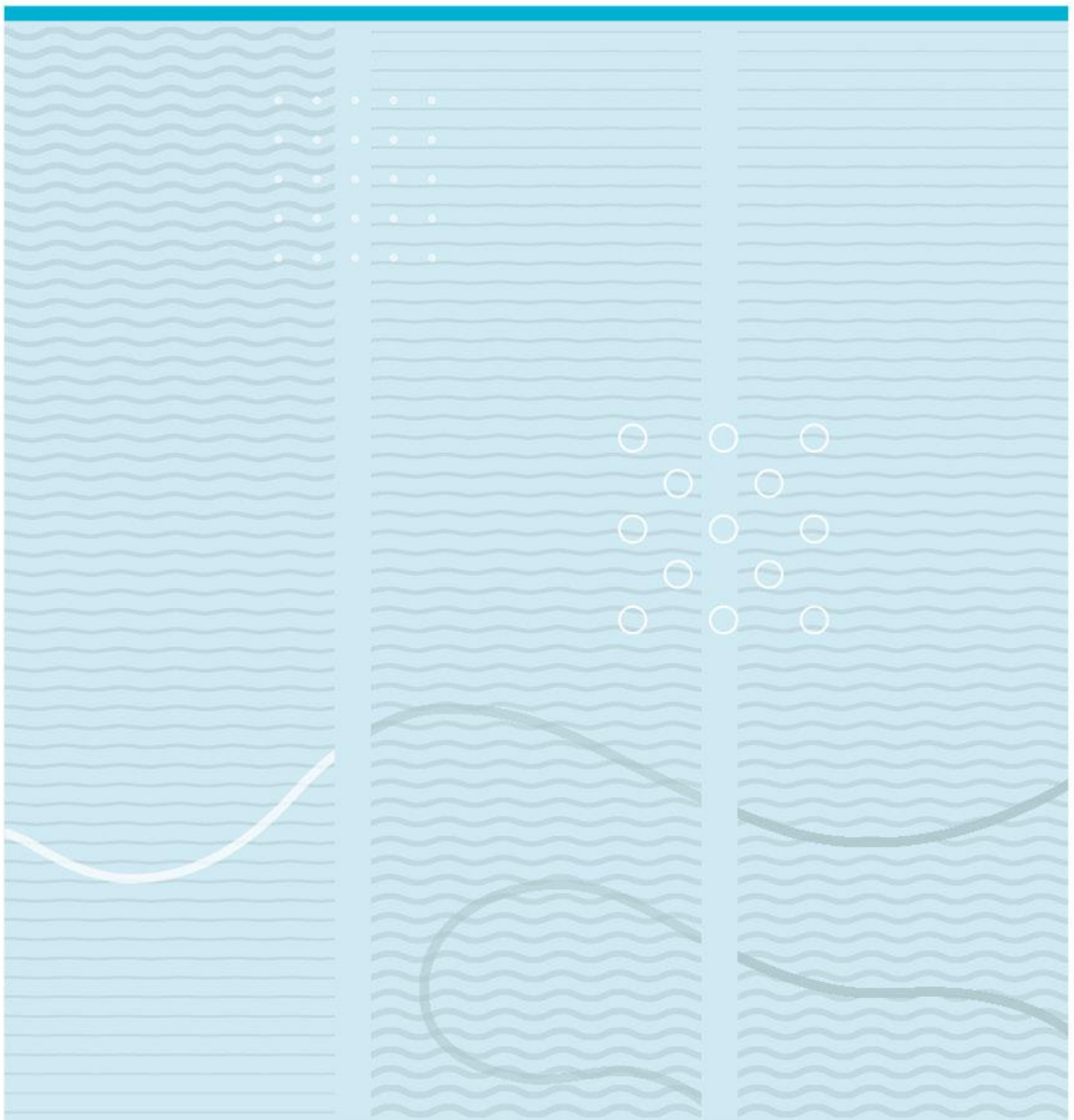


Saad Rabbani

Implantable MEMS Electrode for Neuroprosthesis



University of South-Eastern Norway
Faculty of Technology, Natural Sciences and Maritime Sciences
Department of Microsystems.
Raveien 215
NO-3184 Borre, Norway

<http://www.usn.no>

© 2021 <Saad Rabbani>

Acknowledgement

Throughout the project I have received a great deal of support and assistance.

I would first like to thank my supervisors, Lars-Cyril Blystad and Kristin Imenes. Their doors were always open whenever I ran into a trouble spot or had a question about my research or writing. They consistently motivated me during the ups and downs of the project and steered me in the right direction whenever they thought I needed it. I would also like to thank the lab engineers Zekija Ramic and Birgitte Kasin Hønsvall. They helped me throughout my lab work and guided and assisted me at several places. Here I would also like to thank University of South-Eastern Norway for providing me with such valuable master's program where I studied under supervision of dedicated professors, where I was able to work in state-of-the-art labs and where I was welcomed with warm and welcoming environment.

I would also like to thank Jan Pederson from Elmatica AS for awarding me with the "Dieter Bergman Memorial Scholarship" for my R&D contribution to such research project. This award boosted my interest in electronics and microfabrication pushing me to strive more for such opportunities.

Finally, I must express my very profound gratitude to my parents and to my girlfriend Slsabeel Issa for providing me with unfailing support and continuous encouragement throughout my years of study and through the process of researching and writing this thesis. This accomplishment would not have been possible without them. Thank you.

Abstract

In this thesis, we are microfabricating neural cuff electrodes that will be implanted in the human upper limb and will be utilized for neuroprosthesis. This is a research-based thesis that has been conducted in collaboration with the EEA Grants named "ARMIN". The goal of this project is to design a neuroprosthesis arm, which can mimic the human upper limb's motor actions and sensations. The whole prosthesis is the integration of neural implantable electrode including its fabrication, electronics interface, low power wireless communication, a mechanical arm, and its control system. Parts of the mechanical hand will be equipped with artificial skin which will help to receive sensorial feedback. Having many integral parts, this work set its center of attention on the fabrication of MEMS implantable nerve cuff electrodes.

In this thesis, the fabrication of the nerve cuff electrode is described briefly. The task was assigned for the microfabrication of implantable electrodes for neural signals acquisition in the upper limb (arm) neuroprosthesis. For that, three different microfabrication methods are described with the experiments conducted in the cleanroom. For the fabrication material, Pure gold was chosen due to its 100% continuity and conductivity and PDMS was used as substrate material for the electrode. PDMS is used due to its high tensile modulus, physical toughness, elongation, and also it is a good biocompatible material.

After the fabrication of the electrode, laboratory functionality tests were conducted where the electrode was tested with measuring its conductivity, adhesion, rolling test, and biocompatibility test. Different fabrication methods showed different results where the final test showed acceptable results. The adhesion test showed good adhesion between PDMS and gold also conductivity was also measured all over the electrode. Moreover, the biocompatibility test also showed positive results.

Table of Contents

| | | |
|-------|--|----|
| 1 | Introduction..... | 1 |
| 1.1 | Nervous System..... | 2 |
| 1.2 | Evolution of Neuroprosthesis | 5 |
| 1.3 | Types of Nerve Electrodes..... | 9 |
| 1.3.1 | Longitudinal Intrafascicular Electrode..... | 10 |
| 1.3.2 | Transverse Intrafascicular Multichannel Electrode..... | 11 |
| 1.3.3 | Utah Slanted Electrode Array | 11 |
| 1.3.4 | Regenerative Electrodes | 12 |
| 1.3.5 | Nerve Cuff Electrodes | 13 |
| 2 | Materials and Methods..... | 16 |
| 2.1 | Fabrication Process with Chromium as Adhesion Promoter..... | 19 |
| 2.1.1 | Preparation and Deposition of PDMS Substrate..... | 20 |
| 2.1.2 | Plasma Treatment | 20 |
| 2.1.3 | Deposition, Patterning and Etching of metal layer. | 21 |
| 2.1.4 | Peeling off PDMS substrate from Silicon Wafer | 21 |
| 2.1.5 | Electrode Rolling Tests..... | 21 |
| 2.1.6 | Adhesion and Conductivity Test..... | 22 |
| 2.2 | Fabrication Process with (3- mercaptopropyl) trimethoxy silane (MPTMS) as Adhesion Promoter..... | 22 |
| 2.2.1 | Preparation of (3- mercaptopropyl)trimethoxy silane (MPTMS)..... | 25 |
| 2.2.2 | Treatment of PDMS Substrate in MPTMS Saline | 25 |
| 2.2.3 | Deposition and Etching of Gold on Si Wafer | 25 |
| 2.2.4 | Bonding of MPTMS Treated PDMS with Gold | 26 |
| 2.3 | Fabrication Process with Depositing PDMS Substrate on Patterned Gold Electrodes | 27 |
| 3 | Results..... | 29 |
| 3.1 | Fabrication Process with Chromium as Adhesion Promoter | 29 |
| 3.1.1 | Deposition of Substrate | 29 |
| 3.1.2 | Plasma Treatment | 30 |
| 3.1.3 | Thin Film Deposition of Au and Cr..... | 33 |
| 3.1.4 | Patterning and Etching of Gold Film..... | 33 |
| 3.1.5 | Electrode Rolling Test | 34 |

| | | |
|-------|--|----|
| 3.1.6 | Adhesion Test..... | 36 |
| 3.1.7 | Conductivity Test..... | 37 |
| 3.2 | Fabrication Process with (3- mercaptopropyl) trimethoxy silane (MPTMS) as Adhesion Promoter..... | 38 |
| 3.2.1 | Deposition and Etching of Gold Film | 38 |
| 3.2.2 | Bonding of MPTMS Treated PDMS with Gold | 40 |
| 3.2.3 | Plasma Treatment | 41 |
| 3.2.4 | Conductivity Tests | 44 |
| 3.3 | Fabrication Process with Depositing PDMS Substrate on Patterned Gold Electrodes | 44 |
| 3.3.1 | Transfer of Patterned Gold Electrodes | 44 |
| 3.3.2 | Rolling, Conductivity and Adhesion Tests. | 46 |
| 4 | Discussion..... | 50 |
| 4.1 | Fabrication Process with Chromium as Adhesion Promoter | 50 |
| 4.1.1 | Deposition of Substrate and Plasma treatment..... | 50 |
| 4.1.2 | Thin Film Deposition and Etching of Au and Cr | 50 |
| 4.1.3 | Adhesion Test..... | 52 |
| 4.1.4 | Conductivity Test..... | 52 |
| 4.1.5 | Comparison with the Reference Method..... | 53 |
| 4.2 | Fabrication Process with (3- mercaptopropyl) trimethoxy silane (MPTMS) as Adhesion Promoter..... | 53 |
| 4.2.1 | Deposition and Etching of Gold Film | 53 |
| 4.2.2 | Bonding of MPTMS Treated PDMS with Gold | 54 |
| 4.2.3 | Plasma Treatment | 55 |
| 4.2.4 | Conductivity Tests | 56 |
| 4.2.5 | Comparison with Reference Method | 56 |
| 4.3 | Fabrication Process with Depositing PDMS Substrate on Patterned Gold Electrodes | 56 |
| 4.3.1 | Transfer of Patterned Au Electrodes on PDMS..... | 56 |
| 4.3.2 | Rolling, Conductivity, and Adhesion Tests. | 58 |
| 5 | Insulation Layer for the Cuff Electrode..... | 59 |
| 6 | Biocompatibility Tests..... | 62 |
| 7 | Conclusion and Upcoming Work..... | 66 |
| 8 | References..... | 68 |

List of Tables

| | |
|---|----|
| Table 1: Electrodes comparison between their Longevity/ Persistence and Spatial Resolution..... | 14 |
| Table 2: Different plasma dozes with different Adhesion thickness..... | 31 |
| Table 3: Surface Morphology of Electrode before and after Rolling Test..... | 35 |
| Table 4: Pictures of Electrodes before and after adhesion test..... | 36 |
| Table 5: Results of different plasma duration on bonding..... | 42 |
| Table 6: Comparison Between Different Peeling Angles. | 46 |
| Table 7: Rolling and Adhesion Tests of Electrode for 200nm thickness. | 47 |
| Table 8: Buckling and Cracking Difference between 200nm and 300nm Thickness..... | 57 |

List of Figures

| | |
|--|----|
| <i>Figure 1: Nervous System classified in its two types: Peripheral Nervous System and Central Nervous System.</i> | 3 |
| <i>Figure 2: Neuron structure with its neighbors.</i> | 4 |
| <i>Figure 3: The image shows how electrical impulse arrives in the cell and how it is transmitted to other neurons through the axon[17].</i> | 5 |
| <i>Figure 4: Concept of Neuroprosthesis.</i> | 6 |
| <i>Figure 5: Sauerbruch's prosthetic hand design.</i> | 7 |
| <i>Figure 6: Bowden cable powered prosthesis.</i> | 7 |
| <i>Figure 7: Myoelectric Prosthesis, controlled by Electromyographic(EMG) Signals from remains of muscle at the amputation stump.</i> | 8 |
| <i>Figure 8: Connection paths and working of targeted motor reinnervation</i> | 9 |
| <i>Figure 9: Visual description of LIFE electrode.</i> | 10 |
| <i>Figure 10: Schematic diagram of a median nerve implanted with TIME electrode.</i> | 11 |
| <i>Figure 11: Comparison of the Utah Electrode Array (UEA) and the Utah Slanted Electrode Array (USEA).</i> | 12 |
| <i>Figure 12: Left side of the image shows the concept of the sieve regenerative electrode while the right side of the image shows the front view of the electrode with 64 channels residing inside.</i> | 13 |
| <i>Figure 13: Visual description of LIFE electrode.</i> | 14 |
| <i>Figure 14: Research Project Work flowchart</i> | 17 |
| <i>Figure 15: Electrode Design for Animal Test.</i> | 18 |
| <i>Figure 16: Electrode Design for Animal Test.</i> | 19 |
| <i>Figure 17: Fabrication Process Description.</i> | 20 |
| <i>Figure 18: Electrode 1 peeled off from Si wafer.</i> | 21 |
| <i>Figure 19: Electrode rolled over glass rod.</i> | 22 |
| <i>Figure 20: Stage one for activating MPTMS layer on PDMS.</i> | 23 |
| <i>Figure 21: Au deposition and etching of electrodes on Si wafer.</i> | 24 |
| <i>Figure 22: Bonding and peeling off MPTMS treated PDMS with Au.</i> | 24 |
| <i>Figure 23: PDMS deposited wafer immersed in MPTMS on chemical shaker.</i> | 25 |
| <i>Figure 24: PDMS substrate on Au Patterned on Si wafer.</i> | 26 |
| <i>Figure 25: Soft Baking for enhancing PDMS and Au bonding.</i> | 26 |
| <i>Figure 26: Fabrication Process for the Third Experiment.</i> | 27 |

| | |
|--|----|
| Figure 27: Electrode rolled around plastic tube imitating the nerve . | 28 |
| Figure 28: PDMS deposited on Si wafer and its parts. | 29 |
| Figure 29: Measurement of PDMS thickness. | 29 |
| Figure 30: Metal deposited on two different plasma treated PDMS. | 33 |
| Figure 31: Patterned electrode after Au etching. | 34 |
| Figure 32: Electrode surface on PDMS after peeling off from Si wafer. | 35 |
| Figure 33: Parameter 2 showing cracks from multimeter probes. | 37 |
| Figure 34: Parameter 3 showing cracks from multimeter probes. | 37 |
| Figure 35: Parameter 4 showing cracks from multimeter probes. | 38 |
| Figure 36: Thin Au Film on Si wafer | 39 |
| Figure 37: Peeled of Au from Si wafer after rinsing | 39 |
| Figure 38: Patterned Au electrodes on Si wafer. | 40 |
| Figure 39: Bubble structure on Au thin film. | 40 |
| Figure 40: Au electrodes transferred on PDMS Substrate. | 41 |
| Figure 41: Au transfer on PDMS with 300nm thickness. | 45 |
| Figure 42: Au transfer on PDMS with 200nm thickness. | 45 |
| Figure 43: Conductive Part of 300nm Au Electrode | 48 |
| Figure 44: Non-Conductive Part of 300nm Electrode | 48 |
| Figure 45: Failed Adhesion test for 300nm Electrode. | 48 |
| Figure 46: Conductivity tests of contact pad and reference pads on 200nm Au Electrode. | 49 |
| Figure 47: Au electrode on PDMS after Peeling off from Si wafer | 51 |
| Figure 48: Au electrode on PDMS after rolling on glass rod | 52 |
| Figure 49: Au Pattern with bubble structure. | 54 |
| Figure 50: Au pattern without bubble structure. | 54 |
| Figure 51: Misprinted Au Pattern on Si wafer. | 55 |
| Figure 52: 3D Printed mold for Electrode Insulation. | 59 |
| Figure 53 :Extracted PDMS Mold from Si wafer. | 60 |
| Figure 54: Side View of Insulated Mold. | 60 |
| Figure 55: Top View of Insulated Mold with comparison to electrode design. | 61 |
| Figure 56: Setup on a 24-well plate for Biocompatibility Test. | 63 |
| Figure 57: Metabolic Activity of PrestoBlue Reagent. | 64 |
| Figure 58: Cell Count from each Sample using Hemocytometer. | 64 |

List of Acronyms

ENG: Electroneurogram.

MEMS: Microelectromechanical Systems.

POC: Point-of-Care.

LOC: Lab-on-a-Chip.

EMG: Electromyogram.

EEA: European Economic Area.

PNS: Peripheral Nervous System.

CNS: Central Nervous System.

SNR: Signal-to-Noise Ratio.

TMR: Targeted Motor Reinnervation.

LIFE: Longitudinal Intrafascicular Electrode.

tfLIFE: thin film Longitudinal Intrafascicular Electrode.

TIME: Transverse Intrafascicular Multichannel Electrode.

USEA: Utah Slanted Electrode Array.

UEA: Utah Electrode Array.

IEEE: The Institute of Electrical and Electronics Engineers.

FINE: Flat Interfaced Nerve Electrode.

PDMS: Polydimethylsiloxane.

MPTMS: (3- Mercaptopropyl)trimethoxysilane.

ISO: International Organization for Standardization.

OH: Hydroxide.

RPM: Revolutions Per Minute.

DI Water: Deionized Water.

UV Light: Ultraviolet Light.

SAM: Self-assembled Monolayer.

-SH: Thiol Functional Group.

Cr: Chromium.

Au: Gold.

RIE: Reactive Ion Etching.

HBSS: Hanks Balanced Salt Solution.

-OCH₃: Three methoxy group.

1 Introduction

People living with limb loss has been increasing profoundly in the recent decade. In United States alone, according to a survey, approx. 1.7 million people suffer with the upper limb loss[1]. In total there are approx. 2 million people in the United States suffering with limb loss[2]. These losses can be categorized in two terms, traumatic and non-traumatic losses. The traumatic losses or amputations are those which are caused by wounds or injuries which destroy the vessels of blood, and can origin from e.g. road accidents, gunshot wounds or any mechanical equipment accidents[3]. On the other side, non-traumatic losses or amputations are caused by impaired blood flow. These amputations happens most frequently in patients of vascular disease, diabetes, infections or certain types of cancer[3]. For this, numerous techniques have been developed from different research to answer the problem of loss of functionality. One of the prostheses technologies of interest is the neuroprosthesis that interact directly with the user's peripheral nervous system. This is made possible by the advancements in micro- and nanotechnology. In the past decade, several different kinds of implantable neuroprosthesis electrodes have been introduced to the world that interface with the peripheral nervous system of the human body. Each of these electrodes have their own way to connect with respective muscle or nerve to the anatomical level. The implantable electrodes are designed to acquire signals from the nerve or to stimulate the nerve, in which nerve stimulation is usually done by electric stimulation of the nerves and/or muscles. Materials used for the fabrication of implantable electrodes should comply with biocompatibility standards as wrong material can easily leave bad impact on the nerve, which can result in the form of nerve irritation or nerve swelling. During implantation, these electrodes should provide good charge transfer to avoid current losses, low impedance to avoid neural damage and long-term electrochemical stability[4]. There are multiple kind of nerve electrodes such as surface electrodes (cuff electrodes), penetrating electrodes and regenerative electrodes[5]. Among these electrodes, cuff electrode has best output results due to its ability to have complete grip on target nerve surrounded by cuff electrode from all sides. These kinds of electrodes have been widely used in both research and clinical practice like vagus nerve[6] stimulation, recording electroneurograms(ENGs), and bladder control[7].

Microelectromechanical Systems (MEMS) devices are now highly involved in the fabrication of implantable neural electrodes. MEMS as its names define, consist of a process flow technology which is utilized for the fabrication of devices combining both mechanical and electrical components at microlevel. Due to their capability of controlling, sensing, and actuating on the micro level, they can produce results at macro scale. With the advancement in biotechnology, MEMS has also been introduced in the field of medicine and biological applications, and is therefore known as BioMEMS[8]. Using standard fabrication processes from MEMS, miniaturized biocompatible devices have been introduced for the commercial use serving hundreds of thousands of patients worldwide. Some of the most common BioMEMS devices includes blood glucose monitoring machine where transducer of the size of letters on coin works for providing accurate glucose level, and example of Point-of-Care (POC) device used for performing lab experiments with the help of Lab-on-a-Chip (LOC) at micro level, saves both money and time[9].

In this master project, focus is on the microfabrication of an implantable MEMS designed cuff electrode for nerve signal acquisition. It will be used to integrate nerve electrode in a neuroprosthesis where the goal is to provide accurate signals to control a prosthetic arm based on nerve electric signals instead of using electromyogram (EMG) which aims to work by receiving signals from muscles[10]. The master project work is in collaboration with an EEA Grants project named ARMIN "Arm Neuro Prosthesis

Equipped with Artificial Skin and Sensorial Feedback” and the center of attention is to fabricate electrode that can be implanted and used in an arm neuroprosthesis. The motivation behind the implantable electrode is to remove the intermediate path between the electrode and the nerve i.e., muscles using neural interfaced electrode from where signal will be acquired. The whole prosthesis is the integration of neural implantable electrode including its fabrication, electronics interface, low power wireless communication, a mechanical arm, and its control system. Parts of the mechanical hand will be equipped with artificial skin which will help to receive sensorial feedback. Having many integral parts, this work set its center of attention on the fabrication of MEMS implantable nerve cuff electrode. In that respect, literature study regarding the cuff electrode fabrication also becomes an important part before the fabrication process is started. The cuff electrodes designed and fabricated in this project are meant to be wrapped around target nerve so the substrate for the electrode should be flexible and the electrode material should have good electrical conductivity.

This thesis has been organized in different chapters where each chapter discusses in detail about their respective topics and information residing in them. Starting from **Chapter 1** where background of human nervous system, evolution of neuroprosthesis, statistics of amputees and prosthetic arm, and overview of different types of nerve electrodes have been discussed thoroughly. **Chapter 2** is associated with the materials and methods studied and utilized in this research project, where in depth details are provided regarding the scientific methods, hypothesis, and microfabrication processes that has been considered. In **Chapter 3**, results achieved from the methods experimented in **Chapter 2** have been discussed with detailed tables and figures. Whereas **Chapter 4** is corresponding to the discussion that has been observed from the results section. **Chapter 5** explains the method for the insulation of the electrode with PDMS. **Chapter 6** shows the biocompatibility tests conducted with different samples. Lastly, **Chapter 7** winds up the project and gives ideas regarding future work that can be brought in to account and **Chapter 8** consists all the references that has been used in this thesis regarding to literature study and lab work.

1.1 Nervous System

In the Peripheral Nervous System (PNS), there are several nerves made of axons of sensory and motor neurons. They are organized in groups known as fascicles and are covered by the sheath that holds fascicles in bundles, and this fascial layer is surrounded by the nerve itself. The anatomical complexity of the PNS is considered high while designing any device which interfaces with it. The peripheral nerves are bidirectional that means they transfer the signals both for sensation and motor commands to and from spinal cord. In extreme cases like fatal accidents or gunshot wounds, these pathways are suspected to get blocked or destroyed and result in loss of function when suffer through severe injury [11].

This thesis focuses on how neuroprosthesis can facilitate from the deficit of human functionality by using implantable electrodes. Before proceeding into depth of the microfabrication of implantable electrodes, it is important to learn how our nervous system works and what parts of this system are utilized by the prosthesis.

Our nervous system has been categorized in two parts, namely Central Nervous System (CNS) and Peripheral Nervous System (PNS). The CNS consists of the working of brain and spinal cord, and the combination of these two systems helps human body in functioning and sensing, including sensations, thoughts, speech, and movement. The brain controls all these functions while some of the reflex movements are done with spinal cord [12]. **Figure 1** shows the basic structure of our nervous system and its classes.

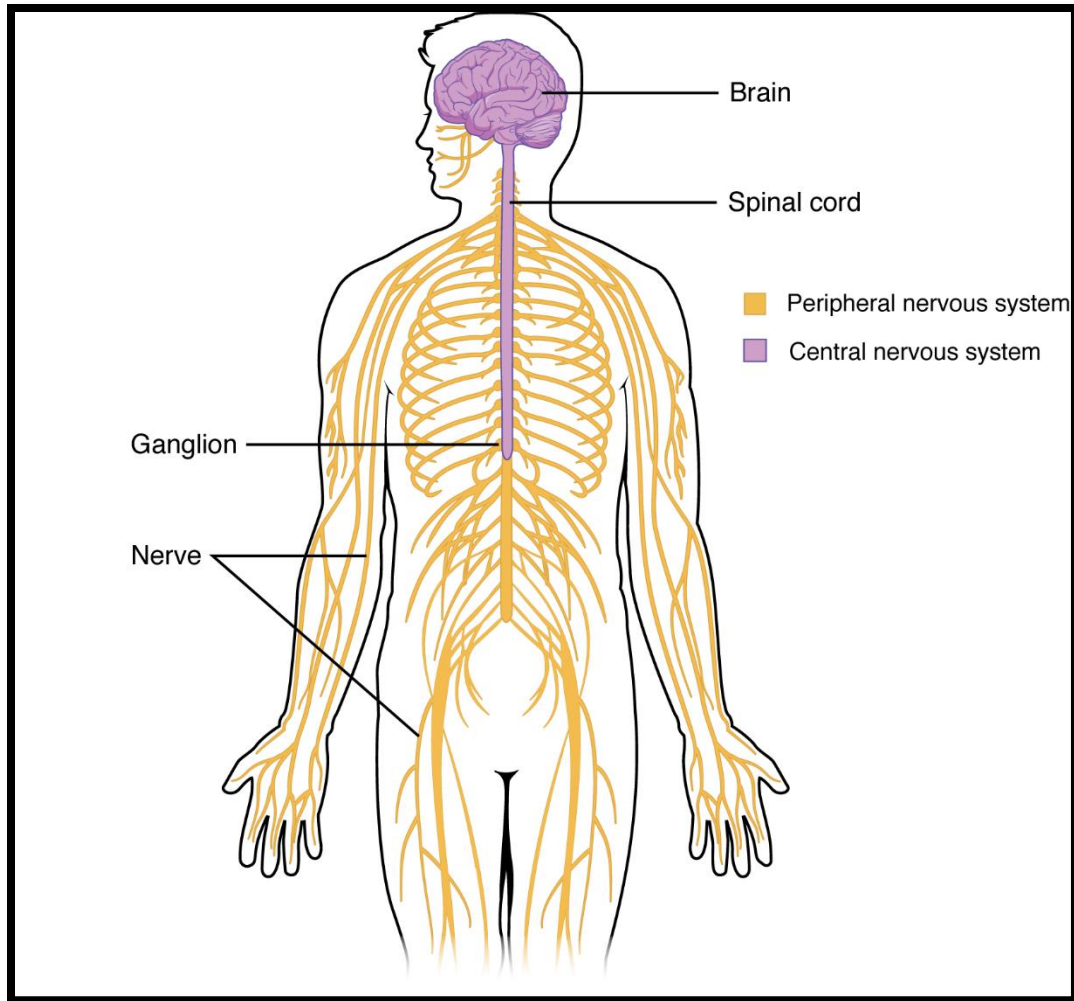


Figure 1: Nervous System classified in its two types: Peripheral Nervous System and Central Nervous System. Reproduced with permission of [Oregon State University](#)[13].

Whereas the PNS controls all the nerves that are lying outside of the CNS. Its main purpose is to connect the CNS with the organs, limbs, and skin. This system actually lets the brain and the spinal cord to transmit and capture information to the other parts of the body that allows us to react in certain situations [14]. The nervous system of a human being consists of billions of nerve cells known as neurons. These neurons are also called messenger cells which transmit messages from one part of the body to another part of the body. The neurons are comprised of a cell body and one or several fibers. These fibers are of two types, as shown in [Figure 2](#). One which carry information towards the cell body called “dendrites” and the other which carries information away from the cell body called “axons”. The nerves are packed in bundles of nerve fibers [15]. Later, these neurons are divided into different types namely sensory neurons, motor neurons and association neurons. The sensory neurons transmit information about the stimulation like heat, light, or touch both from inside or outside of the body and transmits to central nervous system. The motor neurons are those which delivers instructions from central nervous system to the other parts of

the body which includes muscles or glands. Whereas, the association neurons are those that connects sensory neurons to motor neurons [14].

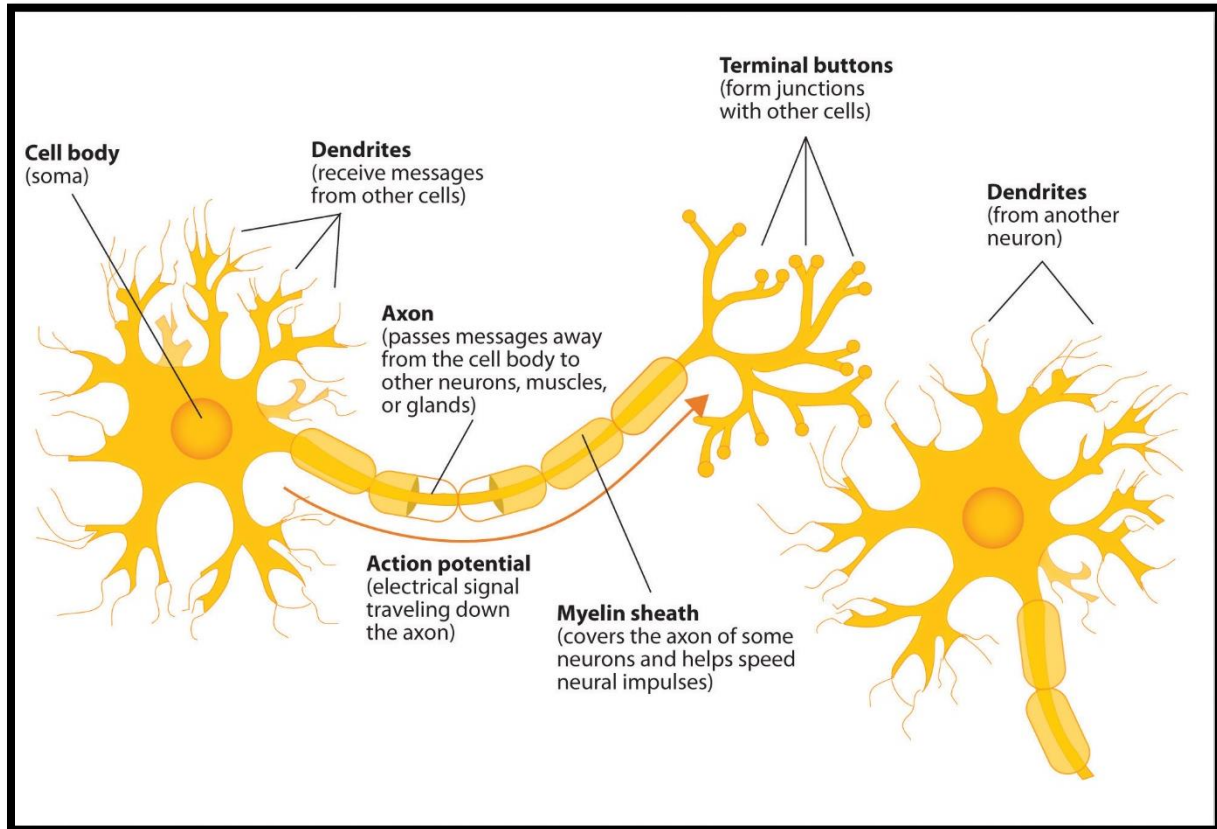


Figure 2: Neuron structure with its neighbors. Reproduced with the permission of [BC Campus open education](#) [16].

All these neurons carry and transmits information in the form of electrical signals which is termed as nerve impulses as depicted in [Figure 3](#). Neurons have to be excited in order to create an impulse which can be in the form of light, sound or pressure [15].

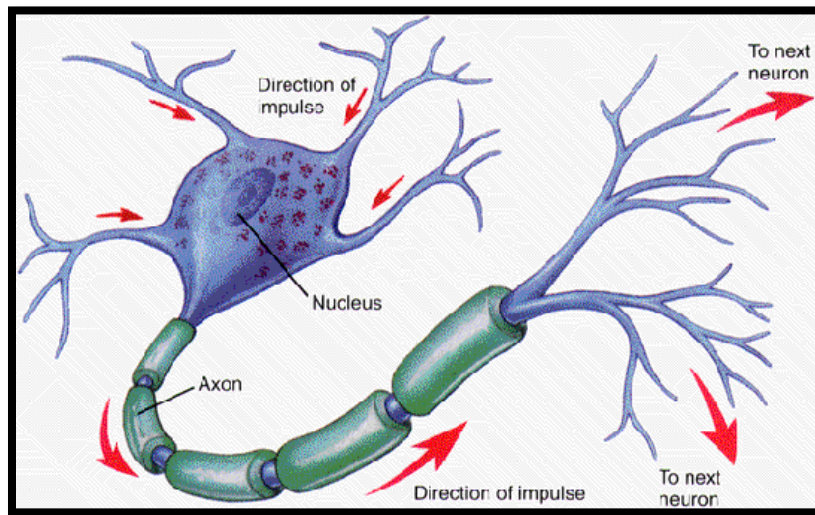


Figure 3: The image shows how electrical impulse arrives in the cell and how it is transmitted to other neurons through the axon[17].

1.2 Evolution of Neuroprosthesis

As discussed in [section 1](#), use of neuroprosthesis can be explained by several means. Issues causing limb losses are defining the need of neuro technologies like neuroprosthesis to help and aid with the patients of limb loss. Neuroprosthesis is a sort of devices, which can help restoring the physiological motor functioning, and sensations to its users. Neuroprosthesis merges physiological processes of human body with state of the art engineering concepts to create a functional replacement [18]. Neuroprosthesis is dedicated to the ones suffering from limb loss functionality and by taking advantage of the remaining neural pathways, neuroprosthesis can assist them by controlling robotic limbs [19], [20]. The availability of sensory feedback in neuroprosthesis over other traditional prosthetic arms gives neuroprosthesis dominance and also it is an active area of research in bioengineering world [21].

The neuroprosthesis is comprised of several components depending on its purpose of function. These devices are invasive and must have a sensor or electrodes that interface with the nervous system for recording or stimulating the nerves, a processing unit where the input and output signal will be controlled with the help of defined algorithms and a robotic arm which will be interfaced with the sensors and electrodes on PNS. Furthermore, for the external device i.e., robotic prosthetic arm has some common components which are related to hardware, processing unit for controlling and routing signals and sensors for the feedback purposes bases on the requirement depending if the system needs to function in forward motor control for adjusting artificial limb or the feedback through sensors for restoring sensations [18].

Before moving ahead, it is important to understand difference between motor and sensory prosthesis. For motor prosthesis, nerve electrode reads neural signals generated from amputees' brain and forwards it that is why the devices related to it are known as forward prosthetic devices. On the other hand, in sensory feedback the sensors read the data and assign it to the neural interface which gives perception to the amputee. In prosthetic devices, both these functions need to work along each other to replicate real limb functions. For that, the flow of information is said to be reversed in the prosthetic devices as for in forward motor prosthesis, the signals acquired from the nerves are assessed by the processing unit and

then are forwarded to the prosthetic arm. And in feedback sensory devices, using sensors, data is sent back to nervous system after being processed by microcontroller. While some actions/tasks are predefined in the microcontroller such as for reflex pathways like having sudden grip on slippery object or sensation of pain. These bidirectional devices adds challenges for both hardware designing, fabrication and assigning algorithms for dealing with various signals including filtration of signals [18].

Neuroprosthesis offers wide advantages when it interacts with the PNS as there is no intermediate path between the electrode and the nerve and signals can be acquired directly from the nerves having low Signal-to-Noise ratio (SNR) compared to the myoelectric signals where signals are acquired through the muscles. **Figure 4** Shows the concept of neuroprosthesis. Further, evolution of neuroprosthesis is discussed giving brief idea on the changes and advancements in neuroprosthesis with time.

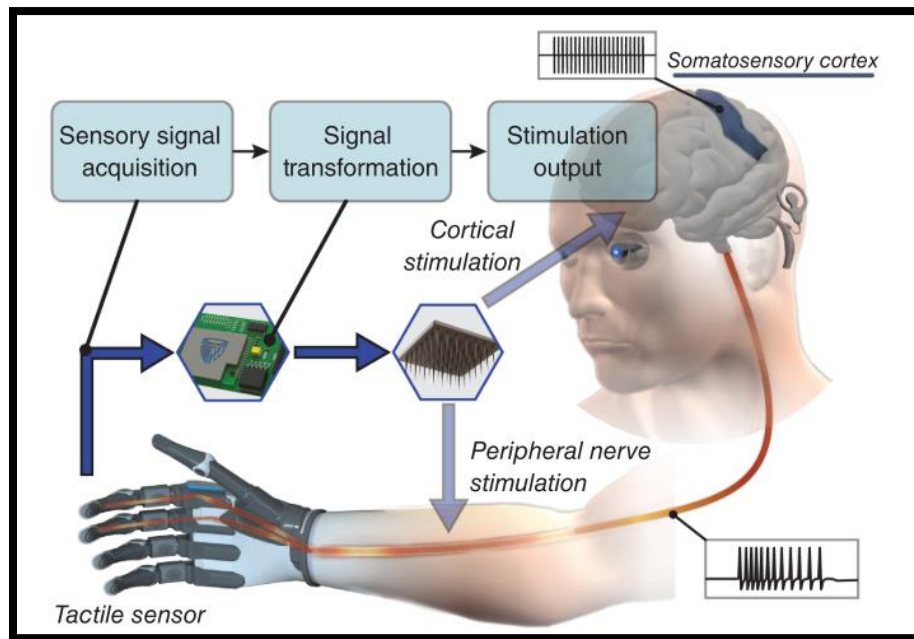


Figure 4: Concept of Neuroprosthesis. Reprinted with the permission of John Wiley and Sons, *Neural Prostheses* (Nitish V. Thakur, Joseph L. Betthausen, Luke E. Osbern)[18]

The first automatic and body-powered upper limb prosthetic arm was developed by German dentist Peter Bailiff in 1818[22]. This prosthesis uses the tension in the transmission with the help of leather straps and let the intact muscles in the shoulder and trunk girdle [23] by which, motion in the terminal device attached to amputation stump was obtained. This was for the first time when an amputee was able to use the prosthetic arm with motion in flow with the body rather than a distinct separate object. Later in 1916, another German surgeon Dr Ferdinand Sauerbruch reported a design which allowed the digits to be controlled with transmission of upper arm muscle movements shown in **Figure 5** [24]. With this prosthesis, amputees were able to drink from cups and even they could light a cigarette with matchstick [25].



Figure 5: Sauerbruch's prosthetic hand design. Reproduced with the permission of the [SAGE Publications](#). [26]

The Bowden cable body powered prosthesis was introduced after three decades in 1948. It changed the way of using prosthetic arm with its durability, portability, and affordability as shown in [Figure 6](#). Rather than using heavy and bulky straps with the sleek, it uses the cables to operate the two prolonged hooks as with the help of cables, changing the tension via shoulder and body movements as shown in below. The amputee must sense the tension in the string so amputee can predict and adjusts the hooks accordingly. This prosthesis was not comfortable as well as motored tasks were limited and appearance was not that good as well [27].

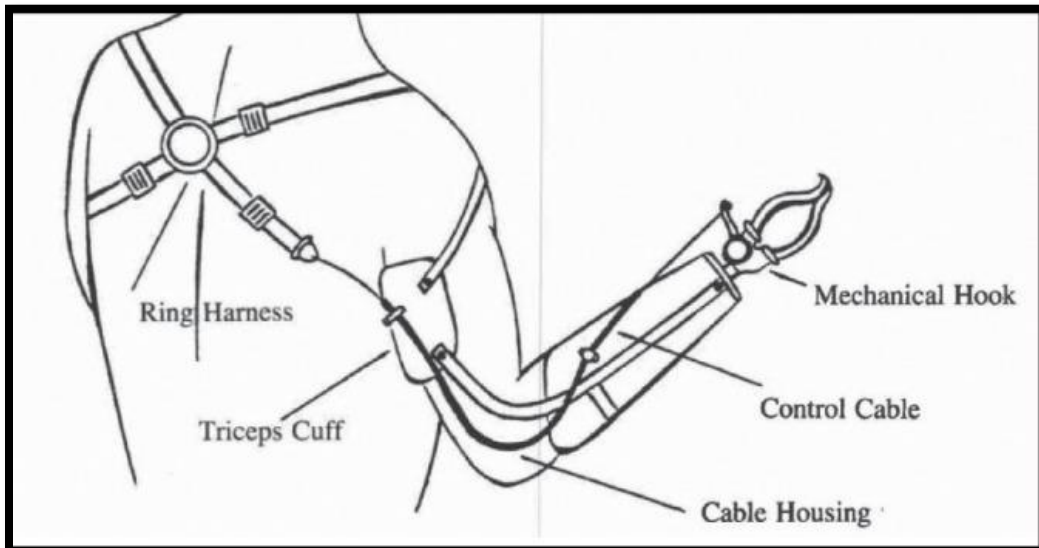


Figure 6: Bowden cable powered prosthesis. Reproduced with the permission of the [SAGE Publications](#) [26].

In late 20th century, myoelectric prosthesis, a prosthesis functions by reading electrical signals from muscles, became common option for the amputees around the world[28]. Myoelectric prosthesis as with its name, is comprised of electrical signals from the muscles. The sensors fabricated in the prosthetic arm reads the nerve signals allowing the prosthetic arm to function[29]. As the technology was getting modernized with the time, improvement in materials and electronics with miniaturized designs was helping this prosthesis. It also helped with the replacement of compressed gas, which had a bulky design and was not portable, with nickel-cadmium batteries, and made these prostheses more reliable [30]. The compressed gas prosthesis was controlled by a vacuum tube amplifier[31]. As shown in **Figure 7** it can be noticed that comparing myoelectric prosthesis with body-powered prosthesis in **Figure 6**, myoelectric prosthesis gave highly increased amount of comfort and aesthetics, also there was no use of mechanical cables in these prostheses anymore. The electric signals from the muscles became easy to detect as the process is noninvasive and its working is similar to that of normal limb[32]. In this prosthesis, control of the arm varies with the level of patients amputation, as transradial amputees[33] uses preserved wrist flexor and external muscle to control the prosthesis while the transhumeral amputees[34] have to involve biceps and triceps muscle to control the prosthesis[35].

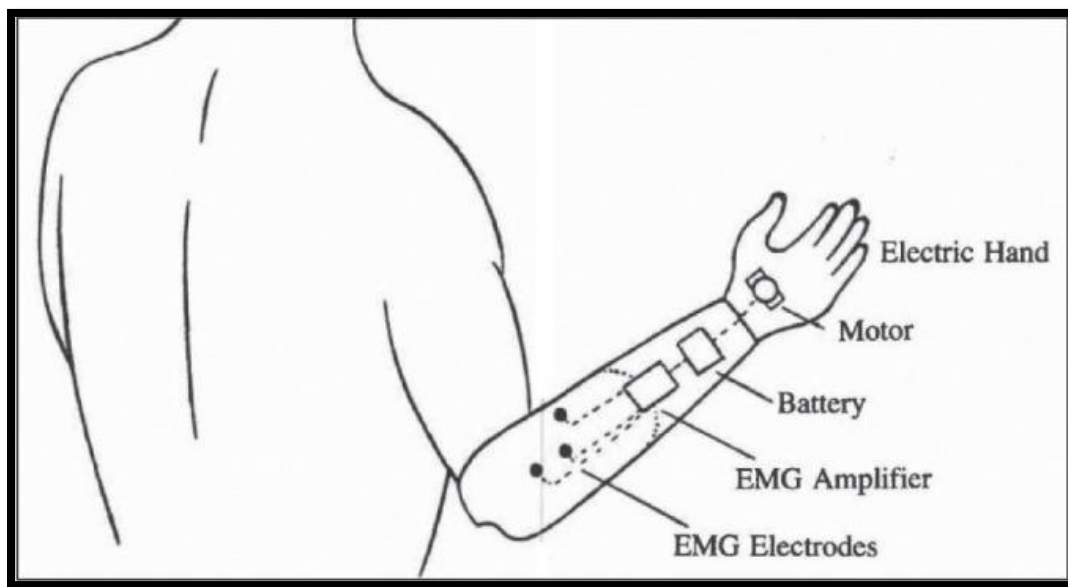


Figure 7: Myoelectric Prosthesis, controlled by Electromyographic(EMG) Signals from remains of muscle at the amputation stump. Reproduced with the permission of the [SAGE Publications](#)[26].

Even though myoelectric prosthesis was appreciated more compared to body-powered prosthesis, it has some issues of its own, like regularly requires recharging battery and its replacement[36], requirement of complex movements articulations at the fingers, wrist and elbow movement was not possible, delay between initiation and its mechanical response, and sweating issues which may interfere with EMG signals[35]. All these issues have been in areas of concern to the researchers and scientists, which have made prosthesis to work on more advanced techniques and methods.

In the start of 21st century, a major development in the field of intuitive limb control with the help of using targeted motor reinnervation (TMR) technique was explained by Dr Todd Kuiken and Dr Gregory

Dumanian in the US[37]. The mechanism of TMR works by rerouting the peripheral nerves from the limbs that are amputated with the target muscle, by which, the resultant EMG signals of the target muscle will then convert it into motor input for the missing limb muscle [38] as shown in **Figure 8**.

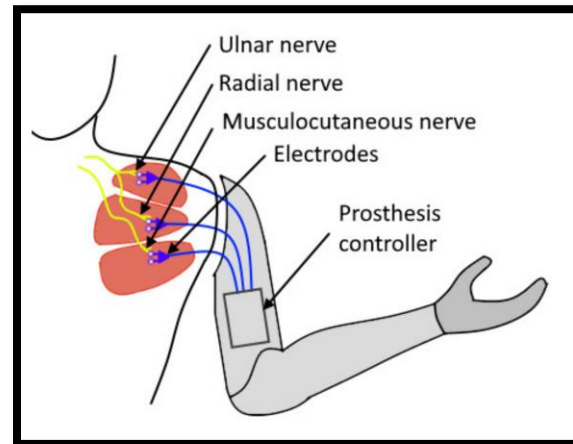


Figure 8: Connection paths and working of targeted motor reinnervation Reprinted with the permission from John Wiley and Sons, Neural Prostheses by Nitish V. Thakor, Joseph L. Betthausen, Luke E. Osborn[39]

With the help and bioengineering technology, combined with surgical techniques and suitable prosthesis can provide a way to overcome deficits faced in old prosthetic techniques[40].

1.3 Types of Nerve Electrodes

Upper limb prosthesis has enhanced the ability to assist the amputees at certain level, but on the other side, it has also caused several problems which have made the prosthetic arm not reliable enough. Some of the problems includes non-availability of sensorial feedback, malfunctioning of prosthetic arm due to uncleanliness of sensors residing inside arm (specifically in myoelectric prosthesis) and limited availability of access in movement of arm[41]. With the passage of time and advancement in bioengineering, a high demand of sensory feedback was noticed which can give an amputee experience same as of real human arm. For this, high quality recording of electric signals and stimulation of nerve is required[42]. And to extract signals from the nerves with low loss of signals, neural electrodes play a vital role. There are various numbers of electrodes that has been introduced in the field of biotechnology in past two decades which consist of different design and their way of use as per the need[43]. These electrodes are discussed in detail under with their pros and cons and compared on the scale of their performance.

For the fabrication of nerve electrodes, it is mandatory that the material used to fabricate avoid any sort of reaction to the nerve which can leave devastating results by using non compatible or non-biocompatible materials. Longevity/persistence is one of the basic requirements by which it means that electrode should be good enough to work for a long time using them in chronic in vivo implantations. Secondly, a higher spatial resolution is required for the electrode. Spatial resolution in electrodes can be defined as the interface of electrodes with the fascicles in the nerves or the area of nerve covered by the electrode. Though implanting several electrodes is unappealing as it might cause irritation to the patient

and risk of sensitivity will increase and to avoid this, an electrode should be fabricated and designed where it can both cover less area and gives best spatial resolution for recoding and stimulation of nerve [44].

1.3.1 Longitudinal Intrafascicular Electrode

Longitudinal Intrafascicular Electrodes (LIFE) are flexible wire electrodes, which are inserted in the nerve until it reaches the fascicle. The wire is insulated apart from the area which will be used for recording signals and that are in contact with nerve fascicle. The electrode is inserted in the nerve using surgical round needle and is aligned parallel to the nerve with fascicle[45]. This electrode is of the size from 25-50 μ m in diameter and the material used in its fabrication of LIFE electrodes is either platinum (Pt) or platinum-Iridium (Pt-Ir). The insulated area of the wire is covered using Teflon or medical-grade silicone, and for acquiring the signals an area from 0.5 to 1.5mm is left uncovered[46][45]. **Figure 9** shows illustration of LIFE electrode in nerve within contact of fascicle.

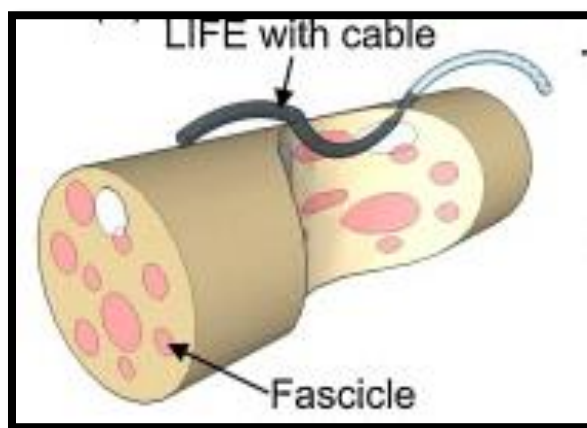


Figure 9: Visual description of LIFE electrode. Reprinted from Biosensors and Bioelectronics, Volume number 26, (Tim Boretius, Jordi Badia, Aran Pascual-Font, Martin Schuettler, Xavier Navarro, Ken Yoshida, Thomas Stieglitz), A transverse Intrafascicular multichannel electrode (TIME) to interface with the peripheral nerve, Pages No.62-69, Copyright (2010), with permission from Elsevier.”[47].

Later, an updated version of LIFE electrode called thin-film LIFE (tfLIFE) was introduced which has specification of more contact sites within electrode allowing more data recording from various groups of fiber and with new substrate that is more flexible [48].

Initially fabricated electrodes were said to be stiff and hard causing the movement of electrode along with the fascicle, and difficulty for electrode to record signal and reduce noise signals. The implantation of LIFE electrode was done on rat on which results were gathered after duration of 3 months [49]. Slight and reversible damages were observed in the nerve. There was a low inflammatory reaction and no sign of nerve degeneration was observed[50]. Despite having 8 individual electrode sites, the electrode was not reliable enough to stimulate or record signals from the specified fascicle if required. Proximity of tfLIFE muscle activation was 2.00 ± 0.89 in an experiment conducted on pig animal[51].

1.3.2 Transverse Intrafascicular Multichannel Electrode

The Transverse Intrafascicular Multichannel Electrode (TIME) is meant to be inserted in the nerve transversely which will provide closer contact with the fibers. Being in contact with several fascicles, it can provide good amount of data to record and analyze. Also due to its transversal insertion, less cross section of tissue will be covered avoiding the error of material mismatch with the tissue of the nerve [47]. **Figure 10** shows schematic diagram of TIME electrode implanted in median nerve.

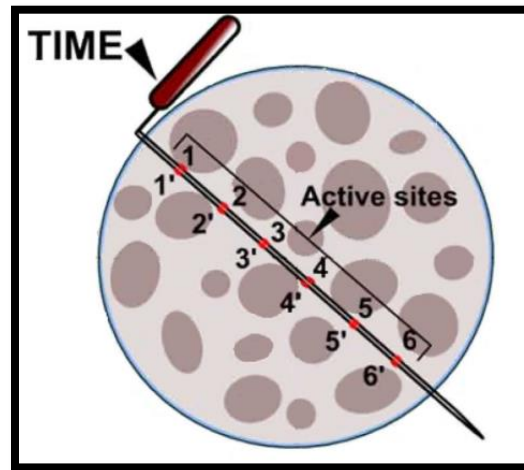


Figure 10: Schematic diagram of a median nerve implanted with TIME electrode. Reprinted with the permission of IEEE Copyright© [2014][51].

These electrodes are developed using platinum material with polyimide substrate as an insulation. The basic electrode is comprised of 10 electrode sites with the gap of 230 μ m in-between each electrode site. There are already researches made on this TIME electrode as they have been used for the sensory stimulation as feedback for controlling the prosthetic arm [52].

To check biocompatibility of TIME electrodes, they were implanted in Gottingen minipigs for the duration of approx. 40 days. As TIME interfaces with multiple fascicles in one implant, the risk of damaging nerves is minimized. Moreover, fibrosis [53] which is thickening and scarring of the tissue was observed but no necrosis [54] that is dead body tissue was observed [55]. Additionally, it was subjected that with the ability of TIME electrode to be in closer contact with the fascicles, it would help in recording and stimulating in required or specific fascicle which was not possible with LIFE electrodes. Here to o, pig animal experiments were conducted which activated 3.68 ± 1.49 selective muscles [51].

1.3.3 Utah Slanted Electrode Array

For Utah Slanted Electrode Array (USEA), an array of electrodes is set in a plane with the spacing of 400 μ m between each electrode. The aim of this electrode is to record and stimulate fascicles present at different distances in a nerve. This is a 10 by 10 electrode array usually made of p-doped silicon substrate with the platinum on the tips of electrode for making it conductive with the silicon nitrate or glass to create insulation. An updated version of USEA is also available where electrodes are aligned with different heights to again record data from different fascicles for better response [56]. **Figure 11** shows comparison between UEA and USEA electrode with differences in them.

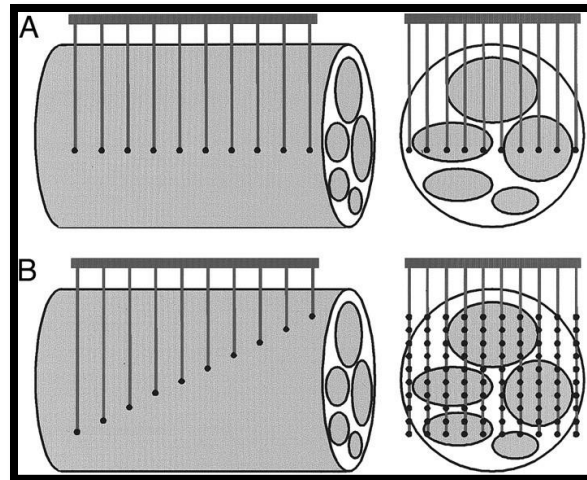


Figure 11: Comparison of the Utah Electrode Array (UEA) and the Utah Slanted Electrode Array (USEA). A) All Electrode with same length. B) Electrodes with variation in length. Reprinted with the permission of Journal of Neurophysiology, (Almut Branner, Richard B. Stein, Richard A. Normann), Volume No. 85, Copyright(2001), Page No.1585-1594 [56].

This is of the most delicate and fragile electrode as the array consists of large number of wires and a high number of electrodes in it which can break during implantation or post-surgery by movement of surrounding fascicles and tissues [57]. It can also cause serious damage to the nerve and will result in decaying of electrode as with the passage of time, recording of the signals will decrease [58]. To avoid the sensitivity and increase the longevity of the electrodes, it was proposed to make the electrode wireless [59]. From different studies different period were noticed till they observe chronic damages, a research conducted in 2004 showed little damage after 7 months [58], in 2014 after 8 weeks of implantation [60]. In another study the inflammatory reaction was observed after a year of implantation [61].

It was anticipated that with good number of electrodes in USEA, various fascicles can be activated. In a study, two humans with amputated arms were subjected with implantation of 96 recording and stimulating USEA electrodes in median [62] and ulnar nerves [63] for duration of 30 days. It was reported that the subjects were comparatively and equally controlling each finger of a virtual robotic hand [64]. In another study of an animal monkey experiment, it was observed that using USEA, 5 to 10 different muscles were activated in the monkey arm [65].

1.3.4 Regenerative Electrodes

Regenerative electrodes working is different from the other electrodes that has been described until now. These electrodes use the method of regeneration which helps to grow nerve around the electrode. Regenerative electrodes have been divided into two different categories as per their requirements, namely sieve electrodes and regenerative multi-electrode arrays. The concept of sieve electrode is that a piece of material having conductive micropores is placed at the center of the nerve that has to be used for signal acquisition. Once it is placed the nerve regenerates itself through the micropores in the material [66]. The other category of multi-electrode arrays in regenerative electrodes work as same methodology of USEA electrodes but in this, the electrode spikes are designed in a hollow tube covering the nerve [67][68]. Figure 12 shows side and front view of regenerative electrode.

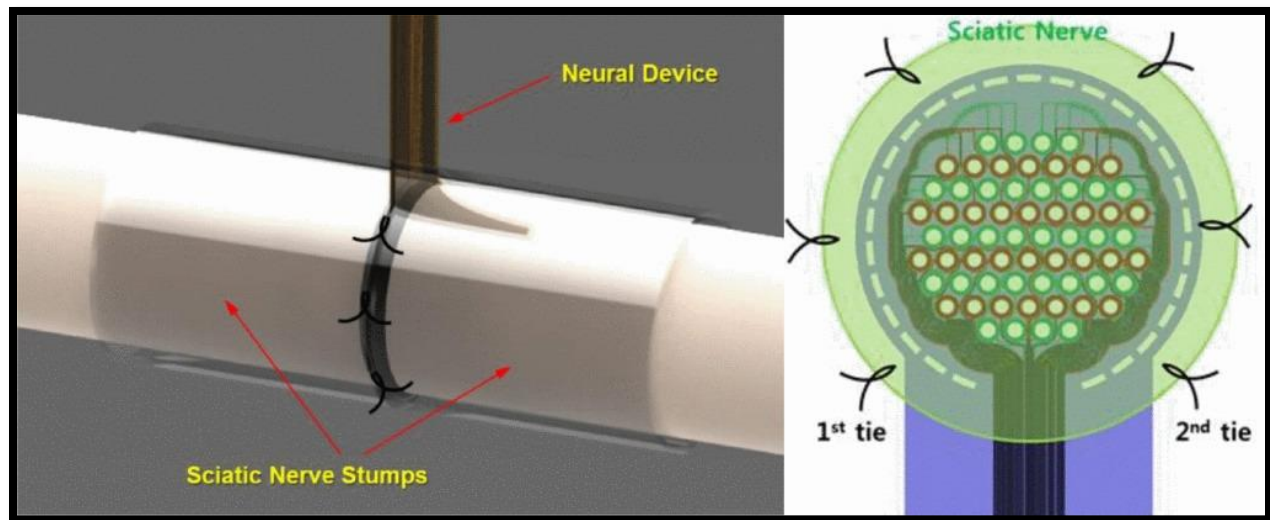


Figure 12: Left side of the image shows the concept of the sieve regenerative electrode while the right side of the image shows the front view of the electrode with 64 channels residing inside. Reprinted with permission of IEEE Copyright© [2016]. [69]

Apart from the other electrodes, before placing the regenerative electrode, the selected nerve must be split down. This is completely different procedure which takes around period of 1 week to a month to regenerate nerves though the electrode [70]. As being one of the most invasive electrodes, complete regeneration of nerve differs in any sort of in vivo experiment. Though in these types of experiments, it has been observed that fascicles in every implant do regenerate through electrode and is capable of recording or stimulating signals up to 3 to 4 months and it was shown that the regenerative electrode array can activate 2.9 ± 0.6 neurons surrounding electrode [71][72][73][74].

1.3.5 Nerve Cuff Electrodes

Nerve cuff electrodes are also known as surface electrodes as they are wrapped around the nerve surface. The principle of cuff electrodes is to acquire and measure the electrical potential of the nerve when there is transmission of signal through the nerve fascicles [44]. There are several types of cuff electrodes like split ring electrode, where a ring type electrode is split from center and is placed around the nerve [75]. The other type is of self-curling or self-wrapping electrodes around the nerve which was designed to avoid fixed sizes of cuff electrodes and helps in safely implantation of electrode [76]. Flat Interface Nerve Electrode also known as FINE were also introduced as a modified form of cuff electrode. They were designed in such a way that when covered around the nerve, the electrode flattens the nerve which gives better accessibility to electrodes to acquire the signals [77]. Figure 13 shows how cuff/surface electrode is rolled over the nerve.

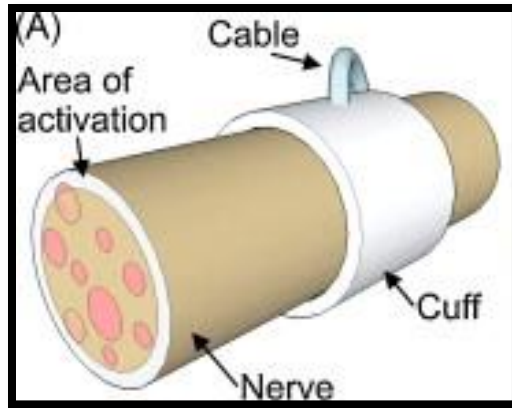


Figure 13: Visual description of LIFE electrode. Reprinted from *Biosensors and Bioelectronics*, Volume number 26, (Tim Boretius, Jordi Badia, Aran Pascual-Font, Martin Schuettler, Xavier Navarro, Ken Yoshida, Thomas Stieglitz), *A transverse Intrafascicular multichannel electrode (TIME) to interface with the peripheral nerve*, Pages No.62-69, Copyright (2010), with permission from Elsevier." [47].

Cuff electrodes provides many advantages over other kind of electrodes like having electrodes on surface and intramuscular level. It reduces the intensity of stimulation required so that the damage ratio of nerve is reduced [78]. Other than that, as electrode is rolled over the nerves, it can acquire stimulation of different axonal fascicles within the nerve. Lastly, cuff electrodes are safer and more reliable than that of interfascicular electrodes which are meant to be placed inside of fascicles and in direct touch with target fiber of nerve [7].

As being covered on the surface of nerve, these electrodes are considered to have best longevity among other implantable electrodes. The results of these electrodes implanted on human peripheral nervous system are said to be good and stable in the study conducted up to 10.4 years [79]. Though being on the surface of nerve, achieving good recording from fascicles inside is difficult, whose solution was given in the modified form i.e., FINE electrodes which by reshaping the nerve can provide better and closer proximity to the fascicles. FINE has minor effects on the nerve functionality due to its working mechanism and pressure applied on nerves through it. Though, another study shows that with the passage of time, nerves have capability to recover and will no longer be disturbed by physiological effects, as the nerve can be reshaped apart from any damage for 3 months of implantation [80][81]. It is reported in another study that using cuff electrodes, researchers were able to stimulate 10 to 15 different precept areas on a phantom hand for the duration of 1 to 2 years. Also, better stability can be carried of using these extra neural electrodes which can help in generating sensory feedback [82].

Each electrode has their own specific points which can be viewed and used at the situation they can be used at. In this section, different electrodes with their experimental data, usage and complications have been discussed. **Table 1** summarizes the types of electrodes reviewed from the literature papers based on their longevity/persistence and spatial resolution.

Table 1: Electrodes comparison between their Longevity/ Persistence and Spatial Resolution.

| Electrode Type | Longevity/Persistence | Spatial Resolution |
|--|---|---|
| LIFE: Inserted in the nerve using surgical round needle and is | Research shows slight and reversable damages has been | Large number of electrodes does not help in recording or stimulation of |

| | | |
|---|---|--|
| aligned parallel to the nerve with fascicle | observed in the nerve. Low inflammatory reaction and no sign of nerve degeneration was observed in 3 months[49]. | nerve. In experiment, muscle activation was limited to 2.00 ± 0.89 [51]. |
| TIME: Inserted in the nerve transversely and is meant to provide closer contact with the fibers. | Research shows fibrosis layer tissue has been observed but no necrosis layer or any inflammatory tissue was observed after period of one month[55]. | As being closer to the nerve fascicles can provide good information for recording and stimulation of nerve. Activated 3.68 ± 1.49 selective muscles in pig animal experiment[51]. |
| USEA: An array of electrodes is set in a plane with the spacing between each electrode and can also be aligned with different heights to again record data from different fascicles for better response. | Different studies showed different results, as some had mild and no inflammatory response after 8 weeks to 7 months, and some had inflammatory reaction after a year[58] [60] [61]. | In a human experiment, 13 different movement on offline decoding and 2 different movements after online decoding were observed[64]. Another study showed 5 to 10 different muscles were activated in the monkey arm[65]. |
| Regenerative: Uses the method of regeneration through conductive micropores which helps to grow nerve around the electrode. | Research shows that it Can take up to one month for regeneration with no surety and maximum recording observed after regeneration was for 3 to 4 months[71][72][73][74]. | Having numerous micropores inside the electrode, it may provide good specificity and high stimulation. Can activate 2.9 ± 0.6 neurons surrounding electrode [74]. |
| Cuff: Surface electrodes which are wrapped around the nerve surface. Measures the electrical potential of the nerve when there is any transmission of signal through the nerve fascicles. | Research shows that cuff electrodes has stable stimulation for long time period on humans reportedly up to 10.4 years[79]. | Using spatial filtering, data from up to 5 fascicles can be recorded and from 10 to 15 different percept areas can be activated[82][83]. |

Reviewing the study on neural electrodes, it can be concluded that the cuff /surface electrodes show higher longevity and good spatial resolution as with in the less covered area, it can record/stimulate nerve better than others. On this basis the fabrication of electrode in this research project is focused on nerve cuff/surface electrode.

2 Materials and Methods

In this thesis, MEMS design, fabrication, and preliminary testing of implantable nerve microelectrodes is described. Gold (Au) is used as the conducting material because of its high conductivity and well-suited biocompatibility. Gold is known for its high strength, and it provides a good resistance to corrosion [84]. Chromium (Cr) is used as an adhesion layer between gold and PDMS because it provides high binding strength with oxygen and can depassivate other material surfaces [85]. PDMS (Polydimethylsiloxane) is used as deposition layer or substrate for gold due to its stretchable electronics applications. It has good substrate properties consisting high tensile modulus of 1.8MPa, physical toughness of 4.77MPa and elongation up to 160%. In addition to this, PDMS is also well known because of its high biocompatibility and nontoxic properties, which makes it feasible to use it as an implantable substrate [86]. PDMS has also wide area usage in the field of sensitive skin, stretchable interconnects and microelectronics for neural interface [87]. As this is a research-based project, different approaches and scientific methods were studied and implemented during the project work, and results from these scientific methods are analyzed, tested, and discussed.

Scientific method can be defined as a process, a process by which different hypotheses are evolved/developed, experimented and by examining the results, it is either accepted or rejected. It is conducted in an organized way where provided scientific theories are carefully observed and tested. A process flow is planned prior to the experiments to define research path and conduct experiments accordingly. The systematic flow of scientific method works in a way that purpose of conducting the work is defined first. After that, a hypothesis is constructed on the base of which experiments are conducted and results are collected. Later, the collected data is analyzed on which conclusions are drawn [88]. Our scientific research methodology is conducted on the basis of Research and Development R&D work where the focus is mostly on developing a product on the needs of the target market. It also focuses on collecting information about the needs and requirements and figuring out feasible ways to improve on an existing product satisfying the identified needs.

Before performing experiments on the fabrication of electrodes various scientific methods were studied in detail and only the methods providing promising results were opted and experimented during the project period. **Figure 14** illustrates the process flow of how this research work has been conducted. The aim of this work is to use MEMS technology to fabricate implantable nerve electrodes with low complexity and provide affordability for using in neuroprosthesis. Emphasis has been on cuff type electrodes because of its wide area advantages discussed in **section 1.3.5**. So, while studying different literature ease of fabrication, and cuff type electrode were of main concern. Keeping these parameters in mind, three research papers were opted due to their feasible fabrication techniques. This thesis discusses (three) different methods for the fabrication of implantable electrodes. First trial method is based on literature study from a research paper and it was implemented with some variations in it [89]. Standard microfabrication processes of photolithography have been applied for designing electrodes.

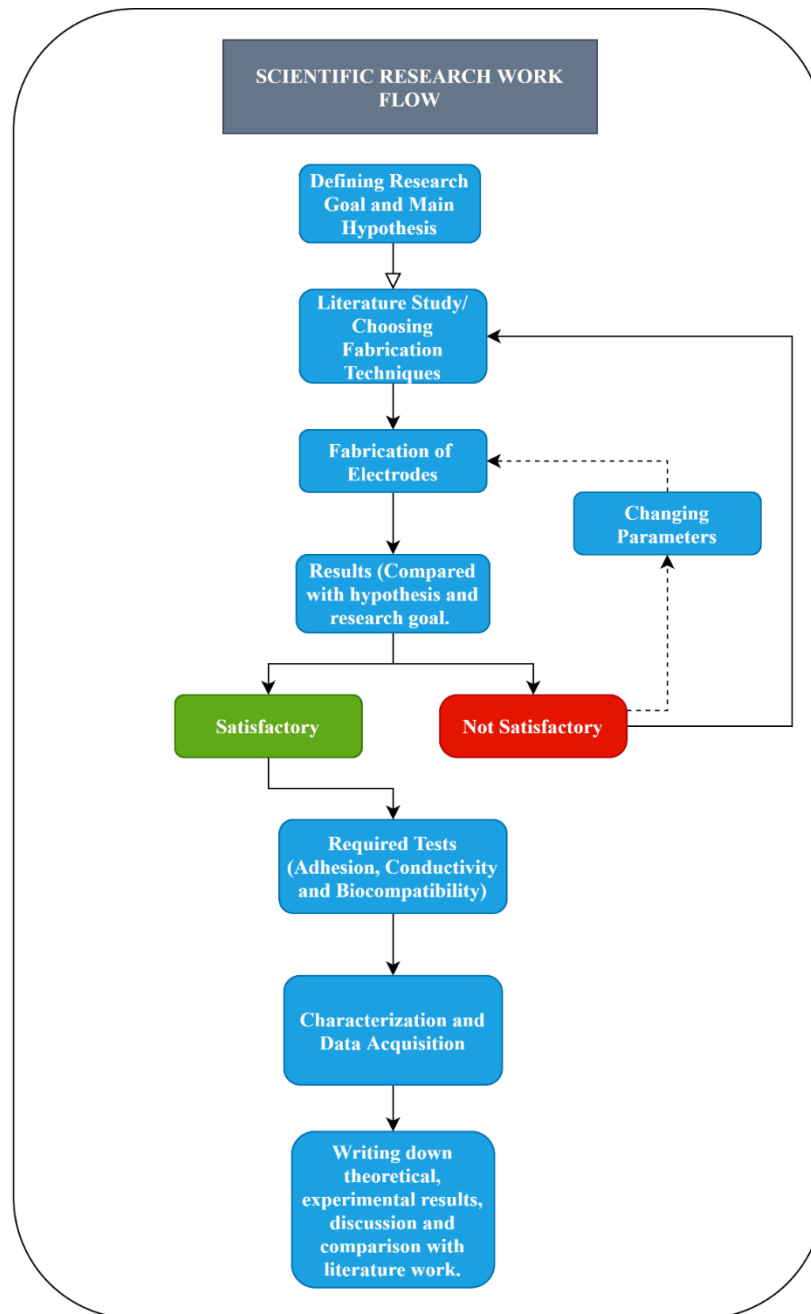


Figure 14: Research Project Work flowchart

Whereas, the second fabrication technique is a bit different than the first method[90]. It was carried out in three different stages, fabrication was divided into various sections and merged in the last stage. For this fabrication method, an additional functionalized layer (3- mercaptopropyl) trimethoxysilane (MPTMS) for enhancing the bond between PDMS and gold was introduced. The fabrication technique here has been divided into three parts for carrying out the whole process.

The third method is based on an hypothesis that has be experimented by undergoing different research papers[89][91]. The process flow has been planned in a bit opposite to what these research papers have experimented. Where, instead of depositing gold on PDMS substate, PDMS has been deposited on etched and patterned gold wafer and was peeled off after curing of PDMS.

All these techniques are described and discussed accordingly in their sections below so that they can be followed up with each other respectively.

Experiments for the fabrication of electrodes were conducted in MEMS labs at the Department of Microsystems, University of South-Eastern Norway [92]. As the fabrication of electrodes has to be in small feature size and clean, all the experiments were conducted in cleanroom of ISO Class 7 and Biochemistry lab. Fabrication approach used in this project consist of layering the patterned gold on PDMS substrate. Oxygen Plasma Treatment was used and applied by Plasma Cleaner PPS(3032) to activate OH- groups on PDMS which enhances the bond between Cr and PDMS. The conducting layer of Au and adhesion layer of Cr was deposited by using Thermal Evaporator Moorfield MiniLab chamber T25M(4030). To pattern the gold electrodes, Mask Aligner MA56 from Karl Suss was used as of its ability to generate small features reliably [89]. Wet Ion Etching was used to build orifices on the material followed by removal of photoresist. The details regarding thicknesses, amount of chemicals used, and types of materials used are described in their respective sections below.

The electrodes that are meant to be fabricated in this master project are predesigned. Two different types of electrodes were designed where each of them has their own features. These designs were made for different animal experiments. The electrode in **Figure 15** is updated as compared to **Figure 16**, it has a reference contact pad and four nerve contact pads. The contact pads are $1000\mu\text{m}$ wide and $4000\mu\text{m}$ long while conducting path to the bottom connector is $\sim 57500\mu\text{m}$ long. Reference electrode is there for measuring potential difference between the signals generated by nerves. While electrode in **Figure 16** is consisted of basic design having only four contact pads with no reference electrode. Here, the width of contact pads is $500\mu\text{m}$, and length of contact pads are $10000\mu\text{m}$ while conducting path to connectors are of $100\mu\text{m}$ width and $12500\mu\text{m}$ long.

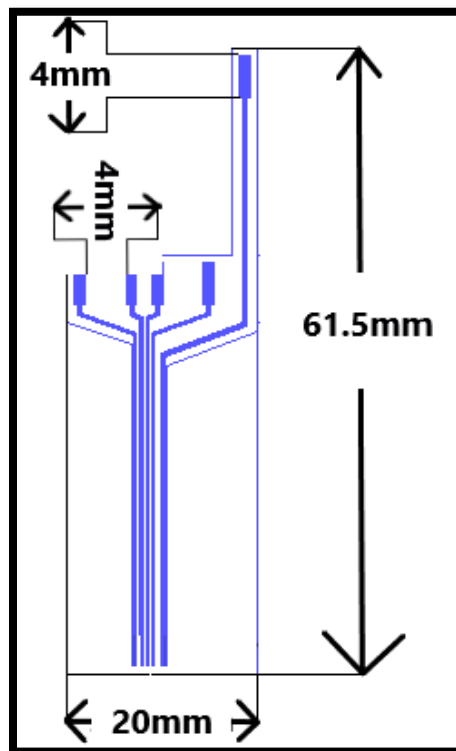


Figure 15: Electrode Design for Animal Test.

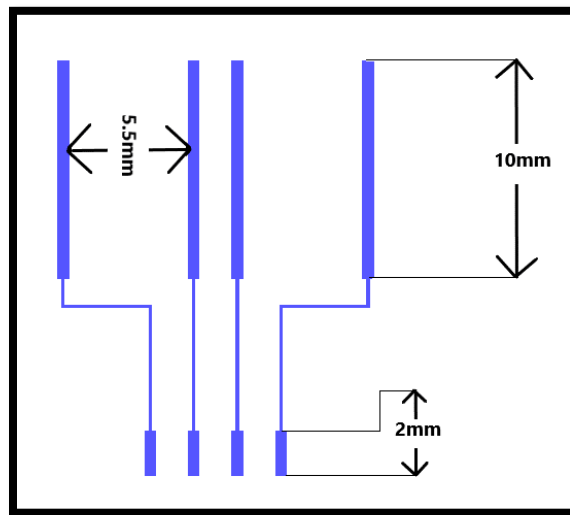


Figure 16: Electrode Design for Animal Test.

2.1 Fabrication Process with Chromium as Adhesion Promoter

In this experiment, PDMS substrate is spin deposited on Silicon(Si) wafer and then cured in oven. After curing, the PDMS substrate on Si wafer is placed in thermal evaporation chamber for the deposition of chromium and gold. The materials (chromium and gold) are placed inside the chamber on a small crucible and are melted by applying current to the crucible and lowering the pressure of chamber which was followed by first chromium deposition and then gold deposition till the desired thickness is achieved. Before patterning of gold electrodes, positive photoresist is spun on the wafer and then using predesigned mask, electrodes are patterned on gold which are later developed using specific chemicals. In the last step, wet etching technique is used to etch gold and is followed by removal of photoresist. Electrodes are then carefully diced from the Si wafer using surgical blade and are processed ahead for testing. [Figure 17](#) shows step wise fabrication technique .

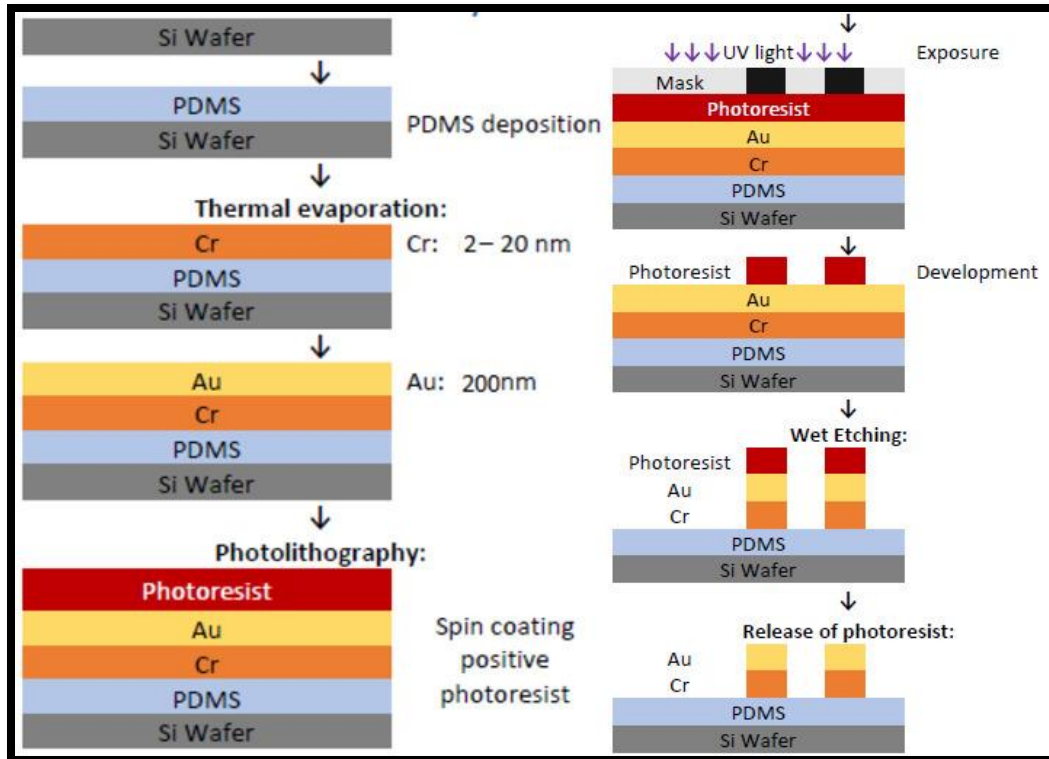


Figure 17: Fabrication Process Description[93]

2.1.1 Preparation and Deposition of PDMS Substrate

For preparing elastomer substrate, PDMS (Polydimethylsiloxane) a biocompatible material is used which is also utilized in implantation within the body because of its nontoxic properties[94]. (Sylgard 184 ©, Dow Corning) at 10:1 PDMS prepolymer is mixed to curing agent ratio. This mixture was spun at 2500 RPM for 4 minutes in Speed Mixer DAC followed by vacuuming the mixture for ~10 minutes to get rid of air bubbles. The mixture was then left for ~20 minutes at room temperature. This mixing process of PDMS was applied in all the experiments.

For the deposition of PDMS substrate, 4-inch (100mm) Si wafers with 525um thickness were used. The wafers were treated with sequential rinsing with Acetone, Isopropanol and deionized (DI) water and soft baked for 20 minutes on hot plate before deposition of PDMS Substrate. Wafer was then gently placed on Spinner 2 AB Plast Spin 150 and PDMS mixture was poured in center of the wafer to be evenly spread. The spinner was set on 350 RPM for 60 seconds. The RPM of spinner and time were kept constants for all the experiments. The wafer was then carefully removed from spinner and placed in oven binder for ~2 hours at 60°C for curing the PDMS.

2.1.2 Plasma Treatment

After the curing of PDMS on Si wafer and before the deposition of Chromium and Gold, PDMS surface was activated with Oxygen layer. Plasma Cleaner PPS(3032) was used to activate OH- layer on surface of PDMS. This was done to give support to Cr to adhere with PDMS and Cr has good adhesion with oxides. To learn about how plasma treatment affects the PDMS, different parameters were set including change in oxygen doze duration, and different thickness of material. **Table 2** discusses the parameters that were applied to the PDMS.

2.1.3 Deposition, Patterning and Etching of metal layer.

Thermal Evaporator Moorfield MiniLab chamber T25M(4030) was used for the deposition of chromium and gold. Thermal Evaporation was preferred as for the deposition of materials on wafer because of its high purity due to low pressures, easy to use/control, and ease in availability. To provide good adhesion between gold and PDMS substrate, a chromium layer from 2-20nm was deposited on PDMS substrate followed by 200nm of gold. As both materials have different properties, their deposition rate must be set carefully. Deposition rate of chromium was set to $\sim 0.05\text{-}0.1\text{A/s}$ while for gold it was $\sim 0.3\text{-}0.4\text{A/s}$. Rotation of PDMS wafer was set to 30RPM during the whole deposition process as the thickness of material should be same at each point of PDMS substrate.

Conventional method of photolithography and etching was applied on the metal deposited wafer to pattern the electrodes. Before exposing wafer to the UV light for patterning of electrodes, positive photoresist 1813 was spun on wafer using spinner followed by exposure of Mask Aligner-Karl Suss MA56 covering it with photomask. Exposure time of the UV light was set to 60 seconds. To develop electrode patterns on Au layer, the wafer was dipped in a developer solution. Etching was done by washing the wafer with GE6 solution (KI, I_2 in H_2O) and again washed with Isopropanol, Acetone and DI water. Lastly, to remove photoresist, the template wafer was washed with Isopropanol, Acetone and DI water.

2.1.4 Peeling off PDMS substrate from Silicon Wafer

Once the Au has been properly etched and photoresist is removed from it, the electrodes are ready to be diced and peel off from the silicon wafer. Using surgical blade, marks have been made around the electrode and later, using tweezers, the electrode is lifted from one edge of the electrode and then manually peeled off from the Silicon wafer. [Figure 18](#) shows the image of electrode peeled off from the silicon wafer.

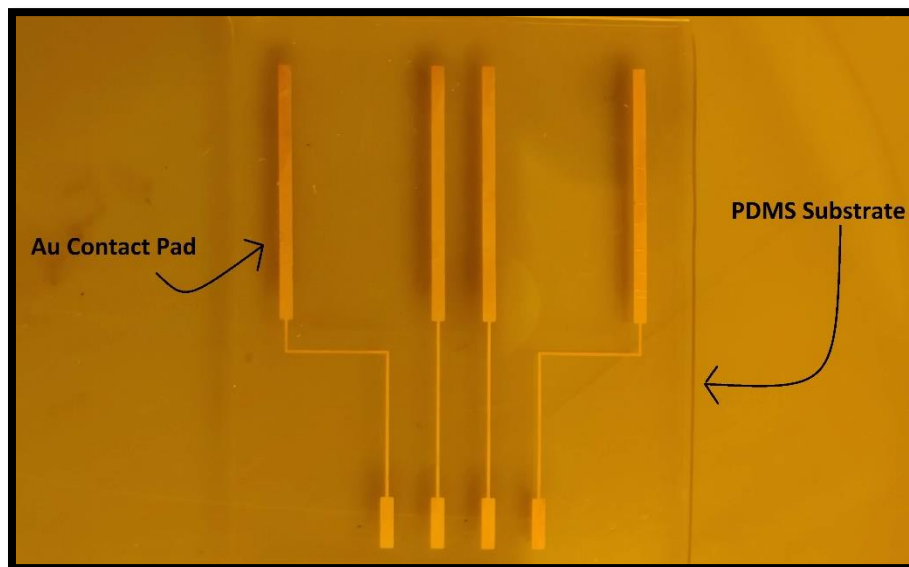


Figure 18: Electrode 1 peeled off from Si wafer.

2.1.5 Electrode Rolling Tests

This test is performed to replicate the placing of cuff electrode around the nerve. Due to the shape of nerve, the electrode has to cover the surface of nerve by rolling over. For this, the electrodes are placed

on a round glass tube of ~6.3mm in diameter and rolled around which is almost near to major median nerve diameter of 5.95mm[95]. The tests were repeated several times, checking both the adhesion and conductivity of the electrodes before and after the rolling. **Figure 19** shows illustration of electrode rolled over the glass tube.

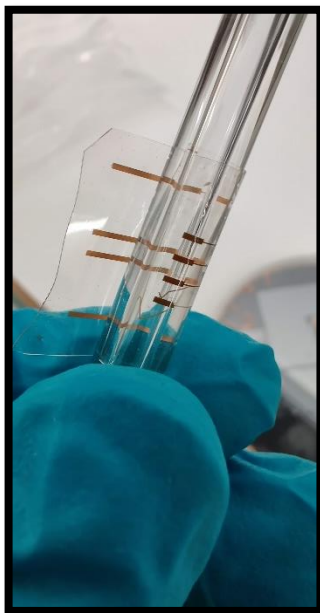


Figure 19: Electrode rolled over glass rod.

2.1.6 Adhesion and Conductivity Test

Following the rolling tests, the electrodes were ready for adhesion and conductivity measurements. Adhesion tests were performed using scotch tape test [96]. A piece of tape was gently placed and pressed on selected electrode. Then the tape was smoothly taken off manually at an angle of approx. 90 degrees from the substrate. Conductivity was measured by measuring resistivity between the two end points on each electrode conductor. For this a multimeter (FLIR MODEL DM284) was used.

2.2 Fabrication Process with (3- mercaptopropyl) trimethoxy silane (MPTMS) as Adhesion Promoter

The second method has used another technique to create good adherence of gold and PDMS. A new saline named (3- mercaptopropyl) trimethoxy silane (MPTMS) was now used instead of an adhesion promoter material like chromium to have good and strong adhesion between gold and PDMS substrate. This fabrication is divided into three stages. In the first stage, PDMS substrate was deposited on a silicon wafer and was cured in oven until it stabilizes. Before treating PDMS substrate with the saline, it was placed in plasma cleaner for a specific time to activate OH- bonds on surface of PDMS. Following that, the PDMS substrate was immersed into the (MPTMS) saline and left until they have SH-Si-O bonds. After a given period, the PDMS substrate is dried well in vacuum chamber and then the substrate was peeled off from Si wafer. **Figure 20** shows process step of activating MPTMS layer on PDMS.

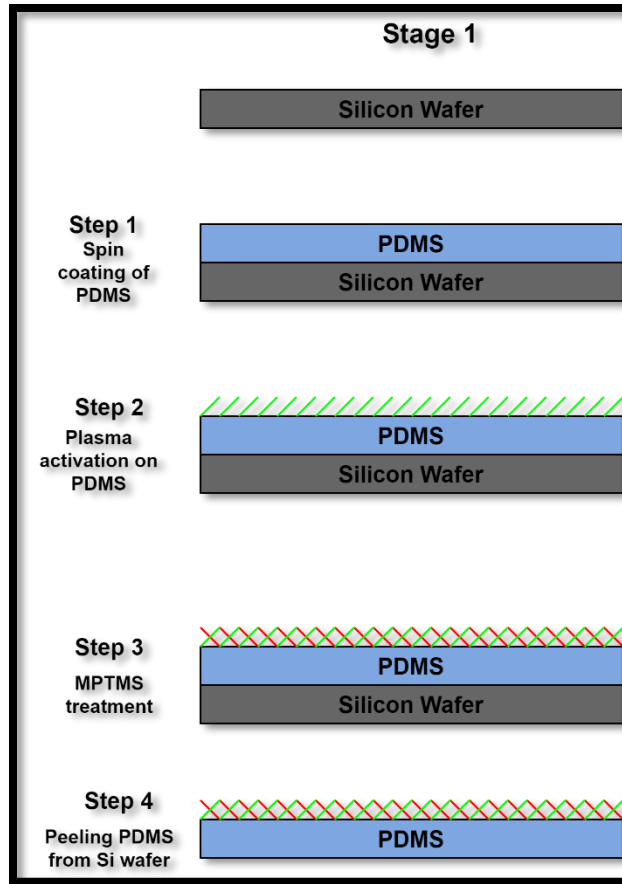


Figure 20: Activating MPTMS layer on PDMS.

The second stage consist of developing patterned Au electrodes on silicon Dioxide wafer as shown in [Figure 21](#). The silicon Dioxide wafer of 4-inch (100mm) with 525um thickness was first deposited with Au film through thermal evaporation and then standard photolithography was applied. The patterned Au wafer was etched using wet ion etching process.

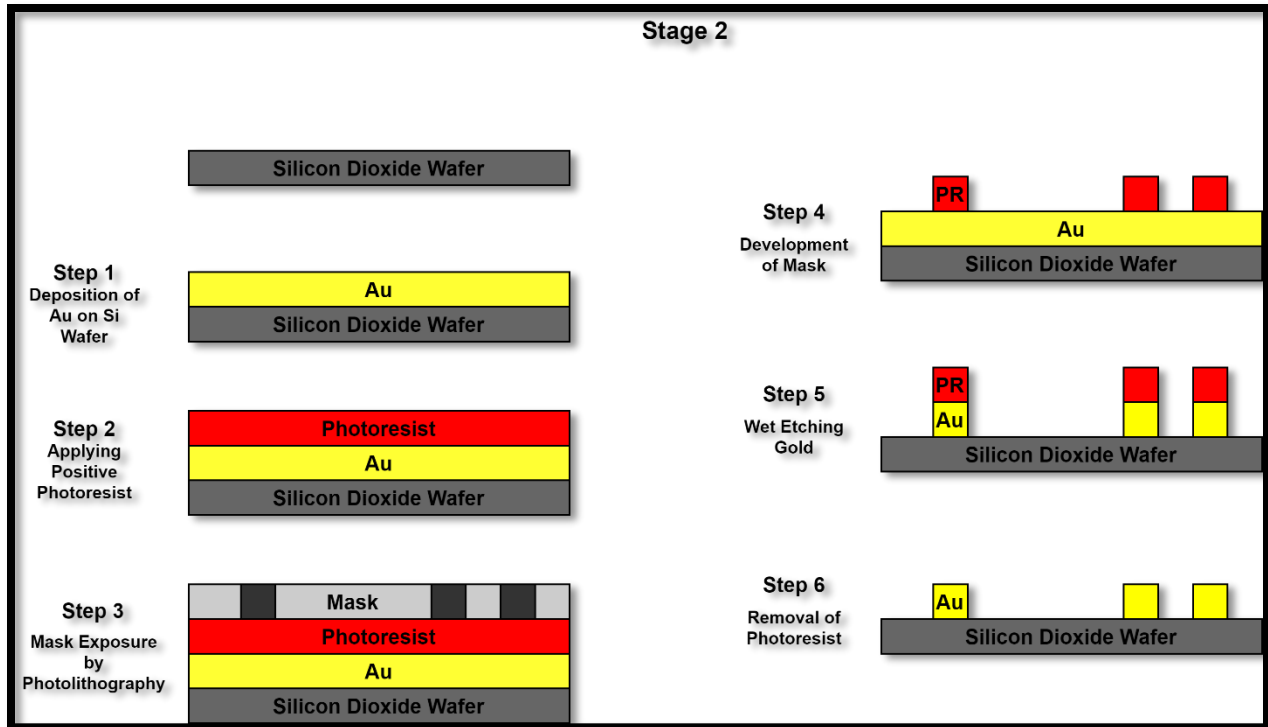


Figure 21: Au deposition and etching of electrodes on Si wafer.

In the last stage, the diced PDMS substrate is evenly bonded with Au patterned wafer and left until it achieves strong bond. The diced PDMS substrate is peeled/lifted off from patterned gold electrodes wafer as illustrated in [Figure 22](#).

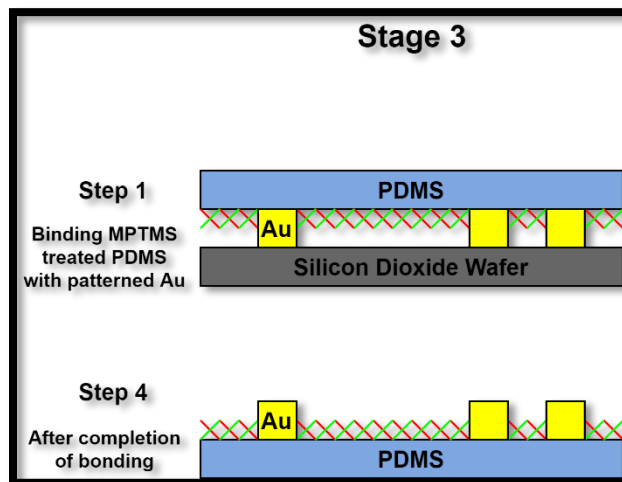


Figure 22: Bonding and peeling off MPTMS treated PDMS with Au.

2.2.1 Preparation of (3- mercaptopropyl)trimethoxy silane (MPTMS)

MPTMS saline is based on the mixture of two chemicals i.e., ethanol and MPTMS saline itself. These two chemicals are mixed in specific amount (92 μ l of MPTMS is diluted in 20 μ l of Ethanol) to achieve the required amount of saline [97]. It works as Self-assembled monolayer (SAM) and due to its different capabilities of two terminal groups, it has versatile usage. It works in such a way that the three methoxy(-OCH₃) group cohere with the oxide surface of plasma activated OH- layer, and the thiol(-SH) functional group attach to the metals i.e. Au in our case [98].

2.2.2 Treatment of PDMS Substrate in MPTMS Saline

For the treatment of MPTMS with PDMS, protocols followed in [section 2.1.1](#), and [section 2.1.2](#) were used to deposit PDMS on Si wafer and activation of OH-layer on surface of PDMS. Here again, different plasma duration was applied to the PDMS substrate before it was immersed in the Saline. To form the MPTMS solution, ethanol of 20ml was mixed with 92 μ l of MPTMS in a petri dish and plasma activated PDMS substrate was immersed in the MPTMS saline and left for duration of 60 minutes. The petri dish was placed on Chemical Shaker (GFL 3006) at 100RPM for 60 minutes so the PDMS surface can be evenly treated with MPTMS saline. Later, the PDMS substrate was dried in vacuum chamber for a period of 15 minutes to dry liquid present on surface. PDMS substrate was then peeled off from Si wafer using surgical blade before bonding it with deposited patterned Au wafer. [Figure 23](#) shows PDMS immersed in MPTMS saline on chemical shaker.



Figure 23: PDMS deposited wafer immersed in MPTMS on chemical shaker.

2.2.3 Deposition and Etching of Gold on Si Wafer

In parallel to [section 2.2.1](#) and [2.2.2](#), a silicon dioxide wafer was deposited with 200nm of gold film using Thermal Evaporator Moorfield MiniLab chamber T25M(4030). The electrode patterns were formed on the gold film using standard photolithography procedure and the gold patterns were etched following the

same procedure as discussed in [section 2.1.3](#). The gold wafer is then ready to bond with MPTMS treated PDMS substrate.

2.2.4 Bonding of MPTMS Treated PDMS with Gold

To transfer patterned gold electrodes on PDMS substrate, two different techniques were implied. One was to directly place PDMS substrate(not peeled from wafer) on Au patterned wafer and the other was to peel off PDMS substrate from wafer and then place it on Au patterned wafer. In both cases PDMS was gently placed on top of patterned gold electrodes wafer. An equal light weight covering the area of the whole wafer was placed on top of PDMS substrate to enhance the bonding. Moreover, this bonded wafer was placed on hot plate for 20 minutes at $\sim 60^{\circ}\text{C}$ to improve the bonding. Later, the PDMS substrate was carefully removed from the Si wafer and patterned gold electrodes were transferred to the PDMS substrate. [Figure 24](#) and [Figure 25](#) shows PDMS substrate placed of Au patterned electrodes and its soft baking, respectively.

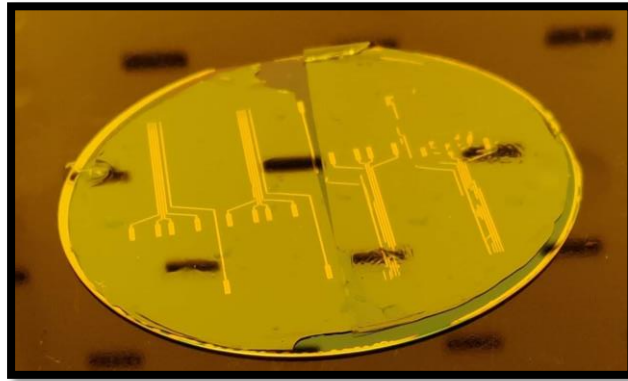


Figure 24:PDMS substrate on Au Patterned on Si wafer.



Figure 25:Soft Baking for enhancing PDMS and Au bonding.

2.3 Fabrication Process with Depositing PDMS Substrate on Patterned Gold Electrodes

The third fabrication method has a simple procedure that has been planned on the hypothesis developed after going through different research papers [89][91]. In the hypothesis, it was proposed that instead of depositing Au on the PDMS substrate, the reverse procedure can also be applied with some proven justifications. The procedure consisted of simple fabrication steps where PDMS is deposited to the patterned gold wafer and is left for curing. Later, the PDMS is peeled off from the silicon dioxide wafer which had complete gold transfer on it and were tested further ahead for conductivity, adhesion, and biocompatibility. The fabrication process flow is shown in the **Figure 26** below and results are discussed in their respective sections.

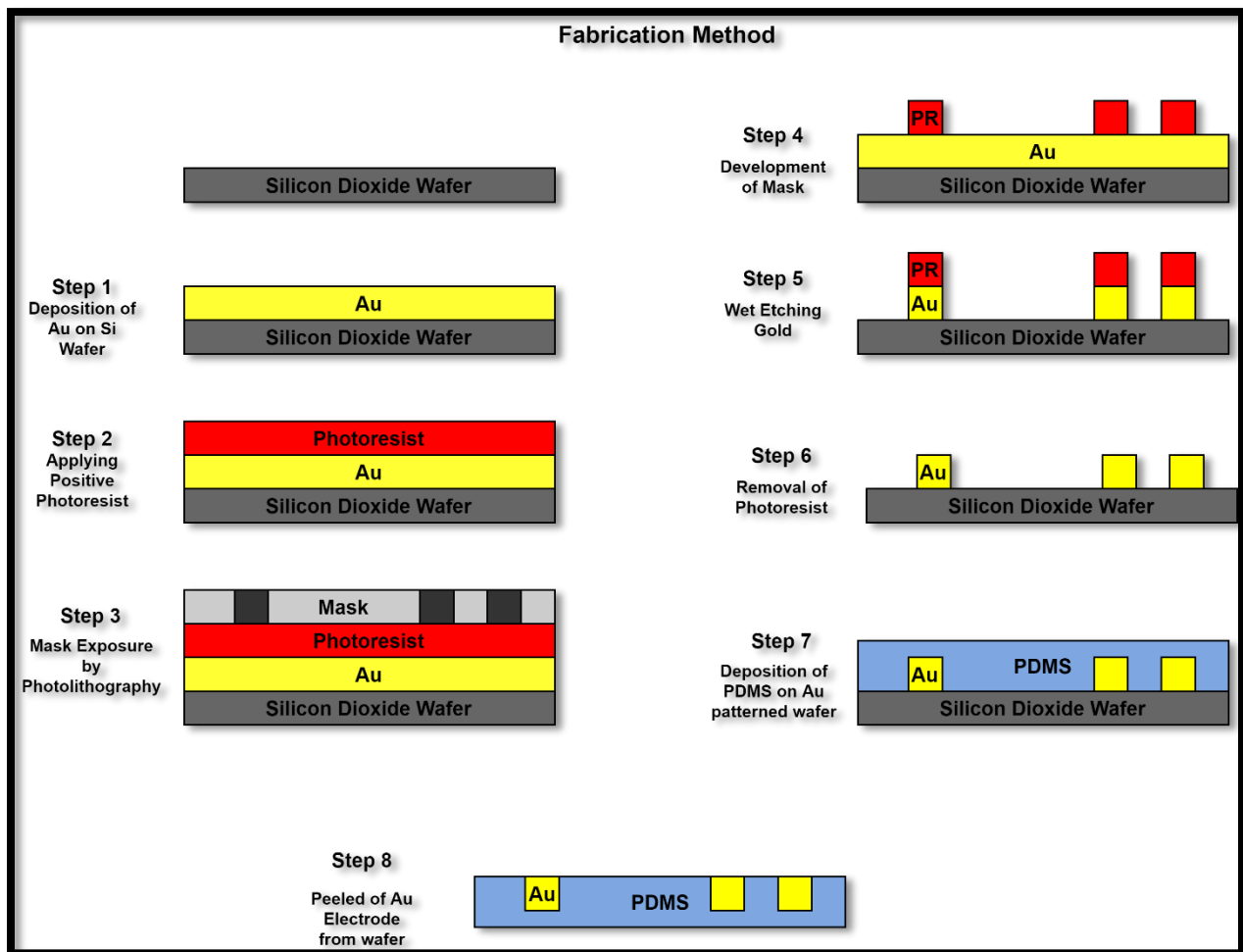


Figure 26: Fabrication Process for the Third Experiment.

Following the [section 2.1.1](#) the PDMS substrate was prepared and was deposited on Silicon Dioxide wafer which was pre deposited with Au and patterned with different Au thicknesses following the [section 2.1.3](#). The deposited PDMS was left for curing in oven at 60C for ~2-2.5 hours. After completion of the curing, the PDMS was left for cooling till it reaches room temperature. Using surgical blade, the PDMS was

carefully diced and using tweezers, it was peeled off from the Silicon Dioxide wafer. Peeling off PDMS was conducted in two different angles. One after dicing the PDMS on wafer was peeled off $\sim 90^\circ$ to the wafer and second was on 135° to the wafer. Electrode was later tested checking its conductivity, adhesion, and biocompatibility. **Figure 27** shows the illustration of patterned gold electrode on PDMS rolled over a plastic tube imitating the nerve.

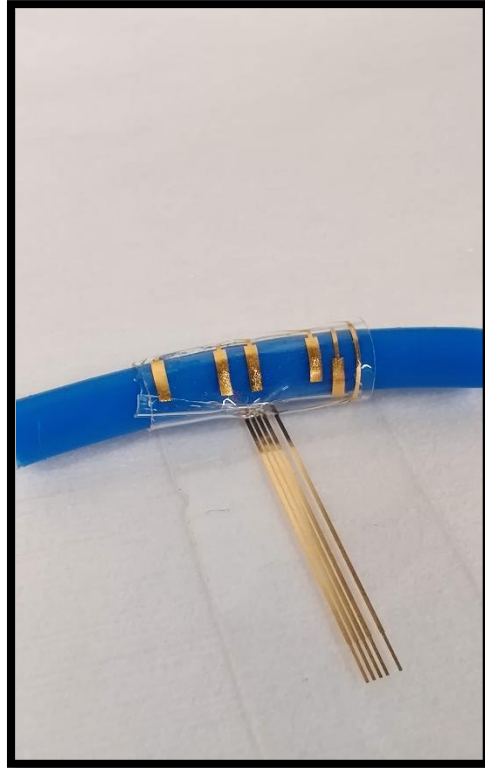


Figure 27: Electrode rolled around plastic tube imitating the nerve.

3 Results

3.1 Fabrication Process with Chromium as Adhesion Promoter

3.1.1 Deposition of Substrate

The deposition method of PDMS substrate on silicon wafer was the same for each experiment, spinning RPM and time was constant which gave approximately same PDMS thickness between 600-800 μm for each wafer. **Figure 28** and **Figure 29** shows the deposition and thickness of PDMS substrate, respectively.

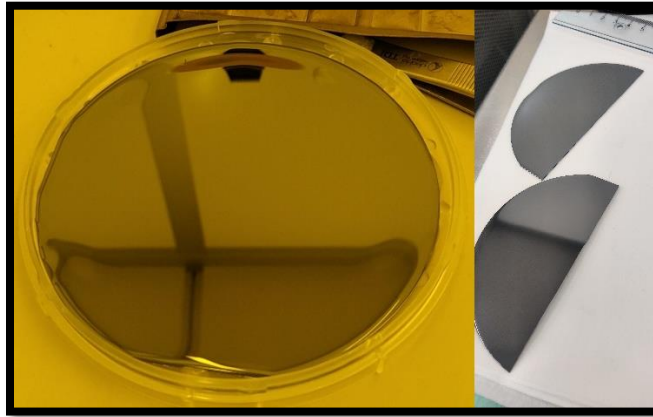


Figure 28: PDMS deposited on Si wafer and its parts.

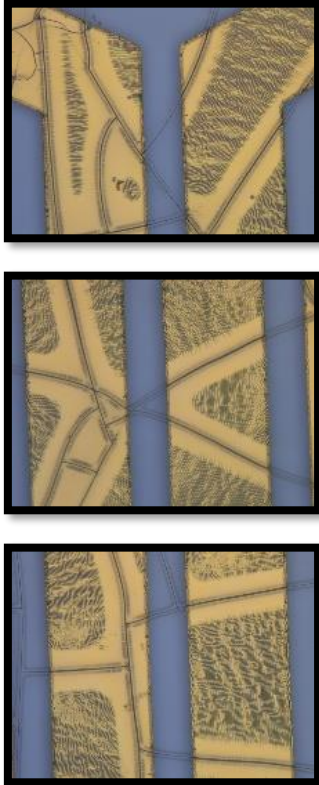



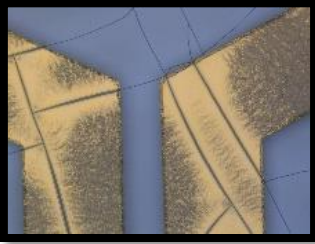
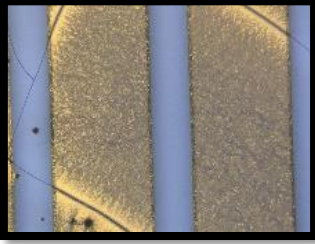
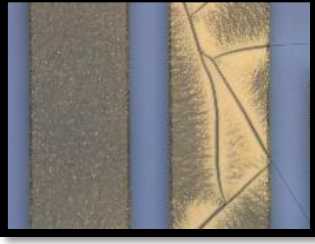


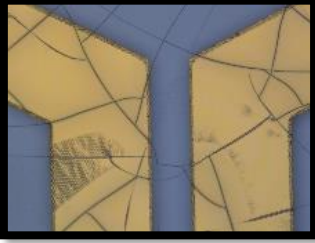


Figure 29: Measurement of PDMS thickness.

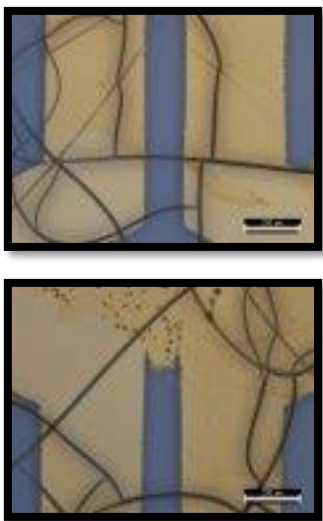
3.1.2 Plasma Treatment

Different parameters were applied to each wafer or part of wafer during its treatment with plasma. Oxygen was used in plasma treatment with different number of doses to each wafer. [Table 2](#) shows results of the applied parameters.

Table 2: Different plasma dozes with different Adhesion thickness

| Parameter # | Cr [nm] | Au [nm] | Plasma Treatment P:300W, O ₂ :200sccm | Results | Pictures |
|-------------|---------|---------|--|---|---|
| 1 | 20 | 200 | 360s | N/A | N/A |
| 2 | 5 | 200 | 180s |  |  |

| | | | | | |
|---|---|-----|------|--|---|
| 3 | 2 | 200 | 180s |    |  |
| 4 | 2 | 200 | 360s |    |  |

| | | | | | |
|---|---|-----|------|--|-----|
| 5 | 2 | 200 | 540s |  | N/A |
|---|---|-----|------|--|-----|

3.1.3 Thin Film Deposition of Au and Cr

Thermal evaporator chamber was used to deposit thin layers of chromium and gold. The wafer was placed upside down in chamber and chromium was set to deposit first as an adhesion layer followed by the conductive Au layer. The results can be seen in [Table 2](#). [Figure 30](#) shows different plasma treated metal depositions.

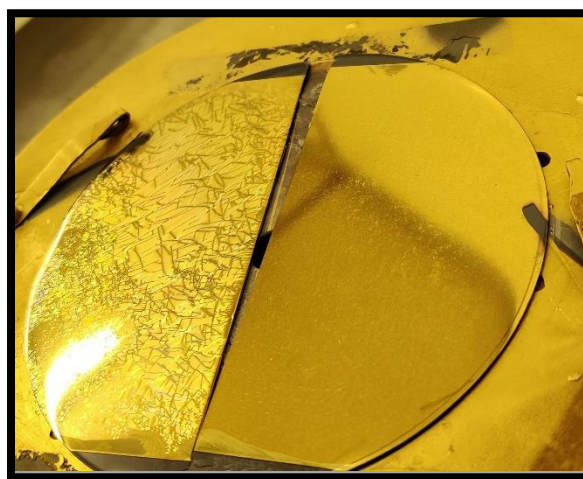


Figure 30: Metal deposited on two different plasma treated PDMS.

3.1.4 Patterning and Etching of Gold Film

The standard method of photolithography was applied to transfer electrode pattern on the substrate and was dipped in developer to enhance the photolithography results. The process was followed by etching gold by dipping the electrodes patterned wafer in gold etchant and was later cleaned and dried with DI water and nitrogen gun, respectively. Result after etching of Au can be seen in [Figure 31](#). After etching,

the thickness of Au was checked through profilometer, and it was noticed that the actual thickness of Au was ~110-120nm.

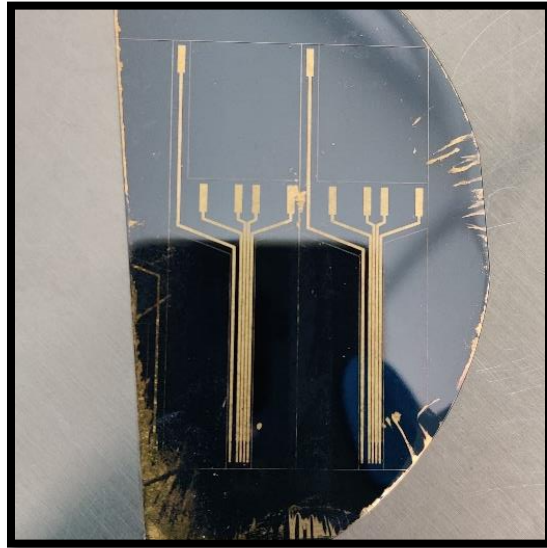


Figure 31: Patterned electrode after Au etching.

3.1.5 Electrode Rolling Test

After dicing electrodes from the Si wafer, the thickness of the electrode was measured, and the fabricated electrode was ~224 μm thick. Later, these electrodes were tested for the rolling tests to know how change in PDMS shape affects patterned Au. The rolling electrodes were later observed under microscope to have better visual of the Au surface. **Figure 32** shows surface morphology after electrode was diced and peeled off from Si wafer and **Table 3** shows results of before and after performing rolling tests.

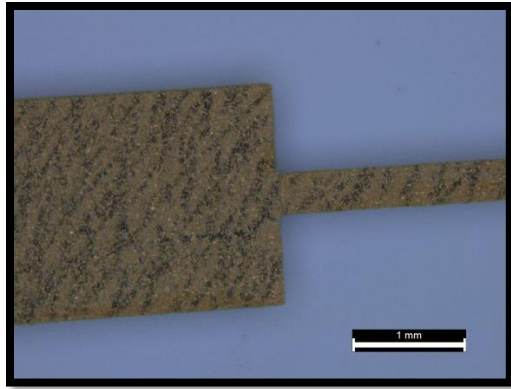


Figure 32: Electrode surface on PDMS after peeling off from Si wafer.

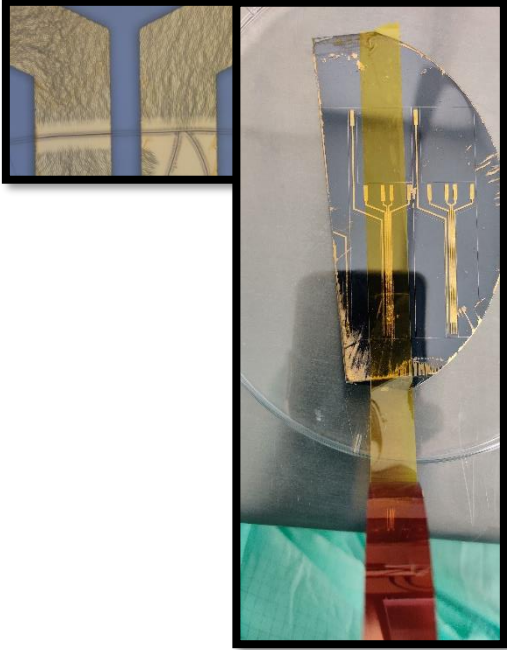
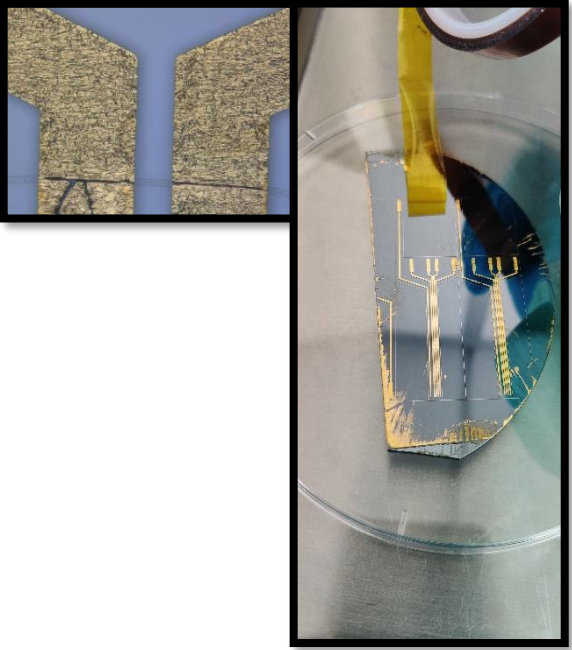
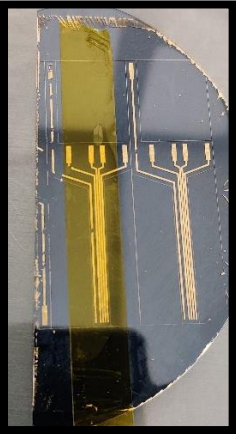

Table 3: Surface Morphology of Electrode before and after Rolling Test.

| Electrode Sample | Before Rolling Test and Peeling from Si Wafer | After Rolling Test |
|------------------|---|--------------------|
| 1 | | |
| 2 | | |

3.1.6 Adhesion Test

Patterned electrodes after etching need to be tested by its adhesion strength and its conductivity. The standard scotch tape and a multimeter were used for the respective testing. **Table 4** shows the results of adhesion before and after of different parameters.

Table 4: Pictures of Electrodes before and after adhesion test

| Parameter | Before Adhesion Test | After Adhesion Test |
|-----------|---|---|
| 2 |  |  |
| 3 |  |  |



3.1.7 Conductivity Test

The conductivity tests were performed by using a multimeter where connection paths resistance was measured. The multimeter showed conductivity at contact pads but not on the conducting path to the end till the connector. Conductivity was also lost due to sharp and edgy probes. **Figure 33**, **Figure 34**, and **Figure 35** shows how probes of multimeter affected the thin gold layers.

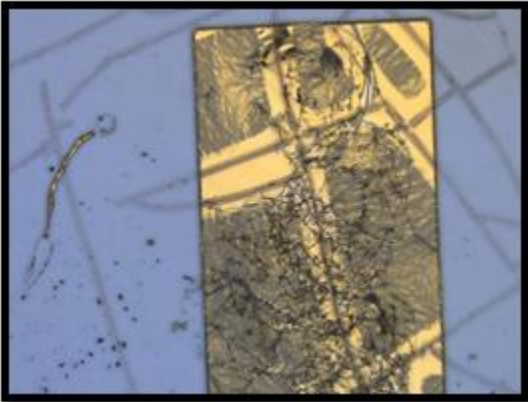


Figure 33: Parameter 2 showing cracks from multimeter probes.

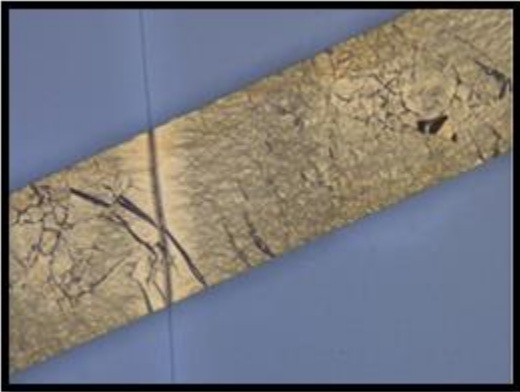


Figure 34: Parameter 3 showing cracks from multimeter probes.

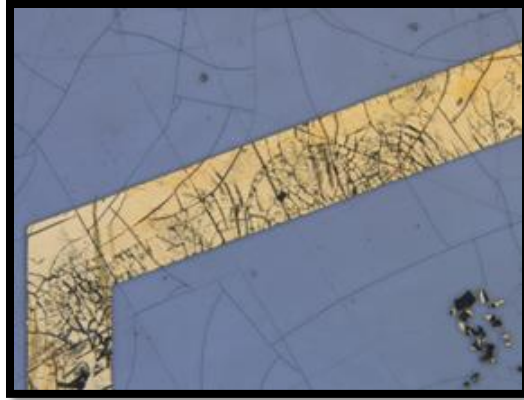


Figure 35: Parameter 4 showing cracks from multimeter probes.

3.2 Fabrication Process with (3-mercaptopropyl) trimethoxy silane (MPTMS) as Adhesion Promoter

3.2.1 Deposition and Etching of Gold Film

A thin film of 200nm of gold was deposited on SiO₂ wafer using thermal evaporation. As there was no adhesion layer used prior to deposition of gold layer, the gold was peeling off easily while cleaning it with isopropanol, acetone, or DI water. Secondly, bubble type structure started appearing on the Au surface after some hours. **Figure 36** shows the Au film right after SiO₂ wafer was taken out from thermal evaporation chamber and **Figure 39** shows bubble structure on wafer after some hours. **Figure 37** shows peeling off Au from the SiO₂ wafer while cleaning and **Figure 38** shows the patterned Au electrodes after etching on SiO₂ wafer. Here too as reported in [section 3.1.4](#), Au thickness was measured with profilometer between ~110-120nm.

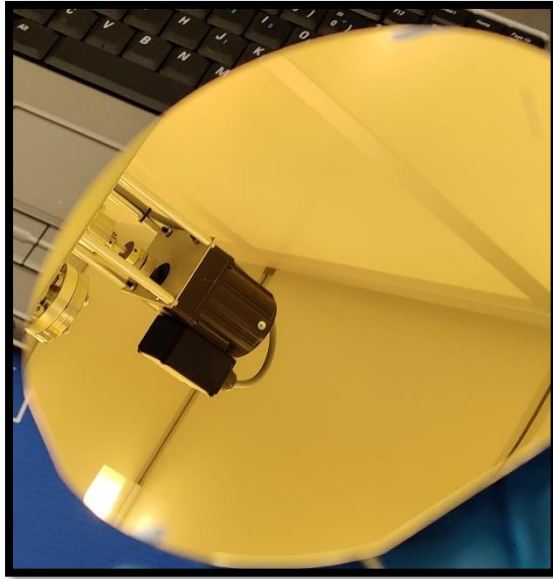


Figure 36: Thin Au Film on Si wafer

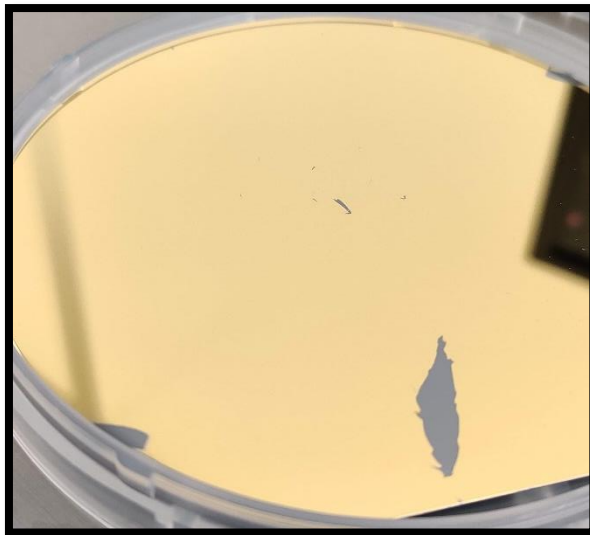


Figure 37: Peeled of Au from Si wafer after rinsing.

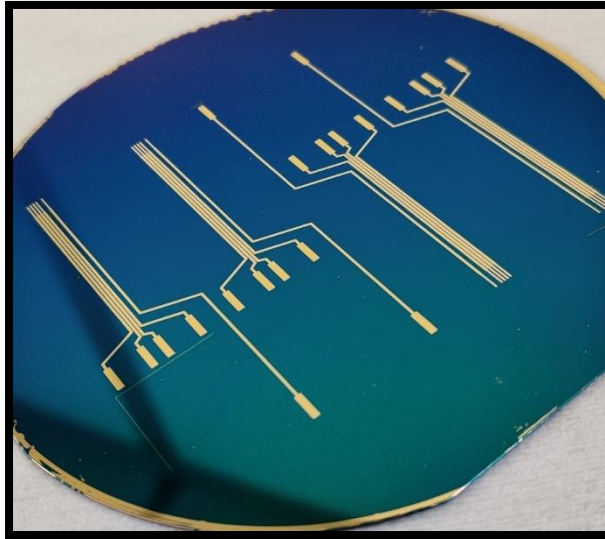


Figure 38: Patterned Au electrodes on Si wafer.



Figure 39: Bubble structure on Au thin film.

3.2.2 Bonding of MPTMS treated PDMS with Gold

PDMS substrate was placed on patterned gold wafer and left on hot plate for ~20 minutes. Heating the wafer worked as enhancing the bond between PDMS and gold. Patterned gold was transferred on PDMS substrate but some of the structure was not transferred. [Figure 40](#) shows the transferred gold from SiO₂ wafer to the MPTMS treated PDMS.

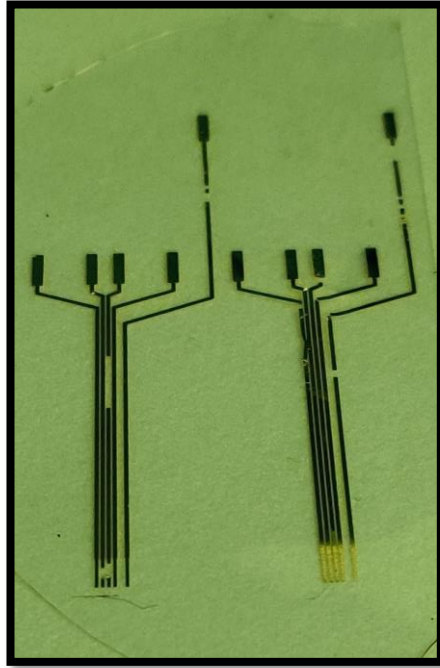
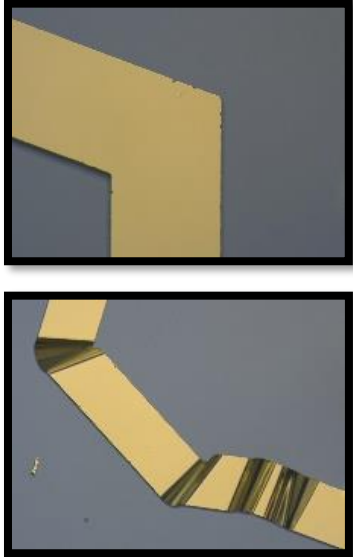
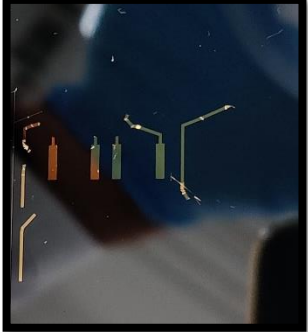
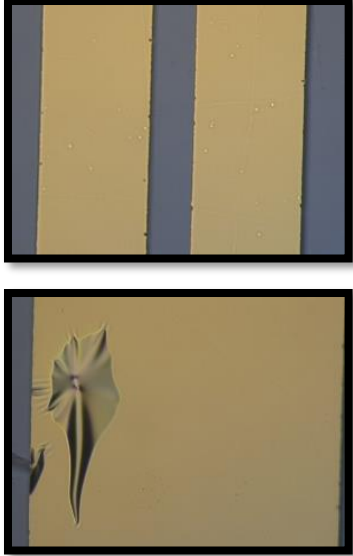



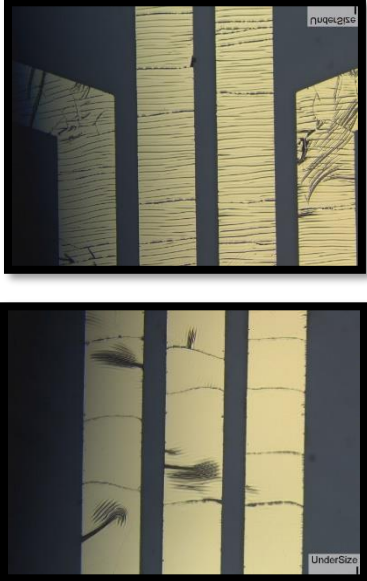
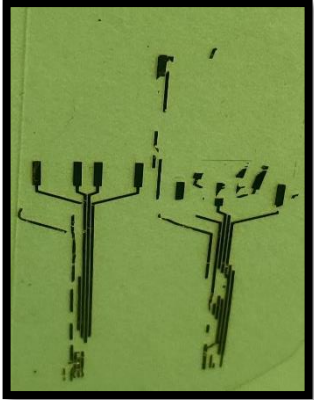
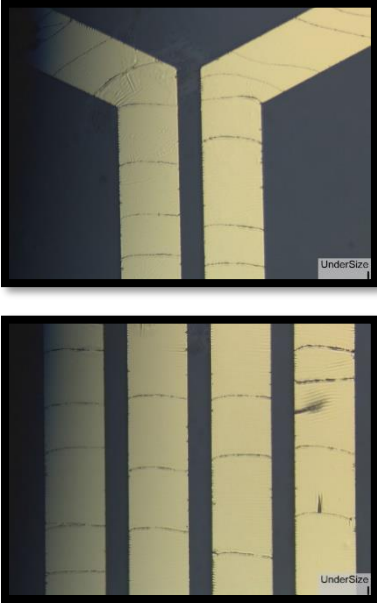
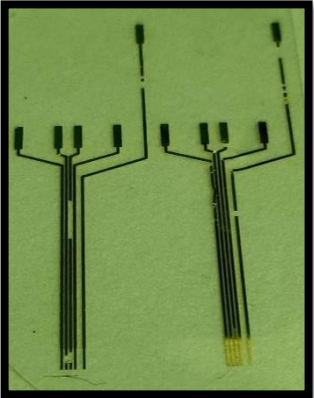

Figure 40: Au electrodes transferred on PDMS Substrate.

3.2.3 Plasma Treatment

Like [section 3.1.2](#), different plasma treatments were experimented to get enough OH- activated layer on PDMS substrate without having cracks on it. Following [Table 5](#) shows different plasma durations and their results.

Table 5: Results of different plasma duration on bonding.

| Parameter | Plasma Doze(min) Power:100W, O ₂ :100sccm | Microscopic Image | Optical Image |
|-----------|--|---|---|
| 1 | 3 |  |  |
| 2 | 5 |  |  |

| | | | |
|---|----|---|--|
| 3 | 7 |  |  |
| 4 | 9 |  |  |
| 5 | 12 |  | N/A |

From the table, it can be noticed that plasma duration for parameter 1 had no cracks in the PDMS surface and the Au transfer onto PDMS was smooth. But complete transfer of electrodes was not achieved. While

for the parameter 2, a good transfer of Au patterns can be noticed with smooth surface as compared to parameter 1. For parameter 3, transfer of Au patterns can be observed but with most of the patches missing as well as the surface of Au patterns is not smooth anymore. Lastly, parameter 4 shows best of Au transfer from the remaining parameters but under microscope, it still shows cracks with some buckling in Au. It is important to mention here that for parameter 1 and 2, PDMS was not peeled off from Si wafer and Au patterns were directly bonded on it. Moreover, for the parameter 3 and 4, PDMS was peeled off from Si wafer before bonding with Au patterns. Parameter 5 was not used for the transfer of Au patterns as after its treatment in plasma for 12 minutes cracks started to appear on PDMS surface.

3.2.4 Conductivity Tests

Conductivity tests were performed on both techniques i.e., one by before peeling of PDMS from Si wafer placing PDMS substrate on Au patterned wafer and second by first peeling off PDMS substrate from Si wafer and then placing it on Au patterned wafer. The probes of multimeter were placed on edges of the electrodes to check full path conductivity or if there is any discontinuation. For the first technique, due to smooth surface of printed Au, the paths were end to end conductive. But, for the second method, mid-range conductivity was observed i.e., the paths were conductive at some points and were nonconductive at the rest of test points. This was occurring due to cracks formed in the Au patterns. Though cracks in the surface of parameter 3 and 4 can be seen from [Table 5](#) the path at some test points were still conductive where Au was buckled.

3.3 Fabrication Process with Depositing PDMS Substrate on Patterned Gold Electrodes

3.3.1 Transfer of Patterned Gold Electrodes

As the PDMS was spun deposited on the patterned Au electrodes, the PDMS molded itself around the thin Au films which helped in better transfer of Au electrodes to the PDMS. Though, thickness of the Au films had an impact on the transfer of Au on the PDMS substrate. There were two different wafers prepared with the Au films of having thickness of 200 and 300nm. [Figure 41](#) and [Figure 42](#) shows transfer patterns of 300nm and 200nm thickness.

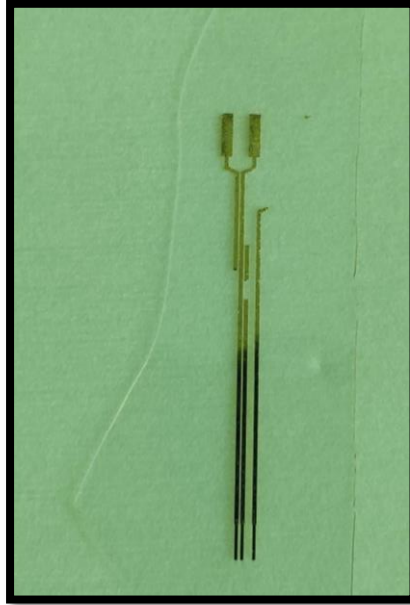


Figure 41: Au transfer on PDMS with 300nm thickness.

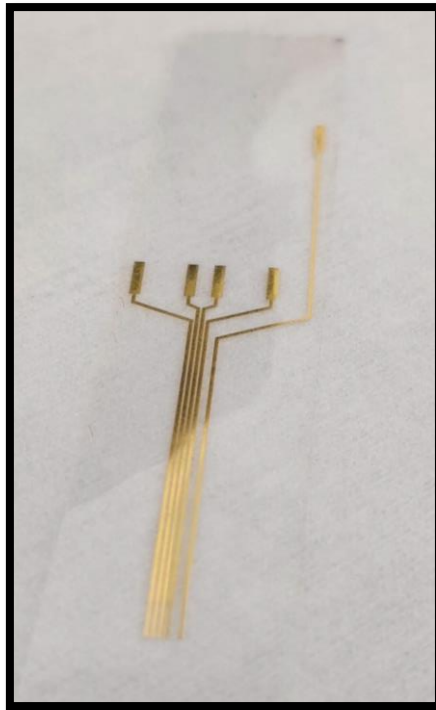
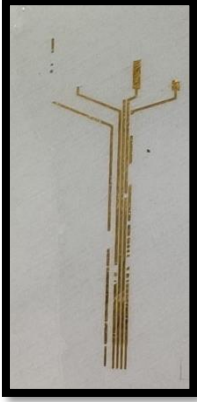
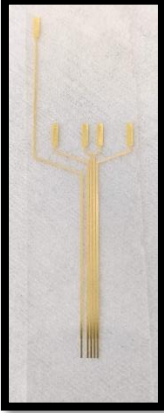
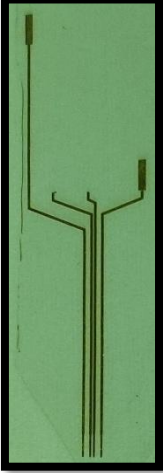
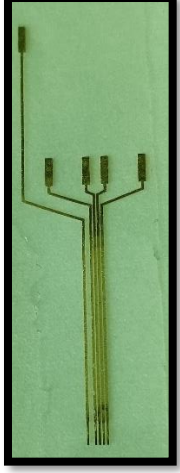


Figure 42: Au transfer on PDMS with 200nm thickness.

Peeling off with two different angles showed different results as well. When PDMS was peeled off with $\sim 90^\circ$ to the wafer, Au patterns did not completely come off with the PDMS while for the $\sim 135^\circ$, Au patterns smoothly and completely came off with the PDMS showing complete transfer of Au electrode on PDMS. [Table 6](#) shows comparison between different angles as how peeling off angles affected the transfer

of Au on the PDMS. The actual measured thickness of Au on 200nm deposited Au was ~115nm and on 300nm deposition through thermal evaporator was ~205nm.

Table 6: Comparison Between Different Peeling Angles.

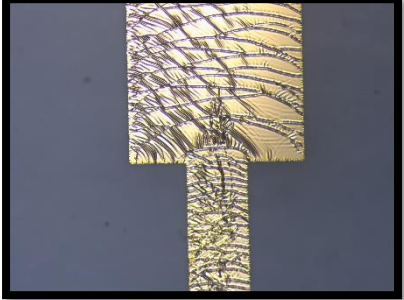
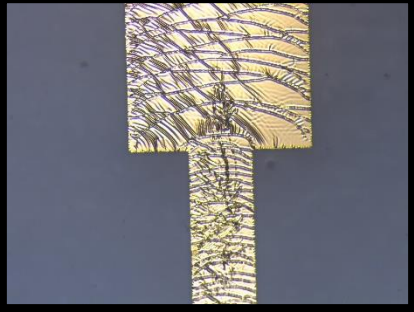
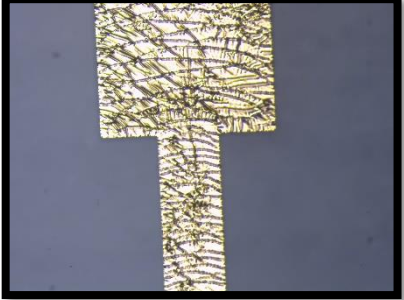
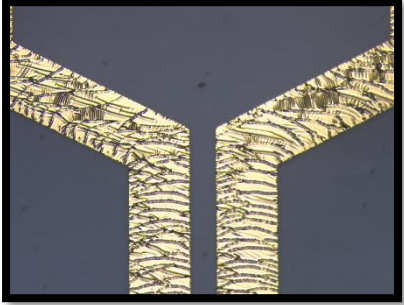
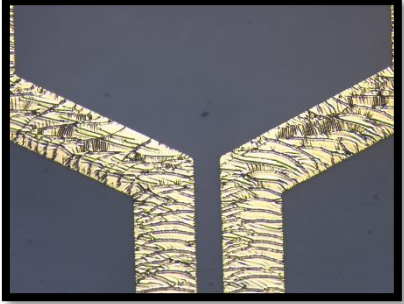
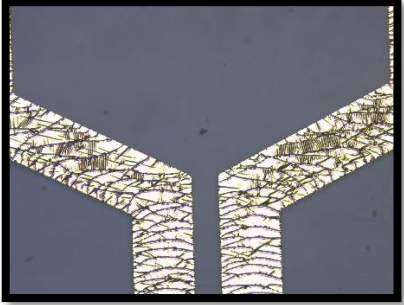
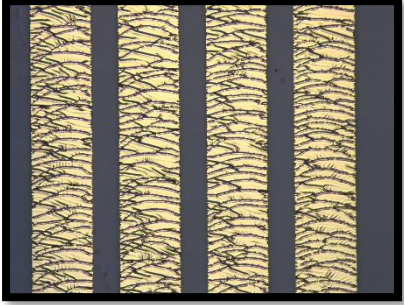


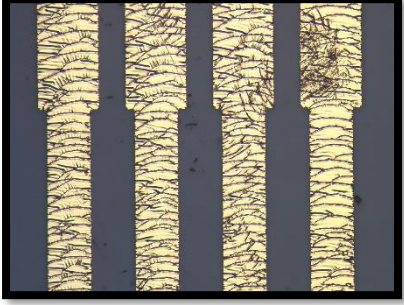
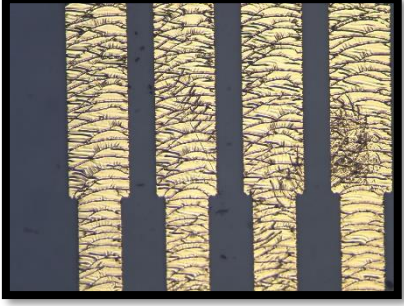
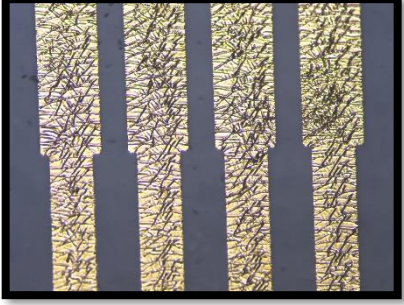
| Au Thickness | 90° Angle Peel off | 135° Angle Peel off |
|--------------|--|--|
| 200nm |  |  |
| 300nm |  |  |

3.3.2 Rolling, Conductivity and Adhesion Tests.

After the successful transfer of the Au with thickness of 200nm, the electrode was proceeded further with the tests to check if the electrode has good conductivity over the electrode, has good adhesion when bought in contact with other materials and if it remains conductive after the electrodes goes though surface changes i.e., rolling of the electrode.

These tests have to be performed systematically so the strength of electrode can be measured and observed stage wise. For that, the first tests performed were the rolling tests following the protocols in described in [section 2.1.5](#). Later, the conductivity of the electrodes was tested which was followed by adhesion tests using the protocol from [section 2.1.6](#). [Table 7](#) shows the microscopic images of the electrodes taken before and after rolling and adhesion tests.

Table 7: Rolling and Adhesion Tests of Electrode for 200nm thickness.

| Before Rolling Test | After Rolling test | After Adhesion Test |
|---|--|---|
|  |  |  |
|  |  |  |
|  |  |  |
|  |  |  |

While results for the 300nm thickness were not that promising, the conductivity was missing at several test points as well as the adhesion was not good enough on it. **Figure 43** and **Figure 44** shows conductive and non-conductive areas of electrode while **Figure 45** shows lack of adhesion on 300nm of Au on PDMS.



Figure 43: Conductive Part of 300nm Au Electrode.



Figure 44: Non-Conductive Part of 300nm Electrode



Figure 45: Failed Adhesion test for 300nm Electrode.

Conductivity was tested using multimeter to measure the resistivity between electrode pads till the connector. **Figure 46** shows measurement of conductivity between the reference pad of the electrode

and the contact pad of the electrode to the other end of the electrode in 200nm thickness of Au. The resistivity measured in the electrode had variations in it. For the reference electrode, the range was in-between $\sim 40\text{-}60\Omega$ and for the contact pads, it varied between $\sim 20\text{-}40\Omega$.

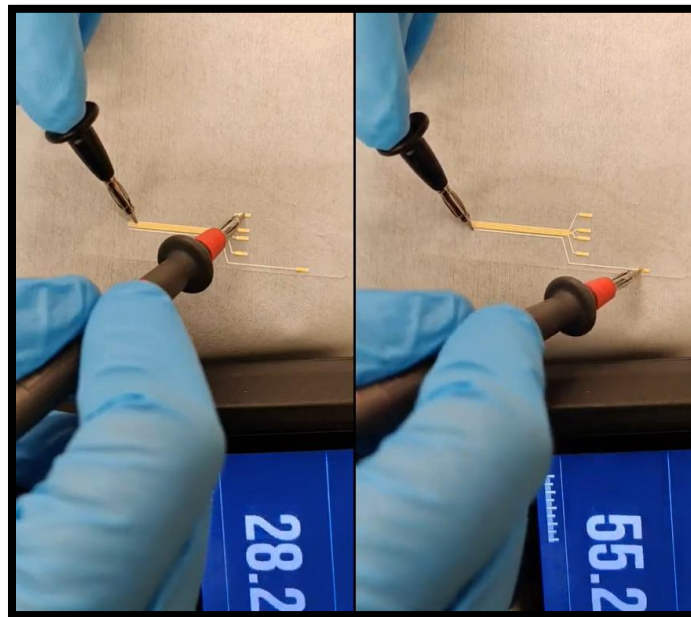


Figure 46: Conductivity tests of contact pad and reference pads on 200nm Au Electrode.

4 Discussion

4.1 Fabrication Process with Chromium as Adhesion Promoter

4.1.1 Deposition of Substrate and Plasma treatment

The deposited PDMS substrate showed equal thickness of PDMS layer on wafer. It was noticed that if the poured amount of PDMS exceeds the required amount, it goes beneath the wafer creating problems for using it later, so an estimated required amount of PDMS should be deposited to avoid the PDMS from going beneath the wafer.

Different parameters of Plasma treatment showed different surface morphology on the PDMS substrate, due to a set of different dosages (change in time) of oxygen. It was noticed that difference in dosage does not put any effect regarding adhesion promoter. The difference in microcracks and buckling can be seen in [Table 4](#). Different parameters were set from the lowest dosage to the highest, but the results were not satisfying as plasma does not affect much in increasing adhesion consequently showing not good conductivity as well. Though, thickness of chromium layer had a great impact on adhesion that is discussed in the [section 4.1.2](#) below.

Plasma was used as adhesion promoter between Cr and PDMS, as Cr itself does not have any adhesion to PDMS so using plasma, the surface of PDMS was oxidized as Cr has good adhesion with oxides. With this, residual tensile stress was introduced in PDMS when it was exposed to oxygen plasma. Plasma treatment can cause cracks (from tensile stress)[99], [100] or wrinkles/buckles (from compressive stress)[101], [102] depending on the pressure of oxygen and duration of exposure. So, a measurable controlled plasma treatment should be used which can create OH-layer as well as not to generate much heat that causes cracks in the PDMS.

4.1.2 Thin Film Deposition and Etching of Au and Cr

Metal deposition plays a vital role both as an adhesion and conductivity. As per the assigned parameters, it was concluded that extreme thin Cr adhesion film cannot hold Au film on to PDMS substrate. During adhesion test 2nm thick Cr layer shows no adhesion at all. While at 5nm thickness and upwards, it shows adhesion. After that, Au layer whose thickness at 200nm showed good adhesion and conductivity to some extent.

After etching, it was noticed that the actual thickness of Au was not 200nm. It was found to be ~110nm thick film of Au. This offset of Au deposition happened because tooling factor of thermal evaporator was not adjusted. This resulted in achieving different thickness from the target thickness. This factor was noticed after multiple depositions. Also, it was observed that after several depositions, thermal evaporator was giving the actual (deposited) thickness of Au around ~110-120nm in the depositions. To encounter this issue, the thermal evaporator needs to be calibrated before the deposition of metal so the target deposition of metal can be achieved.

Moving ahead, as cracks were observed in each of the technique and parameter applied, upon research it was observed that during deposition of Au on PDMS substrate, the thermal evaporator chamber created heat inside the chamber which led to the swelling of PDMS at some extent. It is good to mention here that PDMS is stable thermally till 150°C and its thermal expansion coefficient of PDMS is 310($\mu\text{m}/\text{m}^\circ\text{C}$)[86]. On the other side, thermal expansion coefficient of Au is 14.4($\mu\text{m}/\text{m}^\circ\text{C}$)[103] which is clearly less

than that of PDMS. The temperature inside thermal evaporator chamber was unknown making it is the major drawback. Another factor which is important to be mentioned is the residual tensile stress of thin metal films(both Cr and Au) is occurred because of the metal melting points, their deposition rate and temperature of the substrate. All these factors are important when metal is being deposited on the PDMS with OH-layer on it[100]. Therefore, with these facts, it can be concluded here that as PDMS expands while Cr and Au thermal deposition, as the temperature inside the thermal evaporator rises more than a 150°C, causing expansion of PDMS and when it is removed from the chamber, the PDMS will start curing itself again at room temperature, thus causing cracking in Au leading to non-conductivity of material. So, a controlled deposition of metal is required which can bear the max thermal expansion of PDMS and a good metal deposition can be achieved with it. Electrode Rolling Test

While implanting nerve cuff electrodes, they need to be rolled over the nerve to get full grip and control of it. Electrodes rolling tests were performed to replicate the procedure before actual implantation to view how it affects the surface of electrodes when they are rolled over nerve which was replicated by a glass tube. Before proceeding to rolling test, electrode site has to be diced and peeled off from the Si wafer which can be seen in **Figure 47** which clearly shows change in surface morphology of Au electrodes. As PDMS substrate was stretched while peeling off from the Si wafer, it created stress on deposited Au which in result left cracks and formed buckles on the surface of Au. Moreover, from **Table 3**, it was noticed that there is more change in surface of electrodes before and after rolling over a glass rod. On both tested samples, cracks became denser on Au surface. This occurred due to more mechanical stress on the Au film while being rolled around a rod.

While the diced Au electrode was being peeled off from the Si substrate, tensile stress was forming on the surface, whereas, by rolling it on the glass rod, a compressive stress was forming on the surface of Au electrode. **Figure 47** and **Figure 48** shows microscopic results after peeling off and after rolling around a rod, respectively.

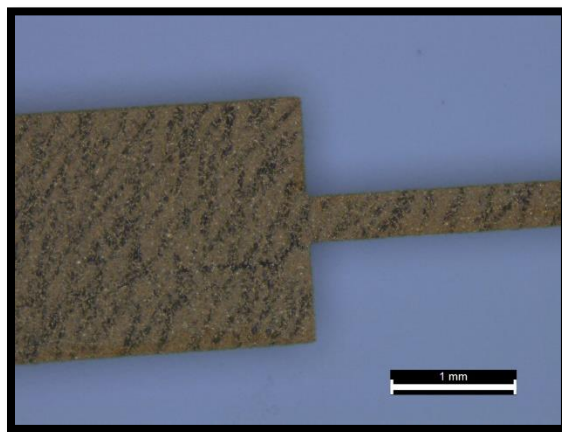


Figure 47: Au electrode on PDMS after Peeling off from Si wafer

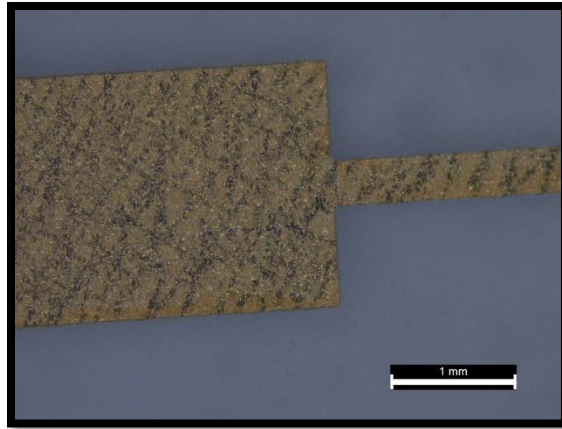


Figure 48: Au electrode on PDMS after rolling on glass rod.

4.1.3 Adhesion Test

Thickness of adhesion layer is important regardless of plasma treatment dosage. From the [Table 4](#) it can be noticed that only on first trial of adhesion test, the patterned Au film peeled off with the tape leaving blank PDMS substrate behind having no adhesion in it. While for the tests with 5nm and 20nm, it shows adhesion to some extent. But it is important to mention that the patterned electrodes after adhesion tests had broken contacts from several places which was not an acceptable result. Therefore, conductivity tests were performed prior to adhesion tests to check conductivity in electrodes.

Another reason affecting the adhesion is the thermal expansion of PDMS. After plasma treatment when PDMS is kept in thermal evaporation chamber for Cr and Au deposition, as PDMS expands with the internal heat, this expansion of PDMS disturbs the OH- layer activated by plasma which results in decreasing the adhesion between Cr and PDMS. PDMS is a stretchable substrate with high elongation factor, while the OH- layer on it does not stretch as that of PDMS comparatively so when PDMS swells, it disturbs the activated OH- layer reducing its effect. This might be the reason for not achieving good adhesion between Cr and PDMS. To reduce the thermal expansion of PDMS, the deposition temperature is required to be controlled.

4.1.4 Conductivity Test

The conductivity was tested with measuring resistance using a multimeter. Conductivity was not constant for each fabricated electrode with different parameter. As probes of multimeter were sharp and larger than the size of fabricated electrodes, they were leaving scratches on the patterned Au on the substrate. These scratches were one of the reasons of breakage in conductivity. It is important to mention here that there was no conductivity found from edge-to-edge electrode in any of these experiments. For improving conductivity, changes in parameters are required as well as to avoid scratching material while measuring conductivity.

4.1.5 Comparison with the Reference Method

The fabrication technique used in this technique has been taken into account with alterations from the reference method[89]. As the changes made in the fabrication technique were not critical, results were expected to be similar or somehow near to the original results. But it was not the actual case, significant differences were encountered after the fabrication was completed and are mentioned as under.

Firstly, differences of etching process were observed, the reference method follows the Reactive Ion Etching (RIE) method whereas, in our fabrication method, metals were etched using wet etching technique. Secondly, the reference method has bought serpentine electrodes traces(parallel and intersecting) for the fabrication of Au electrodes, as per their results, it increased the overall elasticity of the electrode. Their results shows that the intersecting serpentine trace is 8% more stretchable than that of normal straight design which fails if exceeds the limit of 3%. Our design on the other hand had straight design, which if stretched a bit, starts losing conductivity at several points. Thus, it is worth noticing that serpentine trace specifically intersecting trace shows advantage over others. Lastly, testing of conductivity also plays an important role as we used multimeter to check the conductivity, it left scratches on the Au causing loss of conductivity also due to the cracks in the PDMS, conductivity was only measured at the contact pads but not completely to the end of the conducting path i.e., till connector. At several places conductivity was missing due to sharp edges of multimeter which resulted in not accurate measurement of conductivity. Conversely, the reference method used spectrum analyzer with silver wire by dropping Hanks Balanced Salt Solution(HBSS) on the electrode pad. This helped avoiding the directing contact between the electrode pad and the lead by which, electrode can be utilized for several different testings.

4.2 Fabrication Process with (3- mercaptopropyl) trimethoxy silane (MPTMS) as Adhesion Promoter

4.2.1 Deposition and Etching of Gold Film

Au film was deposited on silicon dioxide wafer without any prior adhesion layer on it. As the aim was to transfer Au patterns on PDMS substrate smoothly, so using adhesion layer would have made it difficult. On the other side, not having adhesion layer on such thin Au film causes issues and errors as well. After deposition of Au in high vacuum, bubbles type structure was formed on surface of Au film as shown in **Figure 49**. Moreover, while washing Au surface with Acetone, Isopropanol and DI water, Au was peeling off from surface. To overcome such situations, it was suggested to wash Au deposited wafer in a beaker. The Au wafers were immersed in beaker filled with Acetone, Isopropanol and DI water separately and were rinsed gently to avoid peeling off Au structures.

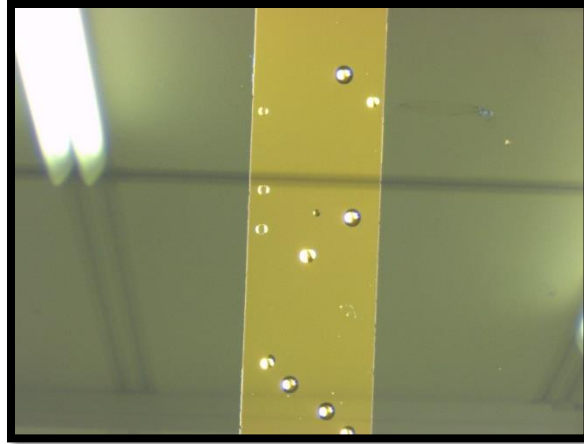


Figure 49: Au Pattern with bubble structure.

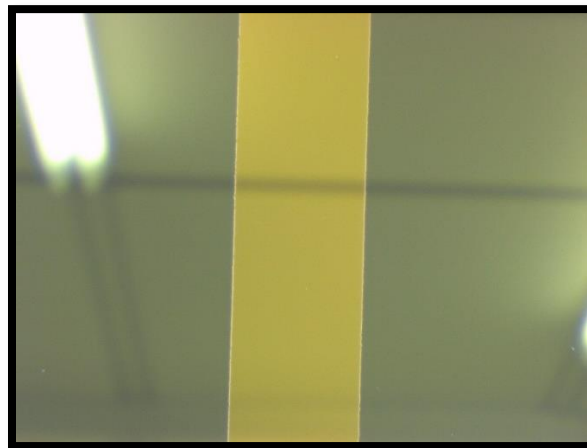


Figure 50: Au pattern without bubble structure.

For the bubble structure on Au patterns, through some research and experiments it can be stated that these bubbles can occur due to two reasons. One is lack of proper cleaning of Si wafer prior to deposition and secondly due to stress on Au film. Due to pressure build inside the metal deposition chamber, it creates stress on the metal while deposition and while releasing the pressure, this might result in forming bubble structures. To resolve this issue, Si wafer were carefully cleaned with Isopropanol, Acetone and DI water followed by drying with nitrogen gas and after that, application of plasma treatment for a minute before deposition was done. Also, the deposition rate was monitored strictly to avoid sudden changes in deposition due to internal temperature of chamber. **Figure 50** shows results of Au pattern after application of the suggested method. This showed us the successful deposition and etching of Au on wafer, ready to be brought in contact with MPTMS treated PDMS.

4.2.2 Bonding of MPTMS Treated PDMS with Gold

Bonding PDMS substrate after its treatment with MPTMS with Au patterns are a crucial stage and requires firm handling of PDMS substrate while making its contact with Au patterns. As PDMS is treated with MPTMS to increase the adherence, it is important to handle it with care and in no-dust environment i.e.,

in cleanroom. Moreover, PDMS substrate becomes sticky after MTPMS treatment, so it is foremost to grasp it gently. Structure shown in [Figure 51](#) is an example of when PDMS is not carefully and properly layered on Au wafer, it can destroy the patterns easily.

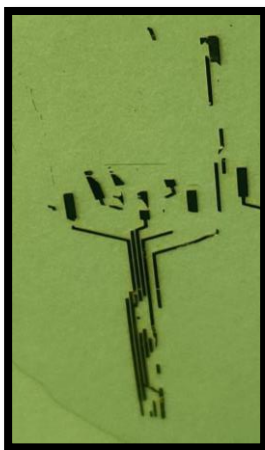


Figure 51: Misprinted Au Pattern on Si wafer

As the transfer of patterns were made in two different ways i.e., one before peeling off PDMS substrate from wafer and bonding with Au patterned wafer and second by first peeling off PDMS substrate from Si wafer and then placing it on Au patterned wafer, two different surfaces of transferred Au electrodes were noticed. While placing PDMS substrate (on wafer) directly on Au patterned wafer, the transfer of Au electrodes is smooth, and no cracks were observed on the surface of Au. On the other hand, by peeling PDMS substrate first and then placing it on Au patterned wafer, cracks were observed on the surface of Au. This caused due to bending of PDMS while peeling. While peeling off, the Au patterns are stretched, and cracks are formed on the Au.

Another technique that can give more understanding regarding formation of cracks on Au is peeling off PDMS from Si wafer after the bonding is completed. This will help in comparing both ways of before and after peeling off and to find significant changes in them.

4.2.3 Plasma Treatment

[Table 5](#) shows interesting results for the bonding in which duration of plasma was varied. It can be noticed from the table that plasma does affect the surface of PDMS which helps OH- layer cohere with the three methoxy (-OCH₃) group of MPTMS. Though, it is worth to mention that calculation of the duration of plasma dose is must to keep PDMS layer activated and not cracked. The low dose i.e., 3 minutes of plasma does not crack the PDMS surface but not completely activates the surface. Furthermore, high dose i.e., 12 minutes can crack the surface of PDMS which, if the bond between PDMS and Au patterned electrodes are made, will leave cracks in the Au patterns as well as which will affect the conductivity. By performing several experiments, an optimum duration was identified to be 9 minutes. It activated the plasma surface completely and did not leave cracks on it. Moreover, the transfer of Au patterns is also found to be good but not perfect.

Upon research, it was observed that cracks that are provoked in the PDMS layer using plasma occur when dose exceeds 1.5kJ and no cracks were observed under this value i.e., $\leq 1.5\text{kJ}$ which is approximated as 50W of power and 30s of duration having pressure of 40Pa [100]. The same phenomenon can be applied in [section 4.1.1](#). Therefore, it can be concluded that to achieve complete transfer of electrodes without impacting the surface of PDMS, more modifications are required e.g., varying oxygen rate of power watts or duration for the plasma dose.

4.2.4 Conductivity Tests

From the results of conductivity test, it can be observed that transfer technique of Au from Silicon dioxide wafer to PDMS substrate plays an important role. Bending of PDMS substrate more than the stress level of Au can leave cracks in it causing discontinuity in the path irrespective of compressive or tensile stress. Thus, it is important to calculate stress level of Au by which, adjustment in the PDMS substrate or deposition rate can also be varied to achieve required conductive path.

4.2.5 Comparison with Reference Method

The fabrication process used in this experiment has been taken from another published paper where the paper describes transfer of Au patterns on PDMS with the help of MPTMS saline [90]. The technique and methods used for fabrication in both reference and our fabrication process are nearly same. Though, after performing experiments, difference in results compared to the reference method has been observed.

The reference method shows that using MPTMS as an adhesion promotor, a good bond can be achieved between plasma treated PDMS and Au patterns. As OH- layer formed by plasma treatment bonds with three methoxy(-OCH₃) group of MPTMS, a strong bond can be achieved which adheres Au-S bond to form. The same technique was utilized in our fabrication method, but the expected results of complete transfer were not achieved. [Figure 40](#) shows the transfer of Au achieved after the bonding but some patches were still missing from the Au transfer. Several trials were made but no complete transfer was observed. This could be occurring due MPTMS treatment did not form uniform bonds over the electrode area. Also, as described in research paper, for high temperature deposition of Au, fluorination of Si wafer is required prior to deposition on Au. Fluorination is a technique of depositing release layer prior to deposition of Au. They spin deposited the release layer solution on Si wafer. The need of release layer addition before the Au deposition is to avoid forming eutectic alloy between Au and Si wafer as they form bond at high temperatures [104] [105]. The eutectic alloy starts forming at $\sim 363^\circ\text{C}$ between Au and Silicon so this might be another reason for not complete transfer as there might be eutectic bond [106]. Moreover, In thermal deposition, thermocouple are not near to the template during evaporation, so it might also be the reason that actual temperature is high enough to reach the eutectic point forming eutectic alloy [90].

This might be the prime reason in our fabrication method for not achieving complete transfer of Au. Though good transfer of Au has been achieved without using the release layer. But it is worth to try using the release layer as to confirm this theoretical factor in our experiments.

4.3 Fabrication Process with Depositing PDMS Substrate on Patterned Gold Electrodes


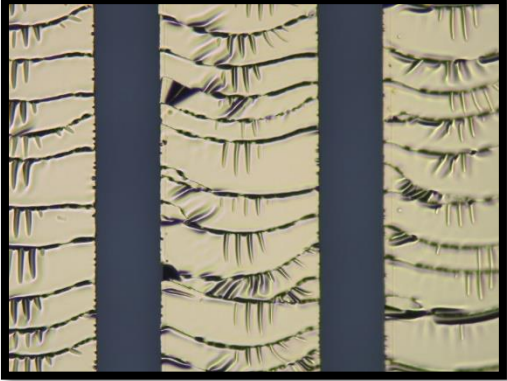
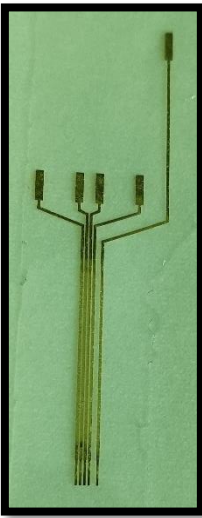
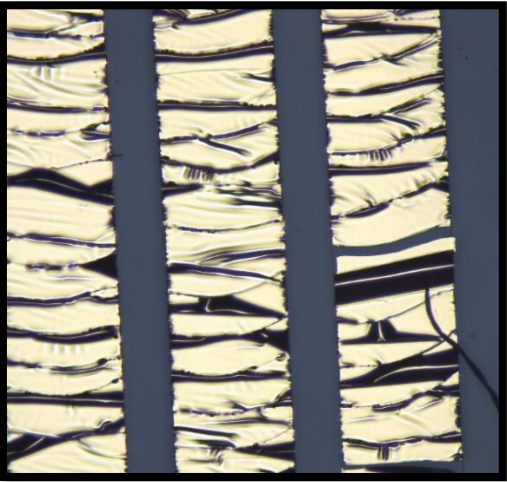
4.3.1 Transfer of Patterned Au Electrodes on PDMS

For the transfer of Au patterned electrodes, two SiO₂ wafers were prepared with Au patterns of different thicknesses i.e., 200nm and 300nm. The idea was to observe the transfer ratio as which thickness adheres more with the PDMS. Moreover, it was also the point of concern that how Au cracking or buckling affects the conductivity, adhesion and while rolled over a tube in a deformed shape. From the results, it was

noticed that the higher thickness did not performed well as that of the lower thickness. For the 300nm thickness, buckling was observed including missing Au patterns. While for the 200nm thickness, symmetrical buckling was observed. PDMS while curing caused the stress in Au resulting in buckling of Au. The buckling in Au formed because of stress form the PDMS when it was cured as forces from the PDMS curing impacted the Au. From [Table 7](#) it can be observed that the difference in buckling before and after rolling test does not changes. After testing adhesion, minor changes or addition to cracks were observed. [Table 8](#) shows the difference in cracks and buckling of both 200nm and 300nm thick Au, respectively.

It can be observed that on 300nm Au thickness there is higher impact of cracking compared to the 200nm. This may be because of the stress forces from the PDMS have more impact on Au and due to that, the Au reached to cracking point. Research is required for understanding impact of thicknesses when PDMS is cured on Au.

Table 8: Buckling and Cracking Difference between 200nm and 300nm Thickness.

| Thickness | Optical Image | Microscopic Image |
|-----------|---|--|
| 200nm |  |  |
| 300nm |  |  |

Another parameter that affected the transfer of Au patterns on cured PDMS, is how PDMS is peeled off. As peeling from PDMS was experimented in two angles, two different transfers of Au on PDMS were observed. With $\sim 90^\circ$ peeling off PDMS, Au patterns were not completely transferred to the PDMS. While for the $\sim 135^\circ$, Au completely transferred to the PDMS. It can be suggested or concluded from these results that PDMS adhesion to Au can affect differently when peeled off in different angles. As forces acting on the Au patterns from the PDMS might act differently. Further research on these parameters is required where possible answers can be mentioned with scientific proofs and reasons.

4.3.2 Rolling, Conductivity, and Adhesion Tests.

After the complete transfers of Au patterns were observed on the PDMS, they were tested ahead observing their conductivity and adhesion after rolling test. The conductivity test for 200nm thickness showed good conductivity at all the tested points, while for the 300nm, conductivity was rarely observed on the electrode. Due to deep cracks and missing Au traces in the electrode, it was difficult to check conductivity over the electrode. Though at some points, conductivity was measured but not throughout the whole electrode.

For understanding the effects of thickness and its relationship with the adhesion, more research is required so that possible changes can be made, and justified explanations can be mentioned for the further research.

5 Insulation Layer for the Cuff Electrode

Apart from the microfabrication of the nerve cuff electrode, insulation of electrode is also a crucial part. As while rolling the electrode over the nerve, the conducting paths needs to be insulated from the conducting pads to avoid any sort of short circuit. The reference and contact electrode pads and needs to expose to the nerves so that they can acquire signals. For this, a 3D printed mold was made by which conducting path of the electrode can be insulated apart from the contact pads and reference electrode. **Figure 52** shows design of 3D mold for the insulation of electrodes.

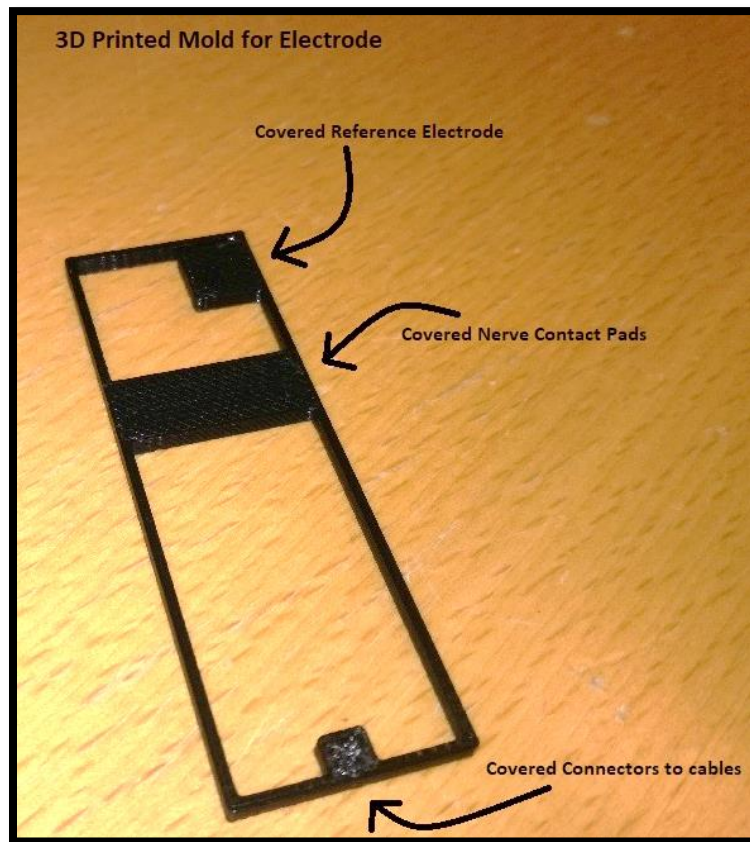


Figure 52: 3D Printed mold for Electrode Insulation.

To check how the mold works, an experiment was performed in which the mold was placed on top of already deposited plain PDMS. The mold was then filled with PDMS in it and left for curing in the oven for 2 hours at 60°C. After the PDMS was cured in the mold, using surgical blade, the mold was diced outside from the edges and peeled off from the Si wafer as shown in **Figure 53**.

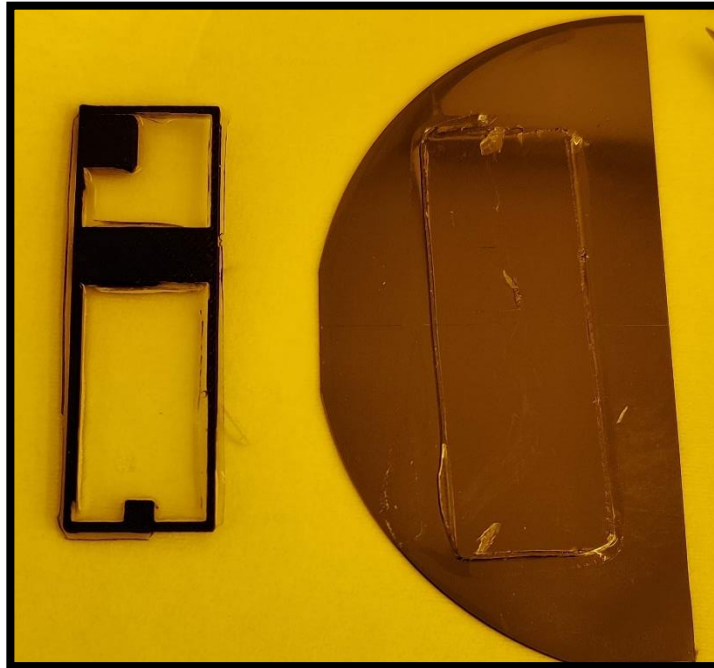


Figure 53 :Extracted PDMS Mold from Si wafer.

The PDMS structure was then carefully taken out from the mold not to destroy the insulation layer or the mold itself. Again, surgical blade was used to make incision inside edges the mold edges for extracting the PDMS. **Figure 54** shows the side view of the insulation layer while **Figure 55** shows top view with comparison to the fabricated electrode.

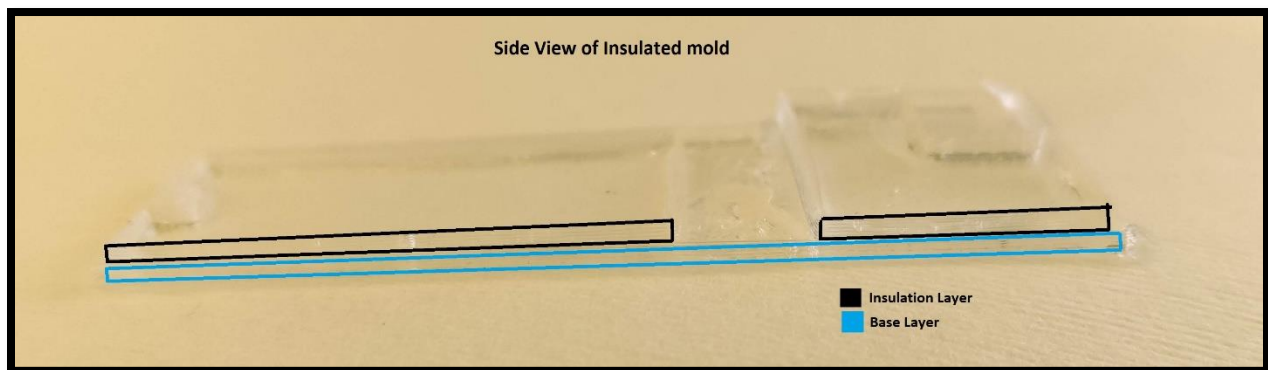


Figure 54: Side View of Insulated mold.

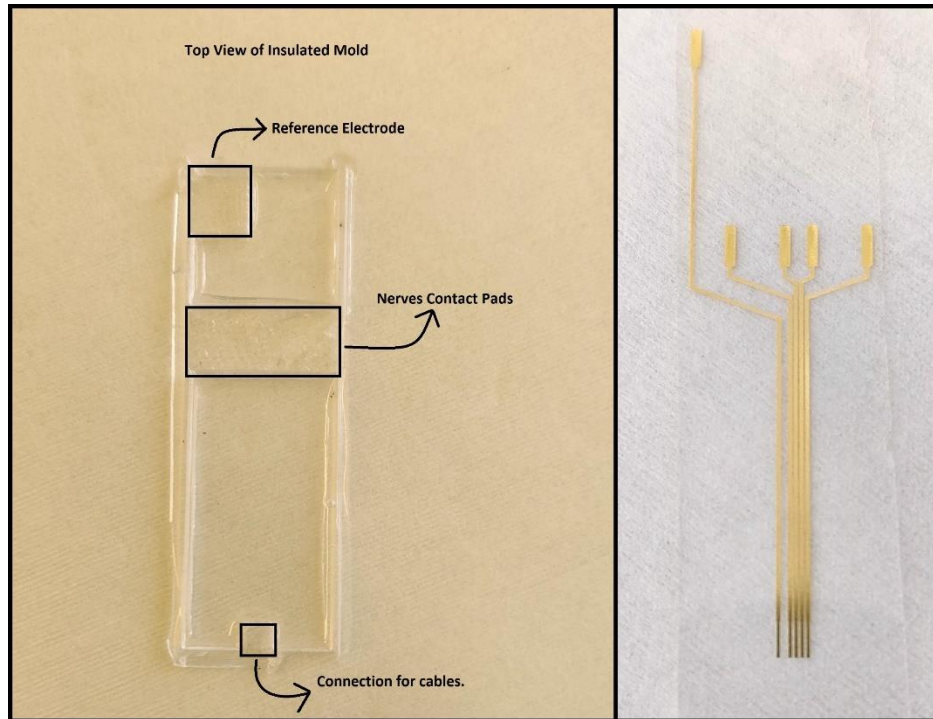


Figure 55: Top View of Insulated Mold with comparison to electrode design.

It can be noticed from the images that there is some thin PDMS layer on the reference electrode, contact pad electrodes and at area for the cable's connection, this happened due to material of the 3D printed mold as it was non resistive to PDMS and while PDMS was curing in oven some small amount of PDMS went under the mold and it also caused trouble while extracting the PDMS from the mold. This problem needs to be encountered by either using PDMS resistive material for 3D mold or to cover edges of this available mold with rubber or other synthetic material so that it can avoid letting PDMS under it.

6 Biocompatibility Tests

Biocompatibility is related to the assessment of medical devices that are in contact with the host (patient) in sort of direct or indirect contact. These devices are evaluated in specific environment, like location where it will be implanted or bring in contact with the host, how they react with the host body both by direct or indirect contacts and if it is good enough to remain stable biologically without causing problem to the host[107][108]. For this these devices must undergo International Standards Organization (ISO) and the local standards to examine their biological capabilities when brought in contact with the body, apart from there other properties from physical, chemical and mechanical aspects[109][110]. These biological properties are verified by inspecting the cytotoxicity, acute systemic toxicity and a number of other tests that are the device must to undergo before it enters the clinical environment so that the safety of the host can be ensured[111]. Cytotoxicity is measurement of how toxic the cells are after the cells have been treated with any agent or process[112], whereas acute systemic toxicity is checked to examine short-term toxic effects that emerge after substance is either swallowed, absorbed through skin or inhaled[113].

From these tests, cytotoxicity is one of the chief biological assessing and screening test which is performed by using cell tissues in vitro for the observation of cell growth reproduction and morphological effects caused by the medical devices[114]. The cytotoxicity tests has developed with time giving more information regarding determining the damages in cell, morphological changes in cells, their metabolic properties and they have grown more from qualitative to quantitative evaluation [115]–[118].

After the completion of microfabricated cuff electrode, it is now important to test its biocompatibility before the electrode is proceeded ahead for animal tests. For that, an experiment was conducted following the protocol[119] and prerequisites for the protocol[120]–[122]. The biocompatibility test was prepared to check the reaction of electrodes including the chemical used and for the substrate as how they react in cell cultures. For that, a 24 well plate was chosen where the wells were filled with test cells and small pieces of electrodes were placed in the wells. **Figure 56** shows the setup arranged for the biocompatibility tests.

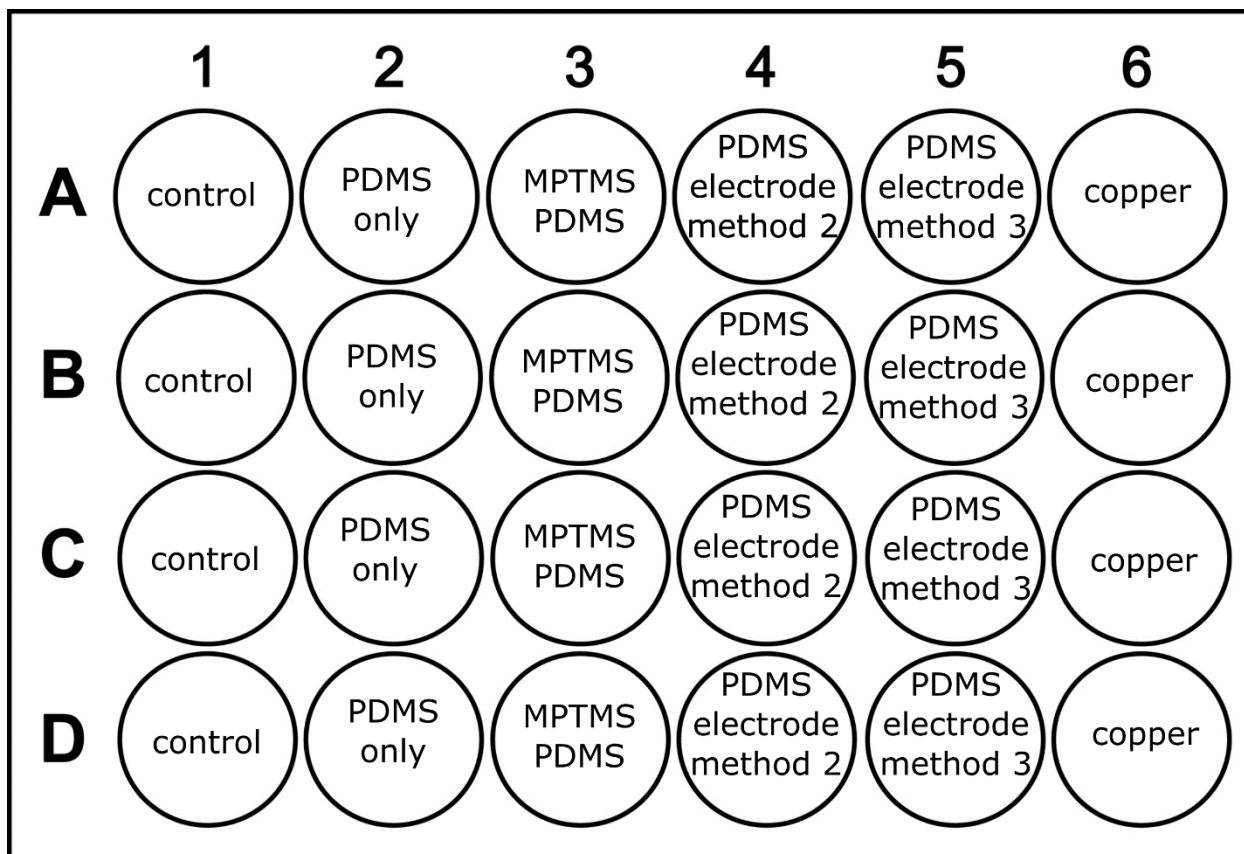


Figure 56: Setup on a 24-well plate for Biocompatibility Test.

Each column consists of four samples which will be used in the end to find mean/average and standard deviation from all four wells. The first column has the positive control which in our case were only Mouse Preosteoblastic cell line, MC3T3-E1 . After 24 h of growth, test substrates were added to the wells of columns 2-6. The second column had only PDMS substrate in it. In third column, each well was given small piece of PDMS that was only treated with the MPTMS saline with no Au on it. The fourth column had the electrodes fabricated from the [2.2](#) i.e., second method. The fifth column had electrodes fabricated from the [section 2.3](#) i.e., third fabrication method. And lastly, the sixth column had negative control which was copper, as copper is highly toxic to the cells. The plate was then incubated for 24hours before cell growth and metabolism was investigated. Metabolism was measured by adding the reagent PrestoBlue (Invitrogen) to each well and was placed in BioTek Synergy2 plate reader to read data using the fluorescence technique (Excitation filter 530/25 (nm), Emission filter 620/15nm) from each well. After the data was collected, a graph was plotted to visualize the differences in each column [Figure 57](#) and shows the metabolic activity of the cells.

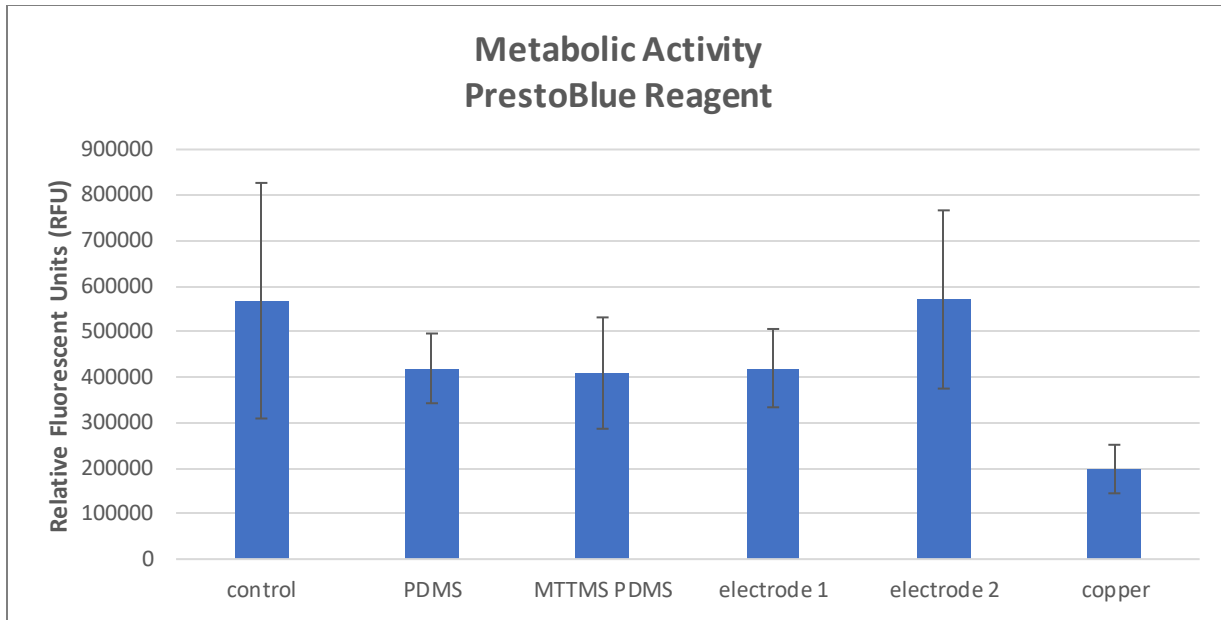


Figure 57: Metabolic Activity of PrestoBlue Reagent.

The cell counts were done after the metabolic activity test using inverted Microscope (Olympus IX51) where samples from each well were transferred to haemocytometer (instrument using for counting number of cells in a fluid) using a pipette.

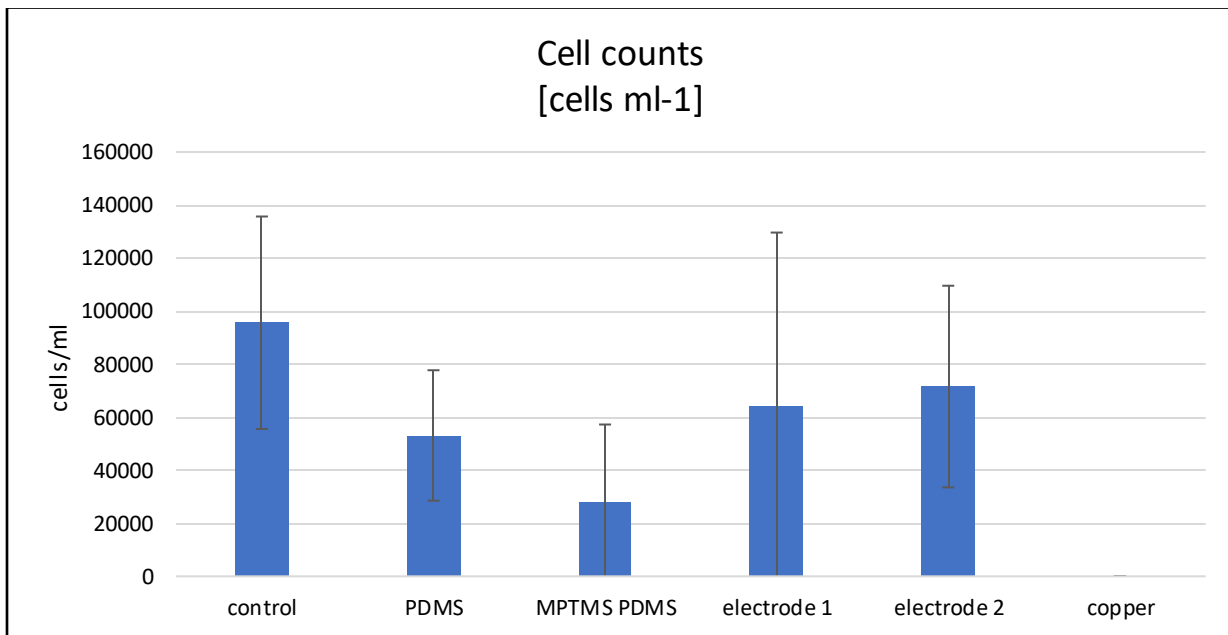


Figure 58: Cell Count from each Sample using Hemocytometer.

From the cell counting, it can be seen from the [Figure 58](#) that being a toxic element to the cells, copper shows no cells in its each well, Electrode 2 that had been fabricated from the third fabrication method shows the high cell count after the positive control. This can be due to the reason that no other chemical was used in the fabrication. While electrode 1 and PDMS with MPTMS treatment shows low cell count

than that of Electrode 2. This can be due to using chemical saline MPTMS in the fabrication of Electrode. The PDMS itself had good cell count showing its feasibility of using for implanted electrodes.

From the graph an uncertainty can also be noticed as PDMS has lower cell count from that of Electrode 2 fabrication where Au and PDMS are used for the fabrication of electrode. This uncertainty might be because experiments with the cell culture, sudden cell death was observed and that might be due to Mycoplasma cell contamination. This usually spreads by aerosols and particulates created during the treatment of the mycoplasma contaminated cell culture [123]. Moreover, due to this factor, variation inside each column was quite high. Overall, the test results are justified as it can be concluded that the materials used in the fabrication of electrodes are in good scale of biocompatibility.

7 Conclusion and Upcoming Work

Limb loss cases are commonly worldwide. And can be caused by traumatic injuries like road accident, gunshot wound or other injuries to non-traumatic injuries like heart and vascular diseases. Effect of these cases have been profoundly noticed in the demand of neuroprosthesis over a decade. Biomedical engineers and scientists have made plenty of research in the respective area and due to that the world have seen prosthetic arms from cable powered prosthesis to updated myoelectric arms. And the research does not stop here, there is huge research still going on in the field of neuroprosthesis [124]. This research master project was planned to contribute to the development of neuroprosthesis currently happening around the world which can be utilized in the field of bionic prosthetic arms.

The motivation of this master project work is the microfabrication of an implantable neural cuff electrode, which can be used for the acquisition of signals from nerves and can become an integrated part of a neuroprosthesis arm. Hence, a thorough literature study was required before moving ahead to the fabrication processes. Different techniques were studied and a few of them were considered based on the feasibility of the fabrication process and availability of equipment's. Three fabrication procedures are performed during the project which are well documented with their fabrication description, results, and discussion. Au was used as conductive electrode metal and Cr was for promoting adhesion between PDMS and Au. MPTMS saline was used replacing Cr for promoting adhesion and strong bond between Au and PDMS, PDMS was used as a substrate material for Au and lastly, oxygen plasma treatment was utilized to promote adhesion between Cr and PDMS.

Both the theoretical part and the practical part of the thesis were extensively conducted as being in a research project. The goal was to achieve results which can be useful for future work and experiments. From the three chosen fabrication methods, different results were observed and each of these results are beneficial in their respective way.

In first fabrication method, Au with an adhesion layer of Cr was deposited on PDMS substrate using oxygen plasma treatment on PDMS. A 224 μm thick electrode was fabricated using standard photolithography technique consisting of $\sim 200\text{nm}$ Au, $\sim 20\text{nm}$ Cr. From the results it was concluded that plasma treatment can be beneficial for the depositing metals on PDMS substrate if doze of oxygen plasma is used in right amount. Secondly, residual tensile stresses can be expected to observe both from plasma treatment and metal deposition which can be causing effect of cracks. This caused missing conductivity in the electrodes. Different parameters related to Au, Cr thickness and plasma treatment were applied which exhibits good research data and will be helpful for future research and fabrication.

From the second fabrication method, a new technique of having Au patterns on PDMS substrate were experimented. Using a saline namely MPTMS, on plasma activated PDMS Au was transferred to it by bonding Au patterns (deposited on SiO_2 wafer) and MPTMS treated PDMS. The results from the experiment were valuable defining importance of plasma treatment for the bonding of metals. Applying different parameters of plasma, it was observed that cracks in plasma can be avoided using optimal oxygen doze and using MPTMS saline, strong bond between Au and PDMS can be achieved. Though, a complete transfer of Au was not observed but as results from these experiments are useful for future work.

Lastly, the third fabrication method enables simpler fabrication of neural cuff electrodes. Implementing the hypothesis after researching from several research papers, a new method was experimented. The electrode in this fabrication method was achieved by depositing freshly prepared PDMS onto the

patterned Au wafer. Then by curing the PDMS in oven, PDMS was molded around the Au giving good strength of adhesion. Buckles were observed on the Au surface that were caused due to residual tensile stress from the PDMS when it was cured. Though, this does not affect conductivity or continuity from the electrode. Also, a good adhesion between Au and PDMS was also observed when scotch tape tests were applied. The electrode fabricated from these techniques was of $\sim 118\mu\text{m}$ thickness.

All these experimented methods revealed using various techniques for the fabrication of neural electrodes. Using different techniques and parameters, desired neural cuff electrode can easily be fabricated. These electrodes also have the potential for affordable fabrication. Though more work is required but this work on electrode fabrication contributes to the completion of the ARMIN project. .

Due to current and previous unfortunate conditions occurred from the COVID lockdown, some of the research work was left behind and is in need to be completed in upcoming stages. One of the important tasks is the insulation of electrode that is mandatory before the electrode is being implanted. In this research, we successfully illustrated and fabricated double PDMS layer using a mold and this technique can be used ahead to cover Au between the two PDMS layers. The Au will be sandwiched between the two PDMS layers and will only allow the required contact pads with the nerves and with the module to be exposed only. Secondly, further tests are required related to conductivity by connecting the electrode with the microcontroller and using oscilloscope, test signals can be generated and passed through the electrode to check SNR and conductivity all over the electrode. Lastly, more biocompatibility tests will be beneficial after having insulation of PDMS on both sides of the Au to check if there are some changes as per the results achieved and mentioned in this research thesis.

8 References

- [1] J. N. Y. M. M. Diane W. Braza MD, "Upper Limb Amputations," *iEssentials Phys. Med. Rehabil. (Fourth Ed.)*, 2020.
- [2] Z.-G. K., M. E.J., E. P.L., T. T.G., and B. R., "Estimating the Prevalence of Limb Loss in the United States: 2005 to 2050," *Arch. Phys. Med. Rehabil.*, 2008.
- [3] K. Barraclough and A. Bradbury, "Chronic limb threatening ischaemia," *BMJ*, vol. 360, 2018, doi: 10.1136/bmj.j5460.
- [4] S. B. Brummer and M. J. Turner, "Electrochemical Considerations for Safe Electrical Stimulation of the Nervous System with Platinum Electrodes," *IEEE Trans. Biomed. Eng.*, vol. BME-24, no. 1, pp. 59–63, 1977, doi: 10.1109/TBME.1977.326218.
- [5] B. Osmani, T. Töpfer, and B. Müller, "Conducting and stretchable nanometer-thin gold/thiol-functionalized polydimethylsiloxane films," *J. Nanophotonics*, vol. 12, no. 03, p. 1, 2018, doi: 10.1117/1.jnp.12.033006.
- [6] "Vagus nerve - Wikipedia." https://en.wikipedia.org/wiki/Vagus_nerve (accessed Apr. 04, 2021).
- [7] H. Yu, W. Xiong, H. Zhang, W. Wang, and Z. Li, "A parylene self-locking cuff electrode for peripheral nerve stimulation and recording," *J. Microelectromechanical Syst.*, vol. 23, no. 5, pp. 1025–1035, 2014, doi: 10.1109/JMEMS.2014.2333733.
- [8] *Prime Faraday Technology Watch An Introduction to MEMS (Micro-electromechanical Systems)*. 2002.
- [9] U. of N. M. Southwest Center for Microsystems Education, "BioMEMS Overview Learning Module," 2017. Accessed: May 16, 2021. [Online]. Available: www.scme-nm.org.
- [10] L. S. Sudarsan and E. C. Sekaran, "Design and development of EMG controlled prosthetics limb," in *Procedia Engineering*, Jan. 2012, vol. 38, pp. 3547–3551, doi: 10.1016/j.proeng.2012.06.409.
- [11] H. J. Seddon, "A classification of nerve injuries," *Br. Med. J.*, vol. 2, no. 4260, p. 237, Aug. 1942, doi: 10.1136/bmj.2.4260.237.
- [12] F. Dangond, "What Is Central Nervous System? Definition, Function & Parts," *Emedicinehealth*. 2017, Accessed: Jan. 15, 2021. [Online]. Available: https://www.emedicinehealth.com/anatomy_of_the_central_nervous_system/article_em.htm.
- [13] L. M. Biga *et al.*, "12.1 Structure and Function of the Nervous System." OpenStax/Oregon State University.
- [14] K. Cherry, "How the Peripheral Nervous System Works," *Very Well Mind*, p. 2020, 2020, Accessed: Jan. 15, 2021. [Online]. Available: <https://www.verywellmind.com/what-is-the-peripheral-nervous-system-2795465>.
- [15] "BBC Science & Nature - Human Body and Mind - Nervous System Layer." https://www.bbc.co.uk/science/humanbody/body/factfiles/nervecellsandnerves/nerve_cells_and_nerves.shtml (accessed Jan. 15, 2021).
- [16] J. Walinga and C. Stanger, "The Neuron Is the Building Block of the Nervous System – Introduction to Psychology – 1st Canadian Edition," in *Introduction to Psychology: 1st Canadian Edition*, 2012.
- [17] J. Mělka, "The neuron," *Sb. Ved. Pr. Lek. Fak. Karlovy Univerzity. Hradci Kralove*, vol. 7, no. 5, p. Suppl:428-31, 1964, Accessed: Jan. 17, 2021. [Online]. Available: <https://bazaarmodel.net/Onderwerpen/neuron/ps2lec1.htm>.
- [18] J. G. Webster, L. E. Osborn, J. L. Betthausen, and N. V. Thakor, "Neural Prostheses," *Wiley Encycl. Electr. Electron. Eng.*, no. 1, pp. 1–20, 2019, doi: 10.1002/047134608x.w1424.pub2.

- [19] V. Aggarwal *et al.*, “Asynchronous decoding of dexterous finger movements using M1 neurons,” *IEEE Trans. Neural Syst. Rehabil. Eng.*, vol. 16, no. 1, pp. 3–14, Feb. 2008, doi: 10.1109/TNSRE.2007.916289.
- [20] S. Acharya, M. S. Fifer, H. L. Benz, N. E. Crone, and N. V. Thakor, “Electrocorticographic amplitude predicts finger positions during slow grasping motions of the hand,” *J. Neural Eng.*, vol. 7, no. 4, p. 046002, May 2010, doi: 10.1088/1741-2560/7/4/046002.
- [21] D. W. Tan, M. A. Schiefer, M. W. Keith, J. R. Anderson, J. Tyler, and D. J. Tyler, “A neural interface provides long-term stable natural touch perception,” *Sci. Transl. Med.*, vol. 6, no. 257, pp. 257ra138-257ra138, Oct. 2014, doi: 10.1126/scitranslmed.3008669.
- [22] R. H. Meier and D. J. Atkins, *Functional restoration of adults and children with upper extremity amputation*. New York, N.Y.: Demos Medical Publishing, Inc., 2004.
- [23] “Shoulder girdle - Wikipedia.” https://en.wikipedia.org/wiki/Shoulder_girdle (accessed Apr. 04, 2021).
- [24] “Sauerbruch: The Arbitrarily Movable Artificial ... - Google Scholar.” https://scholar.google.com/scholar_lookup?title=Die+willkürlich+bewegbare+künstliche+Hand+Eine+Anleitung+für+Chirurgen+und+Techniker&author=F+Sauerbruch&publication_year=1916 (accessed Feb. 06, 2021).
- [25] “VL Library Item: lit38212, p0008.” <https://vlp.mpiwg-berlin.mpg.de/library/data/lit38416> (accessed Feb. 06, 2021).
- [26] K. J. Zuo and J. L. Olson, “The evolution of functional hand replacement: From iron prostheses to hand transplantation,” *Canadian Journal of Plastic Surgery*, vol. 22, no. 1. Pulsus Group Inc., pp. 44–51, 2014, doi: 10.1177/229255031402200111.
- [27] K. Ostlie, I. M. Lesjø, R. J. Franklin, B. Garfelt, O. H. Skjeldal, and P. Magnus, “Prosthesis use in adult acquired major upper-limb amputees: Patterns of wear, prosthetic skills and the actual use of prostheses in activities of daily life,” *Disabil. Rehabil. Assist. Technol.*, vol. 7, no. 6, pp. 479–493, Nov. 2012, doi: 10.3109/17483107.2011.653296.
- [28] C. Behrend, W. Reizner, J. A. Marchessault, and W. C. Hammert, “Update on advances in upper extremity prosthetics,” *Journal of Hand Surgery*, vol. 36, no. 10. W.B. Saunders, pp. 1711–1717, 2011, doi: 10.1016/j.jhsa.2011.07.024.
- [29] Ottobock UK, “Myoelectric prosthetics 101 | Ottobock UK,” ottobock.co.uk, 2019. <https://www.ottobockus.com/prosthetics/info-for-new-amputees/prosthetics-101/myoelectric-prosthetics-101/> (accessed May 02, 2021).
- [30] R. N. Scott and P. A. Parker, “Myoelectric Prostheses: state of the art,” *J. Med. Eng. Technol.*, vol. 12, no. 4, pp. 143–151, Jan. 1988, doi: 10.3109/03091908809030173.
- [31] D. S. Childress, “Historical Aspects of Powered Limb Prostheses,” *J. Prosthetics Orthot.*, vol. 9, no. 1, pp. 2–13, 1985.
- [32] P. Parker, K. Englehart, and B. Hudgins, “Myoelectric signal processing for control of powered limb prostheses,” *J. Electromyogr. Kinesiol.*, vol. 16, no. 6, pp. 541–548, Dec. 2006, doi: 10.1016/j.jelekin.2006.08.006.
- [33] “What Is a Radial Prosthesis? – Human Technology Prosthetics and Orthotics.” <https://humantechpando.com/what-is-a-radial-prosthesis/> (accessed Apr. 04, 2021).
- [34] “Transhumeral Amputation & Elbow Disarticulate | Aspire Prosthetics & Orthotics Inc.” <https://aspirepo.com/services/prosthetics/transhumeral-amputation-elbow-disarticulate/> (accessed Apr. 04, 2021).

- [35] A. E. Schultz and T. A. Kuiken, "Neural Interfaces for Control of Upper Limb Prostheses: The State of the Art and Future Possibilities," *PM R*, vol. 3, no. 1, pp. 55–67, Jan. 2011, doi: 10.1016/j.pmrj.2010.06.016.
- [36] L. V. McFarland, S. L. H. Winkler, A. W. Heinemann, M. Jones, and A. Esquenazi, "Unilateral upper-limb loss: Satisfaction and prosthetic-device use in veterans and servicemembers from Vietnam and OIF/OEF conflicts," *J. Rehabil. Res. Dev.*, vol. 47, no. 4, pp. 299–316, 2010, doi: 10.1682/JRRD.2009.03.0027.
- [37] T. A. Kuiken, G. A. Dumanian, R. D. Lipschutz, L. A. Miller, and K. A. Stubblefield, "The use of targeted muscle reinnervation for improved myoelectric prosthesis control in a bilateral shoulder disarticulation amputee," *Prosthet. Orthot. Int.*, vol. 28, no. 3, pp. 245–253, 2004, doi: 10.3109/03093640409167756.
- [38] T. A. Kuiken *et al.*, "Targeted reinnervation for enhanced prosthetic arm function in a woman with a proximal amputation: a case study," *Lancet*, vol. 369, no. 9559, pp. 371–380, Feb. 2007, doi: 10.1016/S0140-6736(07)60193-7.
- [39] S. Grushko, T. Spurný, and M. Černý, "Control methods for transradial prostheses based on remnant muscle activity and its relationship with proprioceptive feedback," *Sensors (Switzerland)*, vol. 20, no. 17, MDPI AG, pp. 1–32, Sep. 01, 2020, doi: 10.3390/s20174883.
- [40] A. D. Roche, H. Rehbaum, D. Farina, and O. C. Aszmann, "Prosthetic Myoelectric Control Strategies: A Clinical Perspective," *Curr. Surg. Reports*, vol. 2, no. 3, pp. 1–11, Mar. 2014, doi: 10.1007/s40137-013-0044-8.
- [41] C. Pylatiuk, S. Schulz, and L. Döderlein, "Results of an Internet survey of myoelectric prosthetic hand users," *Prosthetics Orthot. Int.*, vol. 31, no. 4, pp. 362–370, Dec. 2007, doi: 10.1080/03093640601061265.
- [42] "Upper limb prosthesis use and abandonment: A survey of the I... : Prosthetics and Orthotics International." https://journals.lww.com/poijournal/Abstract/2007/31030/Upper_limb_prosthesis_use_and_abandonment__A.3.aspx (accessed Mar. 10, 2021).
- [43] D. J. Warren *et al.*, "Recording and decoding for neural prostheses," *Proceedings of the IEEE*, vol. 104, no. 2, Institute of Electrical and Electronics Engineers Inc., pp. 374–391, Feb. 01, 2016, doi: 10.1109/JPROC.2015.2507180.
- [44] E. H. Rijnbeek, N. Eleveld, and W. Olthuis, "Update on peripheral nerve electrodes for closed-loop neuroprosthetics," *Front. Neurosci.*, vol. 12, no. MAY, pp. 1–9, 2018, doi: 10.3389/fnins.2018.00350.
- [45] M. S. Malagodi, K. W. Horch, and A. A. Schoenberg, "An intrafascicular electrode for recording of action potentials in peripheral nerves," *Ann. Biomed. Eng.*, vol. 17, no. 4, pp. 397–410, Jul. 1989, doi: 10.1007/BF02368058.
- [46] S. M. Lawrence, G. S. Dhillon, W. Jensen, K. Yoshida, and K. W. Horch, "Acute peripheral nerve recording characteristics of polymer-based longitudinal intrafascicular electrodes," *IEEE Trans. Neural Syst. Rehabil. Eng.*, vol. 12, no. 3, pp. 345–348, Sep. 2004, doi: 10.1109/TNSRE.2004.831491.
- [47] T. Boretius *et al.*, "A transverse intrafascicular multichannel electrode (TIME) to interface with the peripheral nerve," *Biosens. Bioelectron.*, vol. 26, no. 1, pp. 62–69, Sep. 2010, doi: 10.1016/j.bios.2010.05.010.
- [48] A. K. Thota *et al.*, "A system and method to interface with multiple groups of axons in several fascicles of peripheral nerves," *J. Neurosci. Methods*, vol. 244, pp. 78–84, Apr. 2015, doi: 10.1016/j.jneumeth.2014.07.020.
- [49] E. V. Goodall, T. M. Lefurge, and K. W. Horch, "Information Contained in Sensory Nerve Recordings Made with Intrafascicular Electrodes," *IEEE Trans. Biomed. Eng.*, vol. 38, no. 9, pp. 846–850, 1991, doi: 10.1109/10.83604.

- [50] X. Navarro *et al.*, "Neurobiological evaluation of thin-film longitudinal intrafascicular electrodes as a peripheral nerve interface," in *2007 IEEE 10th International Conference on Rehabilitation Robotics, ICORR'07*, 2007, pp. 643–649, doi: 10.1109/ICORR.2007.4428492.
- [51] A. Kundu, K. R. Harreby, K. Yoshida, T. Boretius, T. Stieglitz, and W. Jensen, "Stimulation selectivity of the 'thin-film longitudinal intrafascicular electrode' (tFLIFE) and the 'transverse intrafascicular multi-channel electrode' (time) in the large nerve animal model," *IEEE Trans. Neural Syst. Rehabil. Eng.*, vol. 22, no. 2, pp. 400–410, 2014, doi: 10.1109/TNSRE.2013.2267936.
- [52] S. Raspopovic *et al.*, "Restoring Natural Sensory Feedback in Real-Time Bidirectional Hand Prostheses," *Sci. Transl. Med.*, vol. 6, no. 222, pp. 222ra19–222ra19, Feb. 2014, doi: 10.1126/scitranslmed.3006820.
- [53] "Fibrosis - Wikipedia." <https://en.wikipedia.org/wiki/Fibrosis> (accessed May 09, 2021).
- [54] "Necrosis - Wikipedia." Accessed: May 09, 2021. [Online]. Available: <https://en.wikipedia.org/wiki/Necrosis>.
- [55] A. Kundu, M. Wirenfeldt, K. R. Harreby, and W. Jensen, "Biosafety assessment of an intra-neural electrode (TIME) following sub-chronic implantation in the median nerve of göttingen minipigs," *Int. J. Artif. Organs*, vol. 37, no. 6, pp. 466–476, Jun. 2014, doi: 10.5301/ijao.5000342.
- [56] A. Branner, R. B. Stein, and R. A. Normann, "Selective Stimulation of Cat Sciatic Nerve Using an Array of Varying-Length Microelectrodes," *J. Neurophysiol.*, vol. 85, no. 4, pp. 1585–1594, Apr. 2001, doi: 10.1152/jn.2001.85.4.1585.
- [57] K. Warwick *et al.*, "The application of implant technology for cybernetic systems," *Arch. Neurol.*, vol. 60, no. 10, pp. 1369–1373, Oct. 2003, doi: 10.1001/archneur.60.10.1369.
- [58] A. Branner, R. B. Stein, E. Fernandez, Y. Aoyagi, and R. A. Normann, "Long-Term Stimulation and Recording with a Penetrating Microelectrode Array in Cat Sciatic Nerve," *IEEE Trans. Biomed. Eng.*, vol. 51, no. 1, pp. 146–157, Jan. 2004, doi: 10.1109/TBME.2003.820321.
- [59] R. R. Harrison *et al.*, "A wireless neural interface for chronic recording," in *2008 IEEE-BIOCAS Biomedical Circuits and Systems Conference, BIOCAS 2008*, 2008, pp. 125–128, doi: 10.1109/BIOCAS.2008.4696890.
- [60] H. A. C. Wark, K. S. Mathews, R. A. Normann, and E. Fernandez, "Behavioral and cellular consequences of high-electrode count Utah Arrays chronically implanted in rat sciatic nerve," *J. Neural Eng.*, vol. 11, no. 4, p. 13, Aug. 2014, doi: 10.1088/1741-2560/11/4/046027.
- [61] M. B. Christensen, S. M. Pearce, N. M. Ledbetter, D. J. Warren, G. A. Clark, and P. A. Tresco, "The foreign body response to the Utah Slant Electrode Array in the cat sciatic nerve," *Acta Biomater.*, vol. 10, no. 11, pp. 4650–4660, Nov. 2014, doi: 10.1016/j.actbio.2014.07.010.
- [62] "Median nerve - Wikipedia." https://en.wikipedia.org/wiki/Median_nerve (accessed May 09, 2021).
- [63] "Ulnar nerve - Wikipedia." https://en.wikipedia.org/wiki/Ulnar_nerve (accessed May 09, 2021).
- [64] T. S. Davis *et al.*, "Restoring motor control and sensory feedback in people with upper extremity amputations using arrays of 96 microelectrodes implanted in the median and ulnar nerves," *J. Neural Eng.*, vol. 13, no. 3, p. 036001, Mar. 2016, doi: 10.1088/1741-2560/13/3/036001.
- [65] N. M. Ledbetter *et al.*, "Intrafascicular stimulation of monkey arm nerves evokes coordinated grasp and sensory responses," *J. Neurophysiol.*, vol. 109, no. 2, pp. 580–590, Jan. 2013, doi: 10.1152/jn.00688.2011.
- [66] C. H. Thompson, M. J. Zoratti, N. B. Langhals, and E. K. Purcell, "Regenerative Electrode Interfaces for Neural Prostheses," *Tissue Engineering - Part B: Reviews*, vol. 22, no. 2. Mary Ann Liebert Inc., pp. 125–135, Apr. 01, 2016, doi: 10.1089/ten.teb.2015.0279.

- [67] J. L. Seifert *et al.*, "Normal molecular repair mechanisms in regenerative peripheral nerve interfaces allow recording of early spike activity despite immature myelination," *IEEE Trans. Neural Syst. Rehabil. Eng.*, vol. 20, no. 2, pp. 220–227, Mar. 2012, doi: 10.1109/TNSRE.2011.2179811.
- [68] K. Garde, "Early Interfaced Neural Activity from Chronic Amputated Nerves," *Front. Neuroeng.*, vol. 2, no. MAY, p. 5, May 2009, doi: 10.3389/neuro.16.005.2009.
- [69] J. Jeong *et al.*, "64-channel double-layered sieve electrode with increased porosity for improved axon regeneration and high spatial resolution," in *Proceedings of the IEEE RAS and EMBS International Conference on Biomedical Robotics and Biomechanics*, Jul. 2016, vol. 2016-July, pp. 1148–1153, doi: 10.1109/BIOROB.2016.7523786.
- [70] K. Garde, E. Keefer, B. Botterman, P. Galvan, and M. Romero-Ortega, "Early interfaced neural activity from chronic amputated nerves," *Frontiers in Neuroengineering*, vol. 2, p. 5, 2009, [Online]. Available: <https://www.frontiersin.org/article/10.3389/neuro.16.005.2009>.
- [71] A. F. Mensinger *et al.*, "Chronic Recording of Regenerating VIIIth Nerve Axons With a Sieve Electrode," *J. Neurophysiol.*, vol. 83, no. 1, pp. 611–615, Jan. 2000, doi: 10.1152/jn.2000.83.1.611.
- [72] A. Srinivasan *et al.*, "Microchannel-based regenerative scaffold for chronic peripheral nerve interfacing in amputees," *Biomaterials*, vol. 41, pp. 151–165, Feb. 2015, doi: 10.1016/j.biomaterials.2014.11.035.
- [73] M. R. MacEwan, E. R. Zellmer, J. J. Wheeler, H. Burton, and D. W. Moran, "Regenerated Sciatic Nerve Axons Stimulated through a Chronically Implanted Macro-Sieve Electrode," *Frontiers in Neuroscience*, vol. 10, p. 557, 2016, [Online]. Available: <https://www.frontiersin.org/article/10.3389/fnins.2016.00557>.
- [74] V. H. Desai *et al.*, "Chronic sensory-motor activity in behaving animals using regenerative multi-electrode interfaces," in *2014 36th Annual International Conference of the IEEE Engineering in Medicine and Biology Society, EMBC 2014*, Nov. 2014, pp. 1973–1976, doi: 10.1109/EMBC.2014.6944000.
- [75] N. Xue *et al.*, "Polymeric C-shaped cuff electrode for recording of peripheral nerve signal," *Sensors Actuators, B Chem.*, vol. 210, pp. 640–648, Apr. 2015, doi: 10.1016/j.snb.2015.01.006.
- [76] G. G. Naples, J. T. Mortimer, A. Scheiner, and J. D. Sweeney, "A Spiral Nerve Cuff Electrode for Peripheral Nerve Stimulation," *IEEE Trans. Biomed. Eng.*, vol. 35, no. 11, pp. 905–916, 1988, doi: 10.1109/10.8670.
- [77] D. J. Tyler and D. M. Durand, "Chronic response of the rat sciatic nerve to the flat interface nerve electrode," *Ann. Biomed. Eng.*, vol. 31, no. 6, pp. 633–642, 2003, doi: 10.1114/1.1569263.
- [78] E. B. J. T. Mortimer, J. M. Brookshart and V. B. Mountcastle, "Motor prostheses." .
- [79] B. P. Christie *et al.*, "Long-term stability of stimulating spiral nerve cuff electrodes on human peripheral nerves," *J. Neuroeng. Rehabil.*, vol. 14, no. 1, p. 70, Jul. 2017, doi: 10.1186/s12984-017-0285-3.
- [80] D. J. Tyler and D. M. Durand, "Chronic response of the rat sciatic nerve to the flat interface nerve electrode," *Ann. Biomed. Eng.*, vol. 31, no. 6, pp. 633–642, 2003, doi: 10.1114/1.1569263.
- [81] D. K. Leventhal, M. Cohen, and D. M. Durand, "Chronic histological effects of the flat interface nerve electrode," *J. Neural Eng.*, vol. 3, no. 2, pp. 102–113, Jun. 2006, doi: 10.1088/1741-2560/3/2/004.
- [82] D. W. Tan, M. A. Schiefer, M. W. Keith, J. R. Anderson, and D. J. Tyler, "Stability and selectivity of a chronic, multi-contact cuff electrode for sensory stimulation in human amputees," *J. Neural Eng.*, vol. 12, no. 2, p. 026002, Apr. 2015, doi: 10.1088/1741-2560/12/2/026002.
- [83] B. Wodlinger and D. M. Durand, "Recovery of neural activity from nerve cuff electrodes," in *Proceedings of the Annual International Conference of the IEEE Engineering in Medicine and Biology Society, EMBS*, 2011, pp. 4653–4656, doi: 10.1109/IEMBS.2011.6091152.

- [84] E. T. K. Demann, P. S. Stein, and J. E. Haubenreich, "Gold as an implant in medicine and dentistry," *Journal of Long-Term Effects of Medical Implants*, vol. 15, no. 6. Begell House Inc., pp. 687–698, 2005, doi: 10.1615/JLongTermEffMedImplants.v15.i6.100.
- [85] B. Moazzez, S. M. O'Brien, and E. F. S. Merschrod, "Improved adhesion of gold thin films evaporated on polymer resin: Applications for sensing surfaces and MEMS," *Sensors (Switzerland)*, vol. 13, no. 6, pp. 7021–7032, 2013, doi: 10.3390/s130607021.
- [86] A. Subramaniam and S. Sethuraman, "Poly(Dimethylsiloxane) - an overview | ScienceDirect Topics," *Biomedical Applications of Nondegradable Polymers*, 2014. <https://www.sciencedirect.com/topics/chemical-engineering/polydimethylsiloxane> (accessed Mar. 19, 2021).
- [87] J. H. Moon, D. H. Baek, Y. Y. Choi, K. H. Lee, H. C. Kim, and S. H. Lee, "Wearable polyimide-PDMS electrodes for intrabody communication," *J. Micromechanics Microengineering*, vol. 20, no. 2, 2010, doi: 10.1088/0960-1317/20/2/025032.
- [88] "Scientific Method Examples and the 6 Key Steps." <https://examples.yourdictionary.com/scientific-method-examples.html> (accessed May 28, 2021).
- [89] K. W. Meacham, R. J. Giuly, L. Guo, S. Hochman, and S. P. DeWeerth, "A lithographically-patterned, elastic multi-electrode array for surface stimulation of the spinal cord," *Biomed. Microdevices*, vol. 10, no. 2, pp. 259–269, 2008, doi: 10.1007/s10544-007-9132-9.
- [90] B. Atmaja, J. Frommer, and J. C. Scott, "Atomically flat gold on elastomeric substrate," *Langmuir*, vol. 22, no. 10, pp. 4734–4740, 2006, doi: 10.1021/la0524420.
- [91] T. Adrega and S. P. Lacour, "Stretchable gold conductors embedded in PDMS and patterned by photolithography: Fabrication and electromechanical characterization," *J. Micromechanics Microengineering*, vol. 20, no. 5, 2010, doi: 10.1088/0960-1317/20/5/055025.
- [92] "Lab facilities « Norwegian Micro – and Nano Fabrication Facility." <https://www.norfab.no/lab-facilities/> (accessed May 17, 2021).
- [93] S. Isabel, G. Hernández, and L. Blystad, "PROJECT : MEMS ELECTRODE DESIGN AND (SENSOR FRONT-END) ELECTRONICS . IMPLANTABLE ELECTRODES FABRICATION Internship report," 2020.
- [94] B. K. Gale *et al.*, "Low-Cost MEMS Technologies," *Ref. Modul. Mater. Sci. Mater. Eng.*, 2016, doi: 10.1016/b978-0-12-803581-8.00530-0.
- [95] N. A. Brill and D. J. Tyler, "Quantification of human upper extremity nerves and fascicular anatomy," *Muscle and Nerve*, vol. 56, no. 3, pp. 463–471, Sep. 2017, doi: 10.1002/mus.25534.
- [96] M. Drdácáký, J. Lesák, S. Rescic, Z. Slížková, P. Tiano, and J. Valach, "Standardization of peeling tests for assessing the cohesion and consolidation characteristics of historic stone surfaces," *Mater. Struct. Constr.*, vol. 45, no. 4, pp. 505–520, 2012, doi: 10.1617/s11527-011-9778-x.
- [97] I. Byun, A. W. Coleman, and B. Kim, "Transfer of thin Au films to polydimethylsiloxane (PDMS) with reliable bonding using (3-mercaptopropyl)trimethoxysilane (MPTMS) as a molecular adhesive," *J. Micromechanics Microengineering*, vol. 23, no. 8, 2013, doi: 10.1088/0960-1317/23/8/085016.
- [98] J. Singh and J. E. Whitten, "Adsorption of 3-mercaptopropyltrimethoxysilane on silicon oxide surfaces and adsorbate interaction with thermally deposited gold," *J. Phys. Chem. C*, vol. 112, no. 48, pp. 19088–19096, Dec. 2008, doi: 10.1021/jp807536z.
- [99] M. J. Owen and P. J. Smith, "Plasma treatment of polydimethylsiloxane," *J. Adhes. Sci. Technol.*, vol. 8, no. 10, pp. 1063–1075, 1994, doi: 10.1163/156856194X00942.

- [100] R. Seghir and S. Arscott, "Controlled mud-crack patterning and self-organized cracking of polydimethylsiloxane elastomer surfaces," *Sci. Rep.*, vol. 5, no. March, pp. 1–16, 2015, doi: 10.1038/srep14787.
- [101] D. B. H. Chua, H. T. Ng, and S. F. Y. Li, "Spontaneous formation of complex and ordered structures on oxygen-plasma-treated elastomeric polydimethylsiloxane," *Appl. Phys. Lett.*, vol. 76, no. 6, pp. 721–723, Feb. 2000, doi: 10.1063/1.125873.
- [102] N. Bowden, W. T. S. Huck, K. E. Paul, and G. M. Whitesides, "The controlled formation of ordered, sinusoidal structures by plasma oxidation of an elastomeric polymer," *Appl. Phys. Lett.*, vol. 75, no. 17, pp. 2557–2559, Oct. 1999, doi: 10.1063/1.125076.
- [103] AZoM, "Gold (Au) - properties, applications," *AZO Materials*, 2013. <https://www.azom.com/article.aspx?ArticleID=9083> (accessed May 20, 2021).
- [104] C.-H. Lin, J.-M. Lu, and W. Fang, "Formation of Silicon-Gold Eutectic Bond Using Localized Heating Method Related content Encapsulation of film bulk acoustic resonator filters using a wafer-level microcap array."
- [105] R. F. Wolffenbuttel and K. D. Wise, "Low-temperature silicon wafer-to-wafer bonding using gold at eutectic temperature," *Sensors Actuators A. Phys.*, vol. 43, no. 1–3, pp. 223–229, May 1994, doi: 10.1016/0924-4247(93)00653-L.
- [106] "Eutectic Bonding - an overview | ScienceDirect Topics." <https://www.sciencedirect.com/topics/engineering/eutectic-bonding> (accessed Jun. 01, 2021).
- [107] J. M. Anderson and M. S. Shive, "Biodegradation and biocompatibility of PLA and PLGA microspheres," *Advanced Drug Delivery Reviews*, vol. 64, no. SUPPL. Elsevier, pp. 72–82, Dec. 01, 2012, doi: 10.1016/j.addr.2012.09.004.
- [108] M. Shim, N. W. S. Kam, R. J. Chen, Y. Li, and H. Dai, "Functionalization of Carbon Nanotubes for Biocompatibility and Biomolecular Recognition," *Nano Lett.*, vol. 2, no. 4, pp. 285–288, Apr. 2002, doi: 10.1021/nl015692j.
- [109] J. Black, *Biological performance of materials: fundamentals of biocompatibility*. Crc Press, 2005.
- [110] T. O. Woods, "Standards for medical devices in MRI: Present and future," *Journal of Magnetic Resonance Imaging*, vol. 26, no. 5, pp. 1186–1189, Nov. 2007, doi: 10.1002/jmri.21140.
- [111] W. LI, J. ZHOU, and Y. XU, "Study of the in vitro cytotoxicity testing of medical devices," *Biomed. Reports*, vol. 3, no. 5, pp. 617–620, 2015, doi: 10.3892/br.2015.481.
- [112] "Cytotoxicity - Wikipedia." <https://en.wikipedia.org/wiki/Cytotoxicity> (accessed May 31, 2021).
- [113] "Acute Systemic Toxicity." <https://ntp.niehs.nih.gov/iccvmreport/2015/activities/acutetox/index.html> (accessed May 31, 2021).
- [114] S. J. Soenen *et al.*, "Cytotoxic effects of gold nanoparticles: A multiparametric study," *ACS Nano*, vol. 6, no. 7, pp. 5767–5783, Jul. 2012, doi: 10.1021/nn301714n.
- [115] C. Uboldi, G. Giudetti, F. Broggi, D. Gilliland, J. Ponti, and F. Rossi, "Amorphous silica nanoparticles do not induce cytotoxicity, cell transformation or genotoxicity in Balb/3T3 mouse fibroblasts," *Mutat. Res. - Genet. Toxicol. Environ. Mutagen.*, vol. 745, no. 1–2, pp. 11–20, Jun. 2012, doi: 10.1016/j.mrgentox.2011.10.010.
- [116] J. Kasper *et al.*, "Inflammatory and cytotoxic responses of an alveolar-capillary coculture model to silica nanoparticles: Comparison with conventional monocultures," *Part. Fibre Toxicol.*, vol. 8, no. 1, pp. 1–16, Jan. 2011, doi: 10.1186/1743-8977-8-6.
- [117] B. A. Damas, M. A. Wheeler, J. S. Bringas, and M. M. Hoen, "Cytotoxicity comparison of mineral trioxide

- aggregates and endosequence bioceramic root repair materials," *J. Endod.*, vol. 37, no. 3, pp. 372–375, Mar. 2011, doi: 10.1016/j.joen.2010.11.027.
- [118] M. J. Piao *et al.*, "Silver nanoparticles induce oxidative cell damage in human liver cells through inhibition of reduced glutathione and induction of mitochondria-involved apoptosis," *Toxicol. Lett.*, vol. 201, no. 1, pp. 92–100, Feb. 2011, doi: 10.1016/j.toxlet.2010.12.010.
- [119] Birgitte Kasin Hønsvall, "Process specification ARMIN Bio05b Biocompatibility test B MST lab Process specification," pp. 1–4, 2021.
- [120] B. K. Hønsvall, "Process specification ARMIN Bio04 Sterilisation of electrodes MST lab Process specification," pp. 4–5, 2020.
- [121] B. K. Hønsvall, "Process specification ARMIN Bio03 Cell passaging MST lab Process specification," pp. 8–9, 2020.
- [122] B. K. Hønsvall, "Process specification ARMIN Bio02 Cell culture start-up MST lab Process specification," pp. 1–2, 2020.
- [123] L. Nikfarjam and P. Farzaneh, "Prevention and detection of mycoplasma contamination in cell culture," *Cell Journal*, vol. 13, no. 4. Royan Institute, pp. 203–212, Dec. 2012, Accessed: May 31, 2021. [Online]. Available: /pmc/articles/PMC3584481/.
- [124] "Neuroprosthetics 2018-2028: Technologies, Forecasts, Players: IDTechEx." <https://www.idtechex.com/en/research-report/neuroprosthetics-2018-2028-technologies-forecasts-players/549> (accessed May 20, 2021).